NATIONAL ADVISORY COMMITTEE FOR AERONAUTICS

WARTIME REPORT

ORIGINALLY ISSUED
January 1945 as
Memorandum Report L5A18

LANGLEY FULL-SCALE-TUNNEL STABILITY AND CONTROL TESTS OF THE BELL YP-59A AIRPLANE

By Gerald W. Brewer

Langley Memorial Aeronautical Laboratory
Langley Field, Va.

NACA

WASHINGTON

NATIONAL ADVISORY COMMITTEE FOR AERONAUTICS

MEMORANDUM REPORT

for the

Army Air Forces, Air Technical Service Command

LANGLEY FULL-SCALE-TUNNEL STABILITY AND CONTROL TESTS OF THE BELL YP-59A AIRPLANE

By Gerald W. Brewer

SUMMARY

Drag clean-up and stability investigations of the Bell YP-59A jet-propelled airplane have been conducted in the Langley full-scale tunnel. At present, very little data are available pertaining to the effect of jets on the stability of an airplane. Some tests were therefore made to investigate in detail the effect of jets on the longitudinal-stability characteristics of this airplane configuration. The results of these tests indicate that with the flaps retracted, approximately 70 percent of the change in longitudinal stability due to rated-thrust operation is caused by the thrust moment of the jet. With the flaps deflected 45°, the thrust moment contributes about 75 percent of the longitudinal-stability change for lift coefficients up to about 0.65. At the higher lift coefficients there is a large increase in the downwash angle at the tail for the rated thrust flap-deflected condition which results in an appreciable increase in the total destablizing moment. For this condition at lift coefficients greater than 0.65 the change in stability due to the thrust moment of the jet is only about 21 percent. The results of the tests also show that with the exception of two neutrally stable conditions (rated-thrust low-speed flight, flaps down 45° and rated-thrust high-speed flight, flaps neutral) the airplane is longitudinally stable, stick fixed, for the design center-of-gravity location. The airplane will be longitudinally unstable, stick free, for rated-thrust engine operation with flaps neutral in the lift-coefficient range of 0.35 to 0.95 and with the flaps deflected 45° above a lift coefficient of 0.8; for any other combination of engine

operation and flap deflection the airplane should exhibit stable elevator stick-force variations with speed. Although a sufficient amount of data for a complete lateral stability and control analysis were not obtained, the tests made with the engines inoperative show that the airplane, with the landing flaps fully deflected, may be laterally unstable in flight at lift coefficients of about 0.8. The rolling response of the airplane due to full aileron deflection is considered low for both high-speed and low-speed flight conditions.

INTRODUCTION

At the request of the Army Air Forces, Air Technical Service Command, tests of the Bell YP-59A jet-propelled airplane have been made in the Langley full-scale tunnel to investigate means to increase the speed of the airplane and to evaluate the stability and control characteristics. This report presents the test results of the stability investigation and a brief analysis of the static stability and control characteristics of the airplane. A discussion relating to the effects of the exhaust jet on the air flow at the tail and on the stability and control of the airplane is also presented. The results of tests made to determine means of increasing the speed of the airplane will be given in a separate report.

In order to determine the static longitudinal stability and control characteristics of the airplane, forces and moments on the airplane and elevator hinge moments were determined for a large range of elevator deflection and angle of attack at several engine-operating conditions. To obtain an indication of the lateral stability and control characteristics of the airplane, rudder-effectiveness tests were made over a range of angle of attack at angles of yaw of 0°, 3°, 6°, 9°, and 10.6°. Aileron-effectiveness tests were made over a range of angle of attack with the landing flaps retracted and fully deflected and with the airplane at zero yaw. Aileron hinge moments were not obtained since the balance of the test ailerons was not identical to that of the latest production ailerons.

AIRPLANE AND APPARATUS

The Bell YP-59A airplane, as tested in the Langley full-scale tunnel, is shown mounted on the balance system in figure 1. A description of this balance and the operation of the tunnel are given in detail in reference 1. The three-view drawing of figure 2 shows the principal dimensions of the airplane. The airplane was in the wheels-retracted condition for all the tests, since the nose wheel and main landing gear were removed and replaced by the tunnel support system.

The Bell YP-59A is a jet-propelled fighter airplane powered by two General Electric I-16 jet-propulsion engines. The engines are housed in underslung nacelles located at the wing-fuselage junctures. The air enters the unit from a large opening at the front of the nacelle; the exhaust passes through a tail pipe and nozzle and is ejected at the rear of the nacelle at the wing trailing edge. These particular units are each capable of developing about 1650 pounds of static thrust at sea level.

The test airplane was equipped with a ventral fin, prism deflectors at the fin trailing-edge, deflector beads at the rudder trailing edge, and internally sealed 60-percent-balance ailerons. Although the arrangement of the balance and seal of the ailerons tested was not identical to that of the latest production configuration, it was assumed that the aileron-control characteristics of the test ailerons would be substantially the same as the production type. A photograph of the ventral fin installation is given in figure 3 while the deflector installations on the fin and rudder are shown by sketches and a photograph in figures 4 to 6. In order to give some detail of the control surfaces, cross-sectional views of the rudder, the elevator, and the aileron are shown in figure 7. The relation between the elevator, aileron, and rudder deflections with control movement for this airplane is given in figure 8. For the tests, the ailerons, the elevator, and the rudder were operated remotely by electrical-type actuators and the control-surface deflections were obtained by measuring the change in resistance of slide-wire rheostats. Elevator and rudder hinge moments were obtained by the use of calibrated cantilever-beam electrical strain-gage units installed in the control systems.

SYMBOLS

The definitions of the coefficients and symbols used in this report are given as follows:

C_D drag coefficient (X/qS)

C_Y lateral-force coefficient (Y/qS)

C_L lift coefficient (Z/qS)

C_l rolling-moment coefficient (L/qSb)

C_m pitching-moment coefficient (M/qSc)

C_n yawing-moment coefficient (N/qSb)

C_{h_e} elevator hinge-moment coefficient $\left(H_e/qb_e\bar{c}_e^{\,2}\right)$

C_{h_r} rudder hinge-moment coefficient $\left(H_r/qb_r\bar{c}_r^{\,2}\right)$

T_c' thrust coefficient (T/qS)

where

X force along X axis, positive when directed rearward

Y force along Y axis, positive when directed to the right

Z force along Z axis, positive when directed upward

L rolling moment about the X axis, positive when the moment tends to depress the right wing

M pitching moment about the Y axis, positive when the moment tends to depress the tail

N yawing moment about the Z axis, positive when the moment tends to retard the right wing

H_e	elevator hinge moment, positive when the moment tends to depress the elevator trailing edge
H_r	rudder hinge moment, positive when the moment tends to move the trailing edge to the left
T	thrust, pounds (for two-engine operation unless noted)
q	free-stream dynamic pressure $\left(\frac{1}{2}\rho V^2\right)$, pounds per square foot
ρ	mass density of air, slugs per cubic foot
V	free-stream velocity, feet per second
S	total wing area (385 sq ft)
b	wing span (45.5 ft)
c	wing mean chord (8.47 ft)
M.A.C.	mean aerodynamic chord (8.85 ft)
b_e	elevator span (16.75 ft)
b_r	rudder span (6.7 ft)
$\bar{c}_e$	root-mean-square elevator chord (1.32 ft)
$\bar{c}_r$	root-mean-square rudder chord (1.39 ft)
pb/2V	helix angle
p	rolling velocity; radians per second
F_e	elevator stick force, pounds
F_r	rudder stick force, pounds
Δn	change in normal acceleration in g units
α	angle of attack of the thrust axis, degrees
ψ	angle of yaw, degrees; positive when the nose of the airplane is to the right

δ control surface deflection relative to the main fixed surface, degrees; positive when the trailing edge is directed downward or to the left

i_t angle of incidence of stabilizer, degrees; positive when the nose is up with respect to the plane parallel with the thrust axis

Subscripts:

e elevator

a aileron

r rudder

f wing flap

T tab

L left

i indicated

t tail

METHODS AND TESTS

In order to obtain data for the determination of the longitudinal-stability and control characteristics of the airplane, forces and moments on the airplane and elevator hinge moments were determined for a range of elevator deflection and angle of attack. These tests were made with the ailerons and rudder locked neutral and with the elevator tab neutral and deflected $\pm 10^{\circ}$. The tests with the elevator tab deflected $\pm 10^{\circ}$ were made only at angles of attack of 0.1° and 15°. The elevator tests were made with the airplane at zero yaw for different combinations of flap deflection and jet-engine operation. Data were obtained with the engines inoperative and with the engines operating at thrust conditions simulating sea-level flight at high-speed, cruising, and idling thrusts.

For the tests with the jet-propulsion units in operation a tunnel-testing technique was employed that provided simulation in the wind tunnel of the flight thrust-lift relationship. The variation of thrust with airplane speed for sea-level flight was obtained from data furnished by the Supercharger Engineering Division, General Electric Company, which give the estimated thrust performance of these I-16 jet-propulsion units over a range of altitude and flight speed. The thrusts developed in flight at sea level by engine operation at rpm's of 16,500 (military rated), 13,000 (cruising), and 6000 (idling) were chosed and shall be referred to in this report as rated, cruising and idling thrust conditions, respectively. The variation of the thrust coefficient with lift coefficient for these three operating conditions is presented in figure 9. The engine-operating conditions for the tunnel tests were determined by means of a static-thrust calibration which was made with the airplane near zero lift. From this calibration the relation of the thrust developed by both engines over a range of engine speed was determined. Since the change in thrust due to tunnel operation was found to be very small for these stability investigations, the thrust calibration for the static condition was used for all the operating conditions tested.

For the determination of the lateral-stability and control characteristics of the airplane, rudder tests were made at angles of yaw of 0°, 3°, 6°, 9°, and 10.6° for a range of angle of attack and for flap deflections of 0° and 45°. Inasmuch as considerable engine-operating time had been consumed during the longitudinal-stability investigation and since further extended operation would require a major overhaul or replacement of the jet units, most of the rudder-effectiveness tests were made with the jets units inoperative. One test at each angle of yaw and at an angle of attack of 3.9° was made with the engines operating at a constant rpm, simulating rated thrust at zero yaw. The rudder tests were made with the rudder tab, the ailerons, and the elevator in the neutral position. The airplane was yawed only to the right for these tests since it was considered that the characteristics of the airplane would be similar for yaw in either direction. The range of yaw angles was the maximum attainable by the particular strut-support setup. Data were also obtained for the determination of the effects of single-engine operation on the lateral-control characteristics of the airplane by operation of only the left unit over a range of thrust conditions with the airplane at zero yaw and at an angle of attack of -0.5°.

In order to determine the effectiveness of the test ailerons, aileron-effectiveness tests were made with the airplane at zero yaw for a range of angle of attack and for flap deflections of 0° and 45°. These aileron-effectiveness tests were made for deflections of the left aileron only and with all other control surfaces locked in neutral. The jet-propulsion units were not in operation for these tests since the air flow over the region of the ailerons was considered unchanged by the exhaust jet.

Inasmuch as very little data are available with regard to the effects on the air flow at the tail due to the exhaust jet of a jet-propulsion system, a few tests were made with the empennage removed to provide a basis for estimating these effects.

RESULTS AND DISCUSSION

The presentation of results and the accompanying discussion relating to the estimated static stability and control characteristics of the Bell YP-59A airplane are given in three sections: (1) longitudinal stability and control, (2) analysis of exhaust jet effect, and (3) lateral stability and control.

The results of the tests are given in terms of the standard NACA force and moment coefficients. The forces and moments have been referred to the system of axes in which the X axis is the intersection of the plane of symmetry of the airplane with a plane perpendicular to the plane of symmetry and parallel with the relative wind direction; the Y axis is perpendicular to the plane of symmetry; and the Z axis is in the plane of symmetry and perpendicular to the X axis. All the moments are based on the wing mean chord and are computed about a center of gravity located at 27.2 percent of the mean aerodynamic chord and 5.1 inches below the root chord line. All test results are corrected for jet-boundary and blocking effects by the methods discussed in references 2 and 3. The tests were made at a Mach number of about 0.1 and no attempt has been made to predict the effect of high Mach numbers on these results.

Longitudinal Stability and Control

Elevator effectiveness and hinge moments.- The results of the elevator tests which show variations of C_L, C_m, and C_{h_e} with δ_e (tab neutral) for the angles of attack, flap deflections, and engine-operating conditions tested are given in figure 10. For the same engine-operating conditions and flap deflections the variations of C_D and C_L with angle of attack at different elevator settings are presented in figure 11. To aid in the analysis of the test results, the elevator data have been cross-plotted (fig. 12) to show the variation of C_m with C_L for the engines inoperative and the rated thrust conditions with the flaps retracted and deflected 45°. The results of tests made with the tail removed are shown in figure 13.

To determine the changes in elevator effectiveness due to variations in engine operation, flap deflection, and angle of attack, the slopes of the pitching-moment curves $dC_m/d\delta_e$, measured at $C_m = 0$, have been obtained and are plotted in figure 14 as a function of angle of attack. The slopes of the hinge-moment curves $dC_{h_e}/d\delta_e$, measured at $\delta_e = 0$, are also presented in this figure. These results show that a change in airplane attitude, flap deflection, and engine operation produce very small variations in the control-surface effectiveness. The value of $dC_m/d\delta_e$, per degree, decreases slightly from -0.0125 at an α of 0° to -0.0115 at an α of 15°. The fairing of a single curve through all values gives a maximum deviation of only ±0.0007 from the average value of $dC_m/d\delta_e$ at any angle of attack. The measured values of $\left(dC_{h_e}/d\delta_e\right)_{\delta_e=0}$ at each angle of attack for all the test conditions do not show quite so consistent a trend as the pitching-moment results, especially in the lower angle-of-attack range. The average value of all conditions of engine operation and flap deflection is about -0.0040 per degree.

The results of elevator tests made with the tab deflected ±10° at angles of attack of 0.1° and 15°

and with the jet units operating at the rated-thrust condition are given in figure 15. A comparison of these data with the tab-neutral results, which have been included in figure 10, shows very small variation in the slopes of the pitching-moment and hinge-moment curves due to tab deflection. The ratio of tab deflection to elevator deflection $(\delta_t/\delta_e)_{C_{h_e}=0}$ is about 1.4 for the two extreme angle-of-attack conditions.

Longitudinal stability and control, stick fixed.- The longitudinal-stability and control characteristics of the airplane with the stick fixed for the conditions investigated are shown by the variation of elevator trim angle with indicated airspeed in figure 16. With the jet-propulsion engines inoperative the airplane is statically stable (flaps up or down 45°) throughout the speed range. Application of jet propulsion decreased the amount of elevator deflection required to trim the airplane throughout the speed range. The static longitudinal stability of the airplane is decreased to about neutral for the rated-thrust flap-down (wave-off) condition in the speed range from about 100 to 200 miles per hour. For the normal low-thrust landing condition (engines idling, flaps down 45°) the rate of change of δ_e with speed indicates satisfactory direction of elevator-control movement for the limited speed range investigated.

It should be noted that these elevator trim variations are presented for the design center-of-gravity location 27.2 percent mean aerodynamic chord. The longitudinal-stability characteristics of the airplane for any center-of-gravity location can be determined from the curves of figure 17. Each curve represents points of the center-of-gravity location at which the longitudinal stability is neutral with the airplane trimmed. As previously discussed from the curves of figure 16 for the design center-of-gravity location of 27.2 percent mean aerodynamic chord, the airplane will be about neutrally stable for the wave-off flight condition in the C_L range from about 0.3 to 1.0. A very small static margin (less than 1 percent) exists for the rated-thrust flap-neutral condition at low lift coefficients (high speeds). For the remaining conditions shown there are greater positive static margins and, in general, the neutral point moves rearward as the lift coefficient is increased.

Longitudinal stability and control, stick free.- An indication of the longitudinal stability of the airplane with the stick free (tab neutral) for the conditions tested is given by the variations of $C_{m_{(C_{h_e}=0)}}$ with C_L in figure 18. Stick-free instability is shown for the wave-off condition (rated thrust, $\delta = 45^\circ$) by the positive slope of the pitching-moment curve at the trim lift coefficient of 1.18. Although a trim point is not shown for the rated-thrust flaps-retracted condition, stick-free instability is indicated at lift coefficients greater than about 0.4 for this case. For the remaining conditions tested, it appears that the airplane will be longitudinally stable with the stick free.

The stability of the airplane, stick free, is also given by the variations of the stick-free neutral points with lift coefficient in figure 20 showing a comparison of the engines inoperative and the rated-thrust conditions with the flaps up and down 45°. In this presentation it was assumed that, since there exists very little change in the dynamic pressure at the tail, the effectiveness of the elevator tab shown for the rated-thrust case will be substantially the same for the remaining conditions investigated. As previously indicated in figure 18 the airplane will be longitudinally stable, stick free, with the engines inoperative and for flap deflections of 0° and 45°. For rated-thrust operation, with flaps neutral, stick-free instability occurs between lift coefficients of about 0.35 and 0.95; for rated-thrust operation with the flaps deflected 45° the airplane will be unstable, stick free, at lift coefficients greater than about 0.8. It should be noted here that the negative value of C_{h_α} is associated with a loss of stick-free stability for the case where the stick-free neutral point is forward of the stick-fixed neutral point.

In order to determine the control-force characteristics of the airplane the tab-neutral hinge-moment results have been adjusted so that the stick force is zero at the trim speeds listed in the following table for the different conditions.

Flight condition	Operating condition	Flap setting (deg)	Speed for trim velocity, (mph)
Glide	Engines inoperative	0	150
Landing approach	---------do.--------	45	120
Do.--------	Idling thrust	45	120
Wave off	Rated thrust	45	100
Climb	---------do.--------	0	230
Cruise	Cruising thrust	0	265
High speed	Rated thrust	0	315

The resulting stick-force variations with indicated airspeed for these conditions are given in figure 20. These results do not include the effects of friction in the elevator control system. The steady flight conditions shown in figure 20 indicate stable stick-force variations for all speeds above and below the trim speeds for the two landing, the gliding, and the cruising conditions described in the above table. For the latter condition, however, with the airplane trimmed for $F_e = 0$ at 265 miles per hour, the stick forces are rapidly decreasing to zero again in the range of low flight speeds. For the three rated-thrust conditions shown ($\delta_f = 0^\circ$ and 45°) instability is indicated by the two or more trim stick-force speeds occurring in the speed range. For the rated-thrust flap-retracted condition with the airplane trimmed at high speeds (over 300 miles per hour), the control-force response will probably be satisfactory for a reasonable range of speeds deviating from the trim speed. An unstable variation of stick force with indicated airspeed within the important speed range is indicated for the wave-off and climb conditions.

A few calculations were made to determine the effect of changes of thrust and flap deflection on the elevator stick forces. It was found that with the tab fixed for trim at 120 miles per hour for the zero-thrust, flap-deflected condition, the changes in control force never exceed the 35-pound limit, accepted in the Army requirements, when any combination of engine operation or flap deflection is suddenly applied.

Additional computations were made to estimate for steady turning flight the variations of stick force and elevator deflection per g with center-of-gravity position for sea-level operation. The results in figure 21 for the engines-inoperative condition with flaps neutral are based on a maneuver which would develop the normal load factor of 9 at a lift coefficient of 1.0. The curve for this condition shows a change of 2.15 pounds per g for a 1 percent center-of-gravity shift and a maneuver point of 34.4 percent of the mean aerodynamic chord. At the normal center-of-gravity location a value of 15.5 pounds per g is indicated. This gradient is higher than that generally accepted for a fighter airplane.

Analysis of Exhaust-Jet Effect

In the analysis of the test data, certain trends and characteristics of the results indicated that the jet action of the exhaust introduced destabilizing effects of the longitudinal stability of the airplane. Some correlation of the test results has been made in order to determine the extent of the jet effect on the air flow at the tail and the more significant results are discussed in the following sections.

The results shown in the foregoing sections and especially the data in figure 14 indicate that the effectiveness of the elevator, which is a direct measure of the dynamic-pressure ratio at the tail plane, is practically unchanged by a large range of thrust conditions and flap deflection. Since the ratio q_t/q_o is substantially unaffected by the jet, it may therefore be concluded that any change in stability is caused either by the thrust moment of the jet or by a change in downwash at the tail.

The over-all change of stability due to rated-thrust operation (flaps up or down 45°) is shown by the stick-fixed neutral-point results in figure 17. The forward shift in neutral-point location due to rated-thrust operation with flaps retracted is nearly a constant value (about 7 percent M.A.C.) throughout the C_L range. It is also shown that with flaps deflected 45° the forward shift is approximately constant (5 percent M.A.C.) only to a C_L of about 0.7 and at lift coefficients greater than 0.7 the destabilizing effect of the jet is considerably greater.

In order to determine approximately the relative contribution of the thrust moment and the downwash angle to the total moment resulting from rated-thrust engine operation, comparisons are shown of experimental and theoretical estimated increments of pitching-moment coefficient over the C_L range in figure 22. The estimated total increments of pitching moment, which were calculated from theoretical estimated downwash angles at the tail for a jet source located at the wing trailing edge, were based on an unpublished theoretical analysis. For the flaps-retracted condition there is good agreement between the estimated and experimental results and for this condition it is shown that about 70 percent of the total change in stability is caused by the thrust moment of the jet. With the flaps deflected 45°, however, there is a marked increase of experimental total moment coefficient as compared to the estimated results for lift coefficients greater than about 0.65. Since the experimental thrust-moment increments are substantially the same as the estimated thrust-moment results, the large change in the total increment for this flap-deflected condition at high-lift coefficients is attributed to a larger change in downwash at the tail than would be expected. For this case it is estimated that about 75 percent of the total change in stability is caused by the thrust moment of the jet for lift coefficients up to about 0.65. At greater lift coefficients, C_L of 1.0, for example, it is found that only about 21 percent of the total destabilizing moment is caused by the thrust action of the jet.

To supplement the foregoing discussion, the downwash angles at the tail are presented in figure 23 to show the effect of rated-thrust engine operation for both the flap-neutral and flap-deflected conditions. There is shown a marked difference in the experimental and theoretical increments in downwash due to engine operation with the flaps deflected. It is believed that much of this increase in downwash at the tail results from a reduction of flow separation at the nacelle inlets and at the wing-nacelle fillet. There is a relatively large destabilizing shift in neutral point due to rated-thrust operation for the flap-deflected condition at high-lift coefficients;

however, it should be noted that for the engines-inoperative condition there is a large degree of stability and as a result the airplane is about neutrally stable for the rated-thrust flap-deflected condition at low speeds.

Lateral Stability and Control

Aerodynamic characteristics in yaw.- The results of tests made with the airplane in yaw, the landing flaps retracted and deflected 45°, and with the engines inoperative are given in figure 24. These results show the variations of C_n, C_Y, C_l, and C_{h_r} with δ_r for angles of yaw of 0°, 3°, 6°, 9°, and 10.6°. Similar results are given in figure 25 for an angle of attack of 3.9° with the engines operating at the rated-thrust condition ($T_c' = 0.09$) and with the landing flaps retracted. The aerodynamic characteristics of the airplane at zero yaw with only the left engine operating are shown in figure 26.

In order to determine the effects of angle of yaw, angle of attack, flap deflection, and rated-thrust engine operation on the rudder characteristics, the slopes of the curves of C_n, C_Y, C_l, and C_{h_r} against δ_r, measured at $\delta_r = 0$, are presented in figure 27. It is seen that within the ranges tested the effects of the conditions mentioned above on the slopes of these curves are negligible although there is a small degree of variation in the values of $dC_{h_r}/d\delta_r$. The average values of the slopes $dC_n/d\delta_r$, $dC_Y/d\delta_r$, $dC_l/d\delta_r$, and $dC_{h_r}/d\delta_r$ for the conditions tested are approximately -0.0007, 0.0015, 0.0001, and -0.0125 per degree, respectively. The results shown for the engine-operating condition indicate that the effect of the exhaust jet on the rudder effectiveness is negligible.

The rudder-effectiveness data of figures 24 and 25 have been cross-plotted for $\delta_r = 0$ to show the effects of yaw on the aerodynamic characteristics of the airplane and these results are given in figure 28. The directional-stability parameter $dC_n/d\psi$, measured between $\psi = 0°$ and 10°, is about -0.0010 per degree for the engines-inoperative flaps-retracted condition at an α of -0.5°.

For the engines-inoperative flaps-deflected condition at an α of 5.7° the directional stability of the airplane will be low; $dC_n/d\psi$ is reduced to approximately zero at angles of yaw between 2° and 8°. The lateral-force effect $dC_Y/d\psi$ with the engines inoperative is decreased about one-half from a value of 0.0055 per degree at an α of -0.5° (flaps retracted) to about 0.0025 per degree at an α of 11.8° (flaps deflected 45°). The dihedral effect $dC_l/d\psi$ shows an increase with flap deflection from 0.0010 per degree for the engines-inoperative flaps-retracted condition at $\alpha = -0.5^\circ$ to approximately 0.0017 for the engines-inoperative flaps-deflected condition at $\alpha = 5.7^\circ$. For the latter condition, this value corresponds to an effective dihedral angle of about 7.5°. It should be noted that at an angle of attack of about 5.7°, with the engines inoperative and with flaps deflected 45°, a condition of lateral-oscillatory instability may occur since the value for $dC_l/d\psi$ (0.0017) is considerably greater than that for $dC_n/d\psi$ (approximately zero) for angles of yaw between 2° and 8°.

The values of $dC_n/d\psi$, $dC_l/d\psi$, and $dC_Y/d\psi$ for the engine-operative condition tested are -0.0012, 0.00265, and 0.0060, respectively, as compared to the values -0.0009, 0.0014, and 0.0050 for the engines-inoperative condition at the same angle of attack of 3.9°. Although the operation of the jet units at rated-thrust influences the dihedral effect to a larger extent than either the directional stability or the lateral-force effect, there are not sufficient engines-operative test results from which to draw any definite conclusions as to the effects of the jet on these parameters.

The results of figure 29 indicate that the longitudinal trim changes due to yaw will be negligible for yaw angles up to at least 10°. There is some evidence that the wing may begin to stall for yaw angles greater than 10° with the airplane in the landing attitude ($\alpha = 11.8^\circ$, $\delta_f = 45^\circ$) and with the engines inoperative.

Rudder-control characteristics.- The rudder-control characteristics of the airplane in yaw were obtained by cross-plotting for $C_n = 0$ the test results of figures 24 and 25. The variations of rudder deflection for trim with angle of yaw for the conditions tested are shown in figure 30. The rudder deflections are conservative since the effects of aileron control, which would tend to decrease the amount of rudder required for trim in yaw, are not included. These curves of rudder deflection for trim against angle of yaw show stable variations for all conditions tested although there is indicated a marked reduction in directional stability as the angle of attack is decreased and the flaps are deflected 45°. With the engines inoperative, the rudder deflection required to trim the airplane at $\psi = 10^\circ$ is reduced from about 15° at an α of -0.5° with the flaps retracted to about 5.5° at an α of 5.7° with the flaps deflected 45°. For this latter condition it will be noticed that the change in rudder deflection for trim with angle of yaw is very small within the yaw-angle range from about 3° to 8°. The effect of rated-thrust engine operation at an angle of attack of 3.9° with the flaps retracted is to increase slightly the trim rudder settings for a given angle of yaw. With the airplane in a high-speed condition, with only one engine operating at rated thrust, a very small rudder deflection will trim out the yawing moment produced by the single jet. However, with the airplane in low-speed flight and with one engine developing rated thrust, the unbalanced yawing moment due to the single jet is estimated to be considerably greater. At a flight speed of 100 miles per hour, for example, a rudder deflection of about 10° will be required to trim out the resulting yawing moment ($C_n = 0.006$). The pedal force for this condition is estimated to be about 30 pounds.

In order to show the rudder-free characteristics of the airplane, the test data have been cross-plotted to obtain the variation of $C_{n\left(C_{h_r}=0\right)}$ with angle of yaw and the results are given in figure 31. All these curves show stable rudder-free characteristics. It may also be deduced from figure 31 that at least for the limited yaw range tested stable rudder-pedal movements will be required to trim out the airplane yawing moments.

The variation of rudder-pedal force with angle of yaw for the conditions tested are given in figure 32 for a speed range from about 97 to 180 miles per hour. As previously discussed, stable pedal-force variations with yaw are shown by increased rudder-pedal forces as the yaw angle is increased. It should be noted that high forces are required for trim at 10° yaw (about 195 pounds) at a flight speed of 180 miles per hour with engines inoperative or operating at rated thrust (flaps neutral). Application of rated thrust for the flap-neutral condition at 180 miles per hour results in only minor changes in the variation of rudder force with yaw. As the speed of the airplane is reduced to about 100 miles per hour for the engines-inoperative flaps-deflected condition the pedal force is reduced to about 40 pounds with the airplane yawed 10°.

These results show a definite tendency for poor lateral stability and control with the airplane in a moderate sideslip and at lift coefficients in the neighborhood of 0.8 with the engines inoperative and landing flaps deflected 45°. At lift coefficients greater than 0.8, however, the directional stability (rudder fixed and rudder free) is increased somewhat and should result in some improvement in directional control for an engines-inoperative landing. The data are not sufficiently complete to afford an estimate of the effect of engine operation on the directional control although there is some indication of a stabilizing influence due to engine operation.

Aileron effectiveness and control characteristics.- The effects of aileron deflection on the airplane yawing and rolling moments are shown in figure 33 for a range of angles of attack and for flap deflections of 0° and 45°. The effectiveness of the ailerons $dC_l/d\delta_{a_L}$, measured at $\delta_{a_L} = 0°$, is practically unchanged over the large range of angles of attack and the two flap deflections tested. With the flaps in neutral, $dC_l/d\delta_{a_L}$ at $\alpha = -0.5°$ is about 0.0015 per degree and decreases slightly to about 0.0013 per degree at an α of 13.4°. The values of $dC_l/d\delta_{a_L}$ with the flaps deflected 45° may be considered the same as for the flaps-neutral test results. The rate of change of yawing-moment coefficient with aileron deflection for the flaps-neutral condition increases with increasing angle of attack; such that, the adverse yawing-moment coefficient due to full-aileron deflection $(\Delta\delta_a = 30°)$ is 0.001 at $\alpha = -0.5°$ and is 0.011 at $\alpha = 13.4°$. The adverse yawing-moment coefficient due to total aileron deflection with the flaps deflected 45° is 0.004 at $\alpha = 3.2°$ and is 0.009

at $\alpha = 12.7^{\circ}$. For the flaps-deflected condition at $\alpha = 12.7^{\circ}$ (95 miles per hour) a rudder deflection of 15° would be necessary to trim out the adverse yawing-moment coefficient resulting from full-aileron deflection.

Although hinge-moment data are not available, a few of the lateral-control characteristics of the airplane can be evaluated from these aileron-effectiveness tests. The control effectiveness of the ailerons can be given in terms of the helix angle generated by the wing tip $pb/2V$ for any aileron deflection. The value of $pb/2V$ based on the total measured rolling moment developed by maximum aileron deflection is calculated to be about 0.066 for the high-speed flight condition ($\alpha = -0.5^{\circ}$, $\delta_f = 0^{\circ}$) and 0.057 for the landing condition ($\alpha = 12.7^{\circ}$, $\delta_f = 45^{\circ}$). The factor of 0.8 which approximates the effects of adverse yaw at low speeds and compressibility and wing twist at high speeds has been applied to the wind-tunnel results. It should be noted that these values of $pb/2V$ are considerably lower than the minimum Army requirement of 0.09. It is estimated that the maximum rolling velocity developed by full-aileron deflection at an indicated airspeed of 300 miles per hour is approximately 73° per second at sea level, provided the $pb/2V$ of 0.066 is attainable at that speed for a limiting stick-force requirement of 50 pounds.

SUMMARY OF RESULTS

The more important information relative to the static stability and control characteristics of the Bell YP-59A airplane as determined from full-scale tunnel tests are summarized as follows:

1. With the center of gravity located at 27.2 percent mean aerodynamic chord, the airplane exhibits neutral longitudinal stability (stick fixed), for rated-thrust low-speed flight with landing flaps deflected 45° and rated-thrust high speed with flaps neutral. For all other conditions tested the airplane is longitudinally stable for this normal center-of-gravity location.

2. Stable stick-force variations with speed occur for the engines-inoperative (flaps retracted and

deflected 45°), idling-thrust (flaps deflected 45°), and cruising-thrust (flaps retracted) conditions with the airplane trimmed for glide, landing, and cruising speeds, respectively, at sea level. The airplane will be unstable, stick free, for rated-thrust operation $\delta_f = 0^\circ$ between lift coefficients of about 0.35 to 0.95 and for rated-thrust operation $\delta_f = 45^\circ$ at lift coefficients greater than 0.8.

3. With the flaps retracted, there is about a 7 percent average forward shift in the stick-fixed neutral point due to rated-thrust engine operation over the C_L range. Of this total change in stability about 70 percent is caused by the thrust moment of the jet about the center of gravity of the airplane. The remainder is attributed to the inflow of the air at the tail due to the action of the jet. With the flaps deflected 45° there is approximately a constant 5 percent forward shift of the neutral point due to rated thrust operation up to a C_L of about 0.7. At a C_L of 1.0 for this condition it is estimated that only 21 percent of the total destabilizing moment is caused by the thrust moment of the jet. The remainder is believed to result from an increased angle of downwash at the tail due to the reduction of flow separation around the nacelles.

4. The dynamic pressure ratio at the tail is considered substantially unaffected by the action of the jet or by flap deflection.

5. For the normal center-of-gravity location the value of 15.5 pounds per g is considered to be a high stick-force variation for sea-level flight.

6. On the basis of test results, the directional stability of the airplane for some flight conditions is considered low. The slope of the yawing-moment coefficient curve $dC_n/d\psi$ for the engines-inoperative flaps-retracted condition at low angles of attack is about -0.0010 per degree and is decreased to about -0.0005 at an α of 11.8°. At an angle of attack of 5.7°, with the engines inoperative and flaps deflected 45°, the $dC_n/d\psi$ is about zero in the yaw-angle range from 2° to 8°.

7. With the engines inoperative, the dihedral effect $dC_l/d\psi$ increases from 0.0010 per degree with

flaps retracted at an α of -0.5° to about 0.0017 with flaps deflected 45° at an α of 5.7°. It is possible that at an angle of attack of 5.7° ($C_L = 0.8$), with the engines inoperative and flaps deflected 45°, the airplane may revert to a condition of lateral oscillatory instability since the effective dihedral is high, whereas, the directional stability is about neutral.

8. The variations of rudder-pedal force for trim with yaw are stable for all conditions tested.

9. The ailerons, as tested, have low-control effectiveness; the $pb/2V$ values of 0.066 and 0.057 are estimated for the high-speed and landing conditions, respectively.

Langley Memorial Aeronautical Laboratory
National Advisory Committee for Aeronautics
Langley Field, Va., January 18, 1945

REFERENCES

1. DeFrance, Smith J.: The N.A.C.A. Full-Scale Wind Tunnel. NACA Rep. No. 459, 1933.

2. Silverstein, Abe, and Katzoff, S.: Experimental Investigation of Wind-Tunnel Interference on the Downwash behind an Airfoil. NACA Rep. No. 609, 1937.

3. Theodorsen, Theodore, and Silverstein, Abe: Experimental Verification of the Theory of Wind-Tunnel Boundary Interference. NACA Rep. No. 478, 1934.

L-626

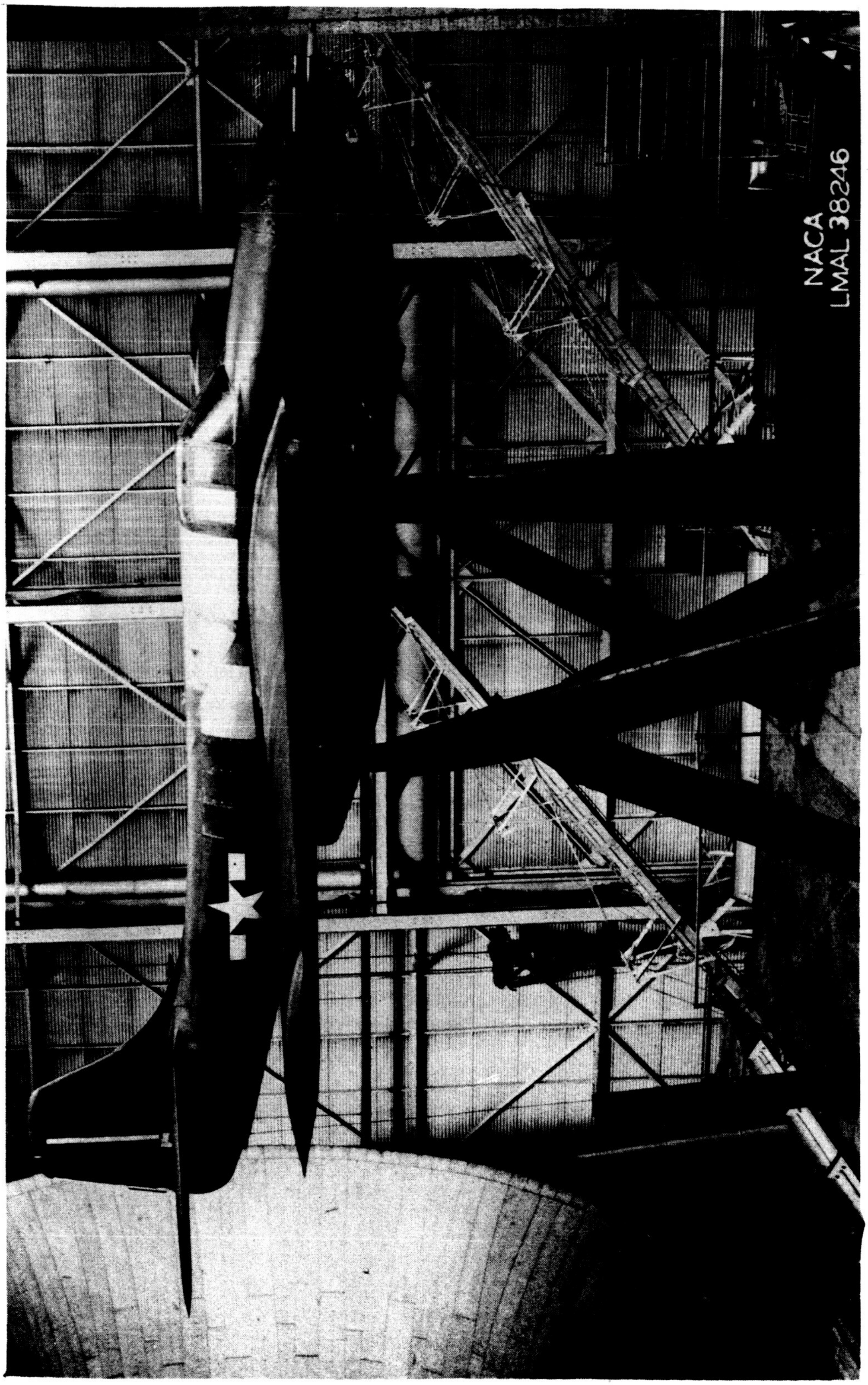

(a) Three-quarter front view.

Figure 1.- The Bell YP-59A airplane mounted on the Langley full-scale tunnel balance.

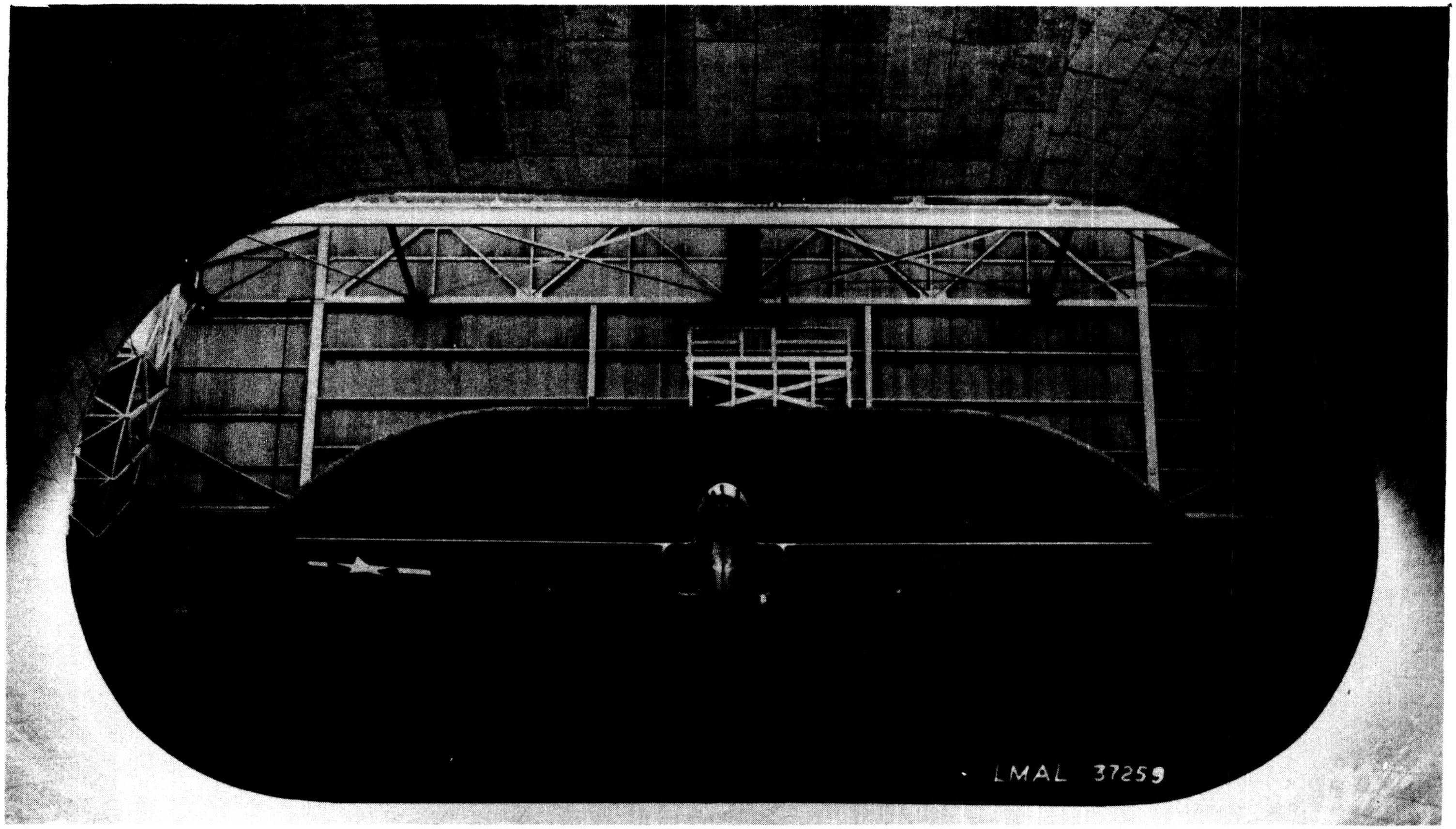

(b) Front view.

Figure 1.- Concluded.

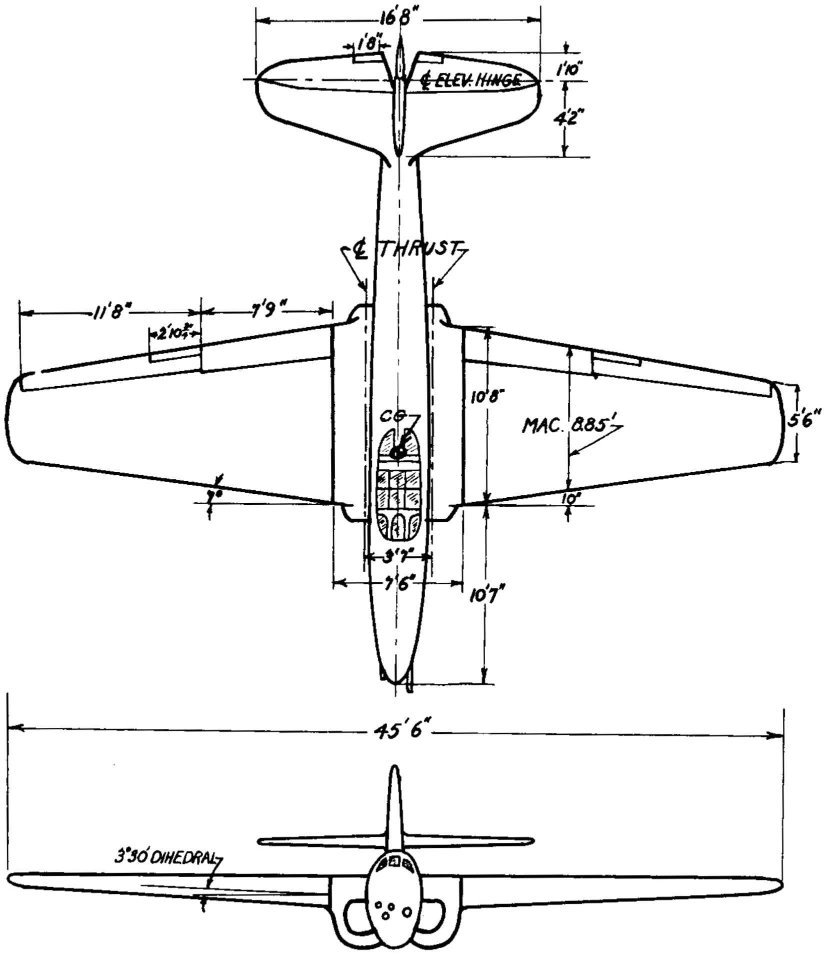

AREAS	Sq. Ft.
Wing area (including ailerons, flaps, fuselage)	385
Control surface areas	
Wing flaps	33.7
Ailerons	22.1
Horizontal tail (total)	69.8
Stabilizer	45.6
Elevator (aft of hinge)	20.1
Vertical tail (total)	29.9
Fin	16.6
Rudder (aft of hinge)	9.2
WEIGHTS	**Lbs.**
Normal gross weight	10,454
Normal empty weight	7,537

Airfoil section

Root	NACA	66,2-014
Tip	NACA	66,2-212

Normal c.g. location - 27.2 percent MAC

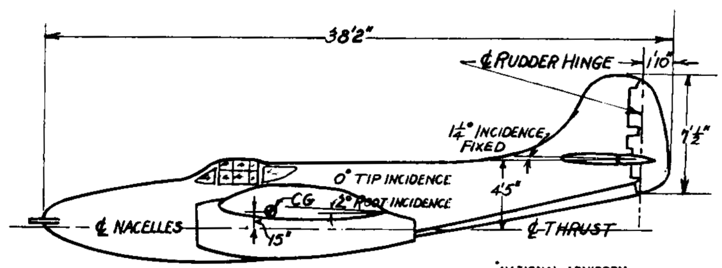

NATIONAL ADVISORY COMMITTEE FOR AERONAUTICS

Figure 2.- Three-view drawing of the YP-59A airplane.

Figure 3.- Rear view of the airplane, with the tail surfaces removed, showing the ventral fin installation.

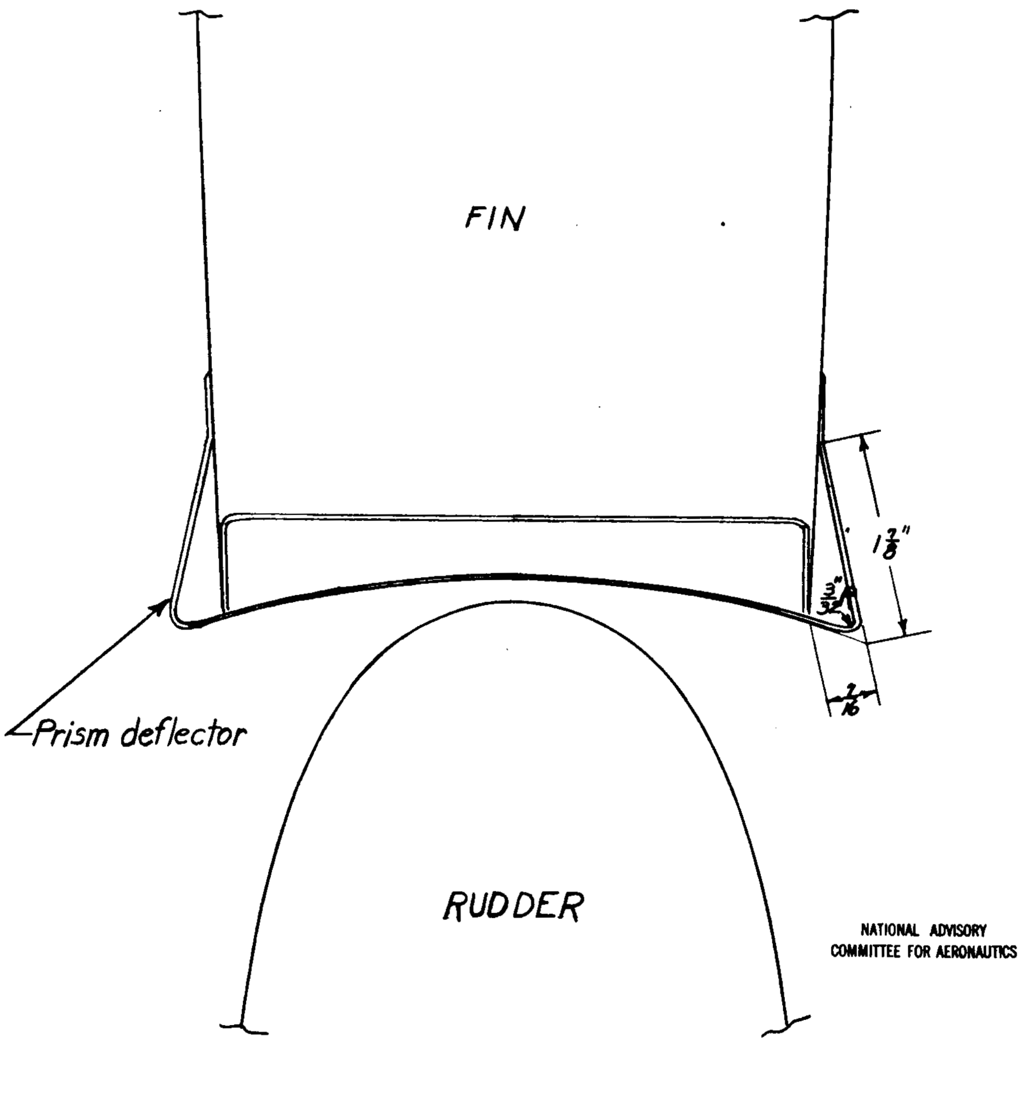

Figure 4.- Section of the fin and rudder showing the installation of the prism deflector at the fin trailing edge.

L-626

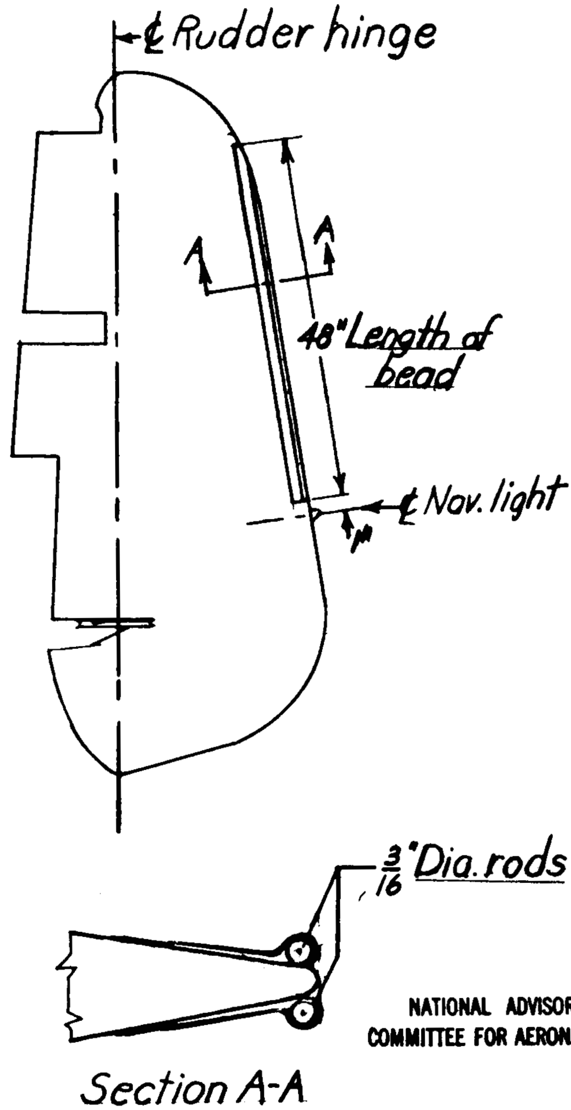

NATIONAL ADVISORY COMMITTEE FOR AERONAUTICS

Figure 5.- Sketch of the modified rudder with the trailing-edge beads installed.

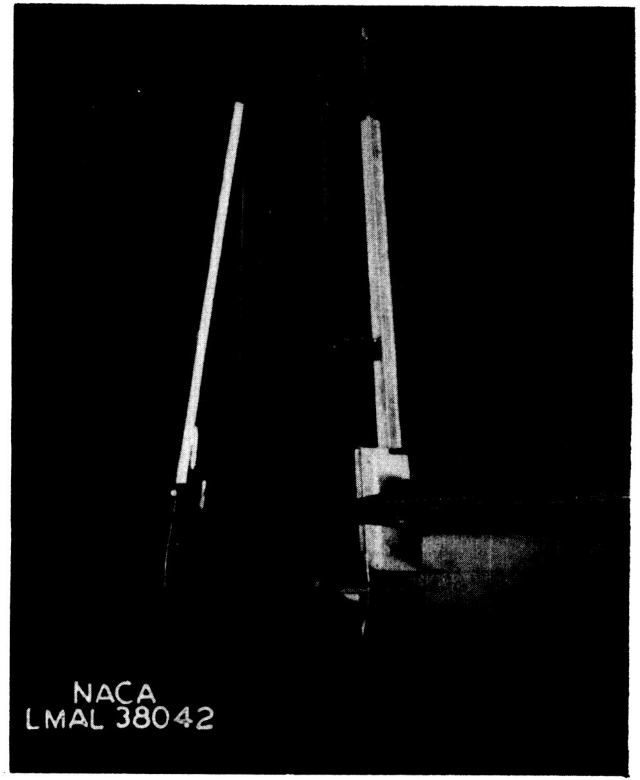

Figure 6.- Photograph of the vertical tail showing the prism deflector at the fin trailing edge and the bead installation at the rudder trailing edge.

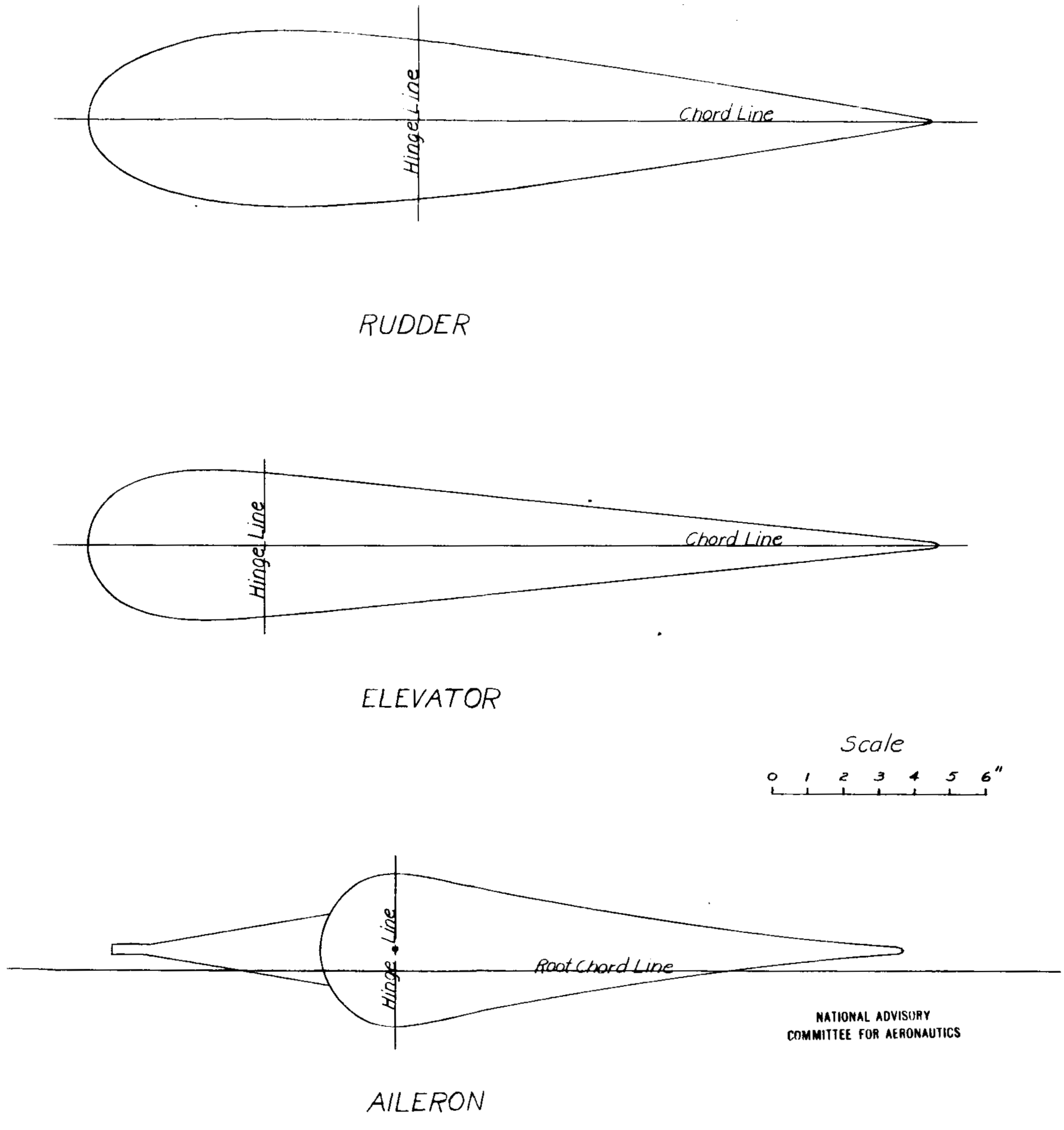

Figure 7 - Section views of the control surfaces on the YP-59A airplane.

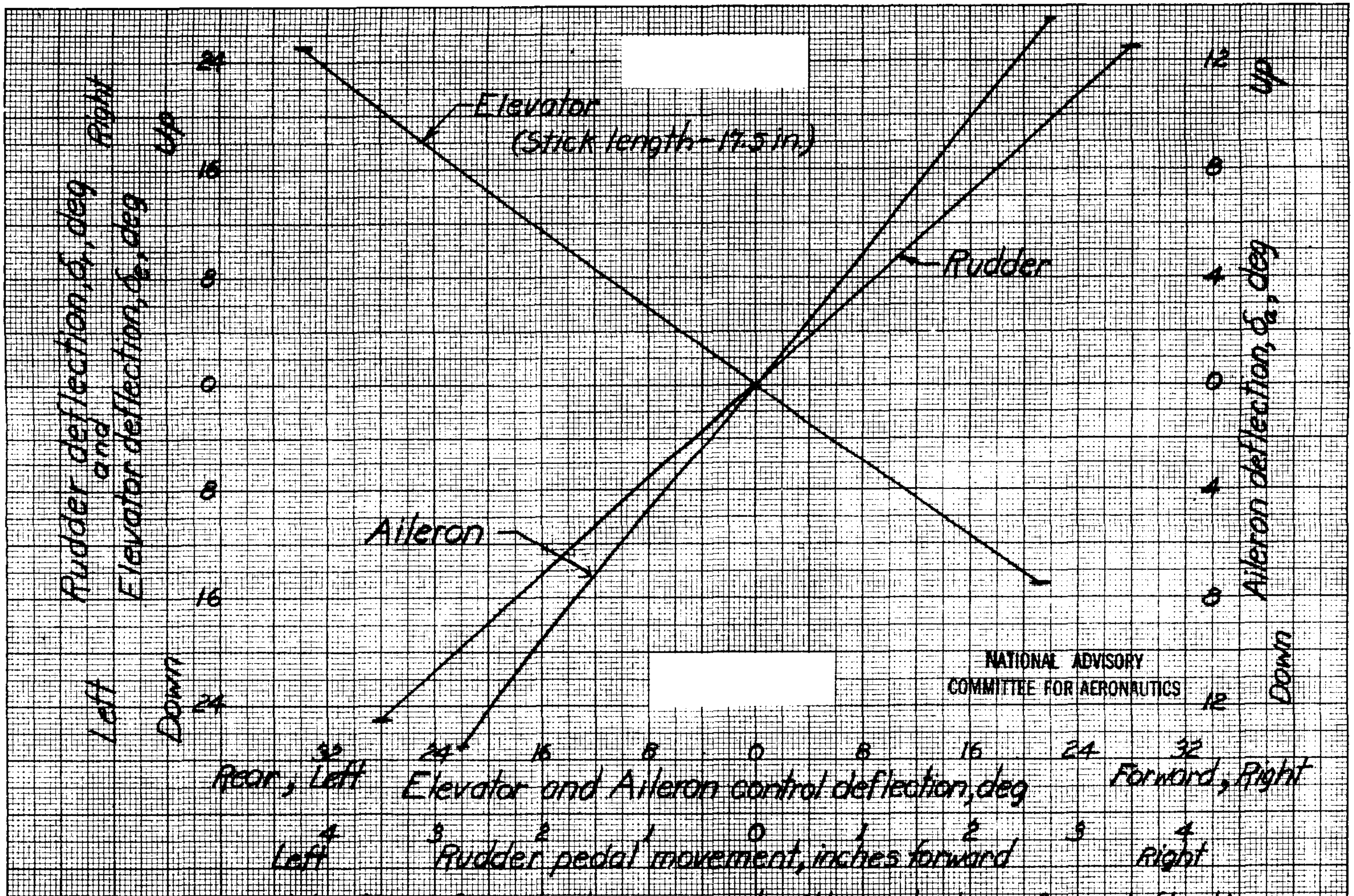

Figure 8.- Calibration of control movement with control surface deflection for the YP-59A airplane.

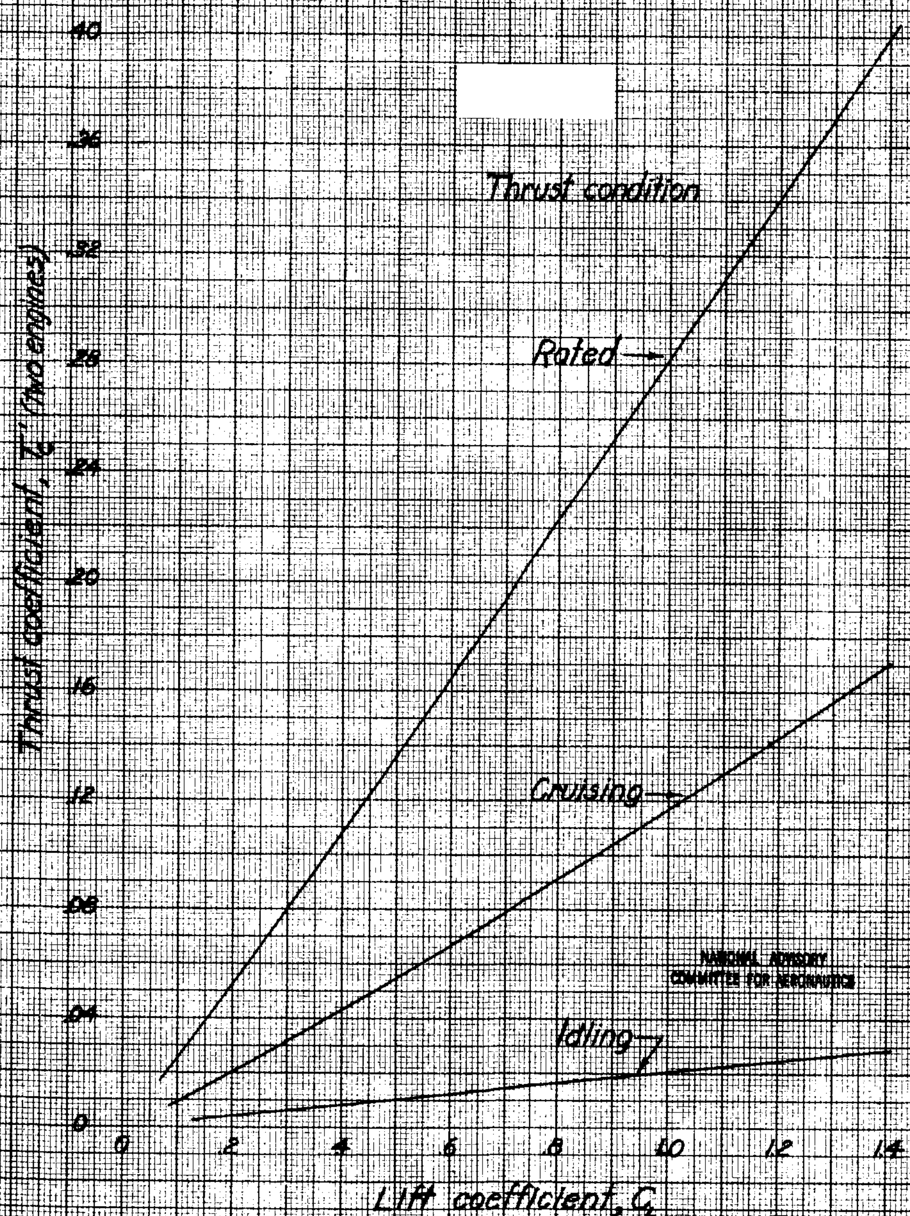

Figure 9.- Variation of T_c' with C_L for two engine operation at sea level. YP-59A airplane with G.E. type I-16 engines. W/S, 27.2.

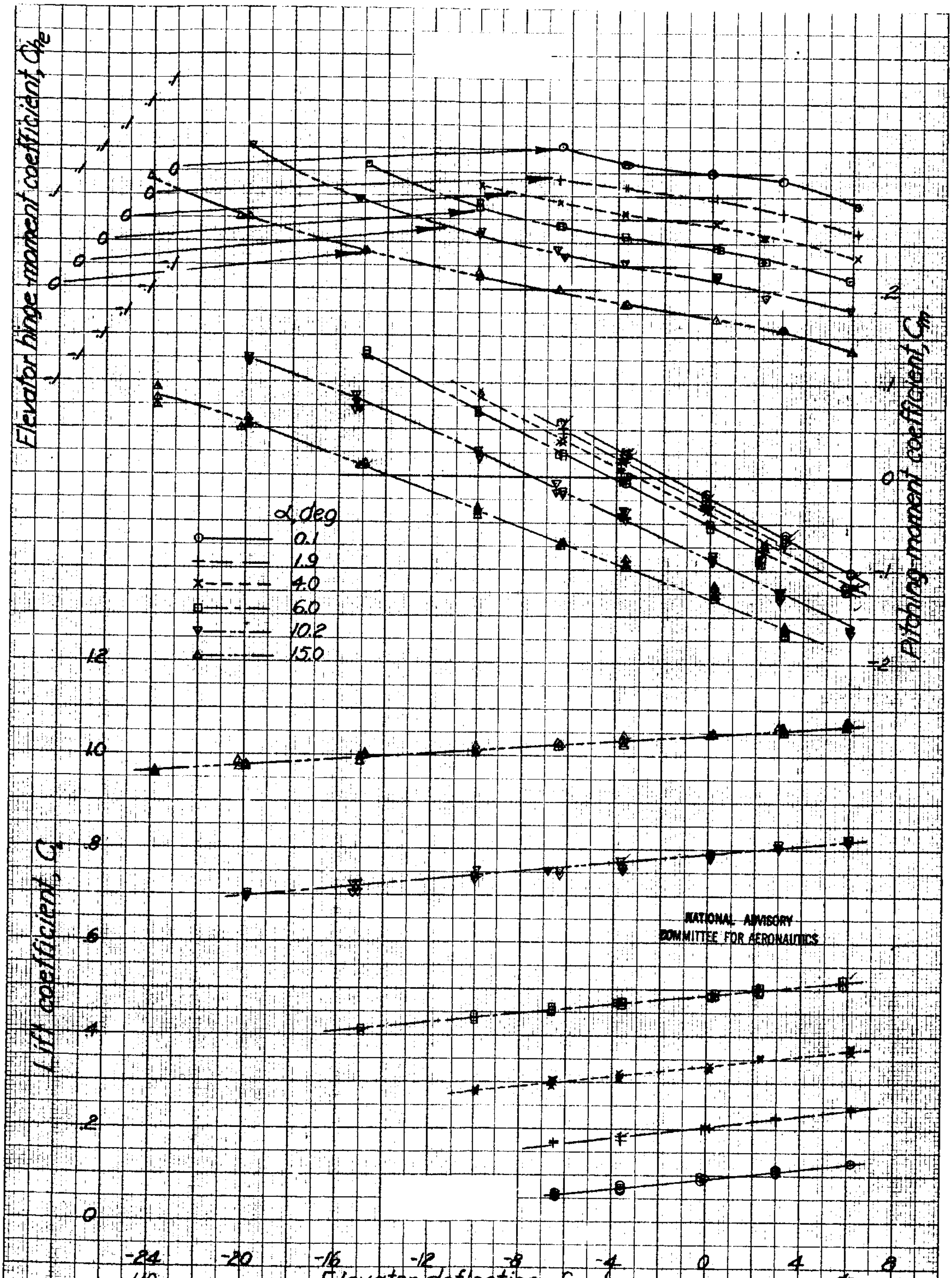

(a) Engines inoperative, δ_f, 0°

Figure 10.- Effect of elevator deflection on the aerodynamic characteristics of the YP-59 airplane. δ_n, 0°; i_t, 1.25°.

L-626

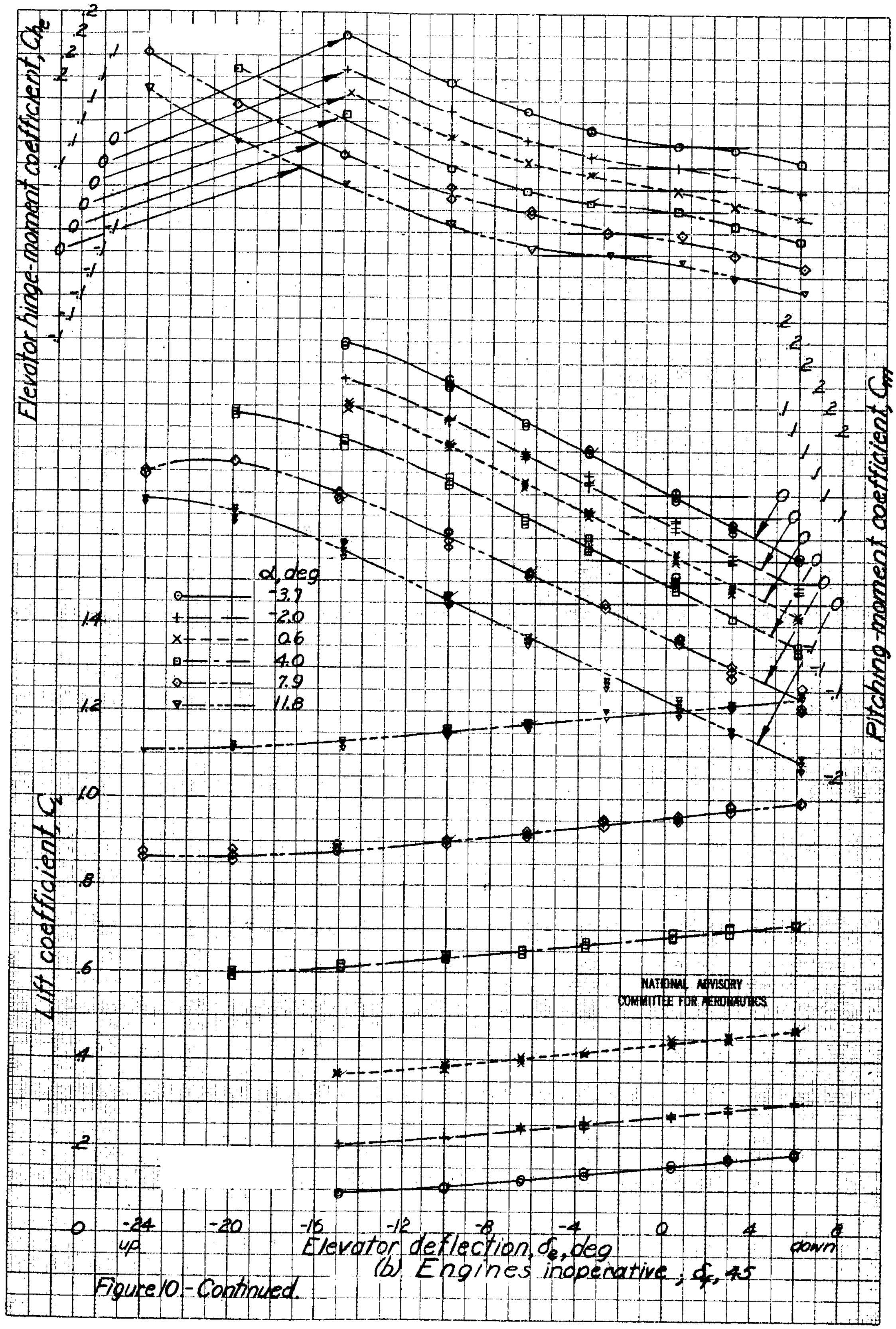

(b) Engines inoperative ; δ_f, 45

Figure 10.- Continued.

L-626

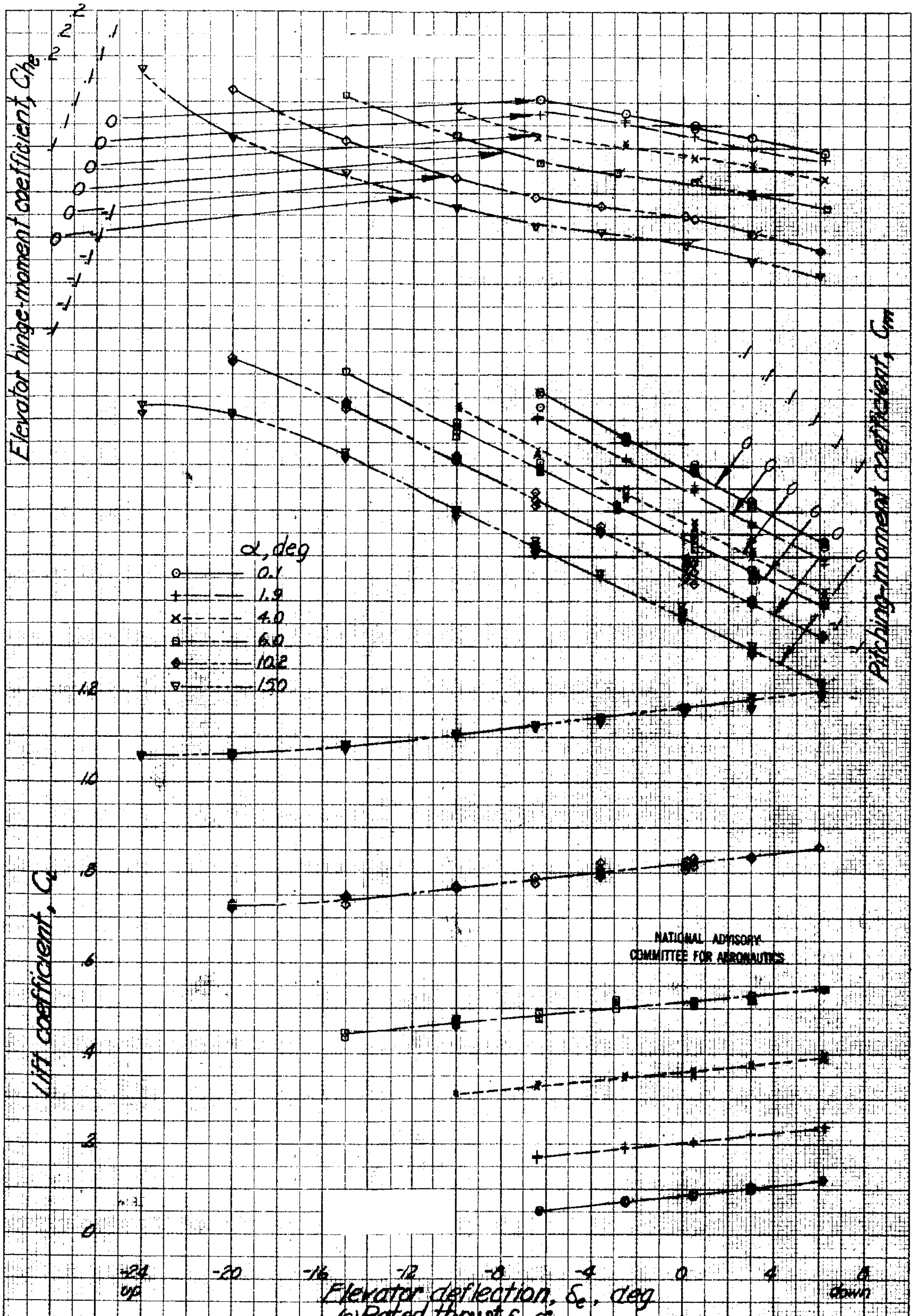

(c) Rated thrust, δ_f, 0°

Figure 10.- Continued.

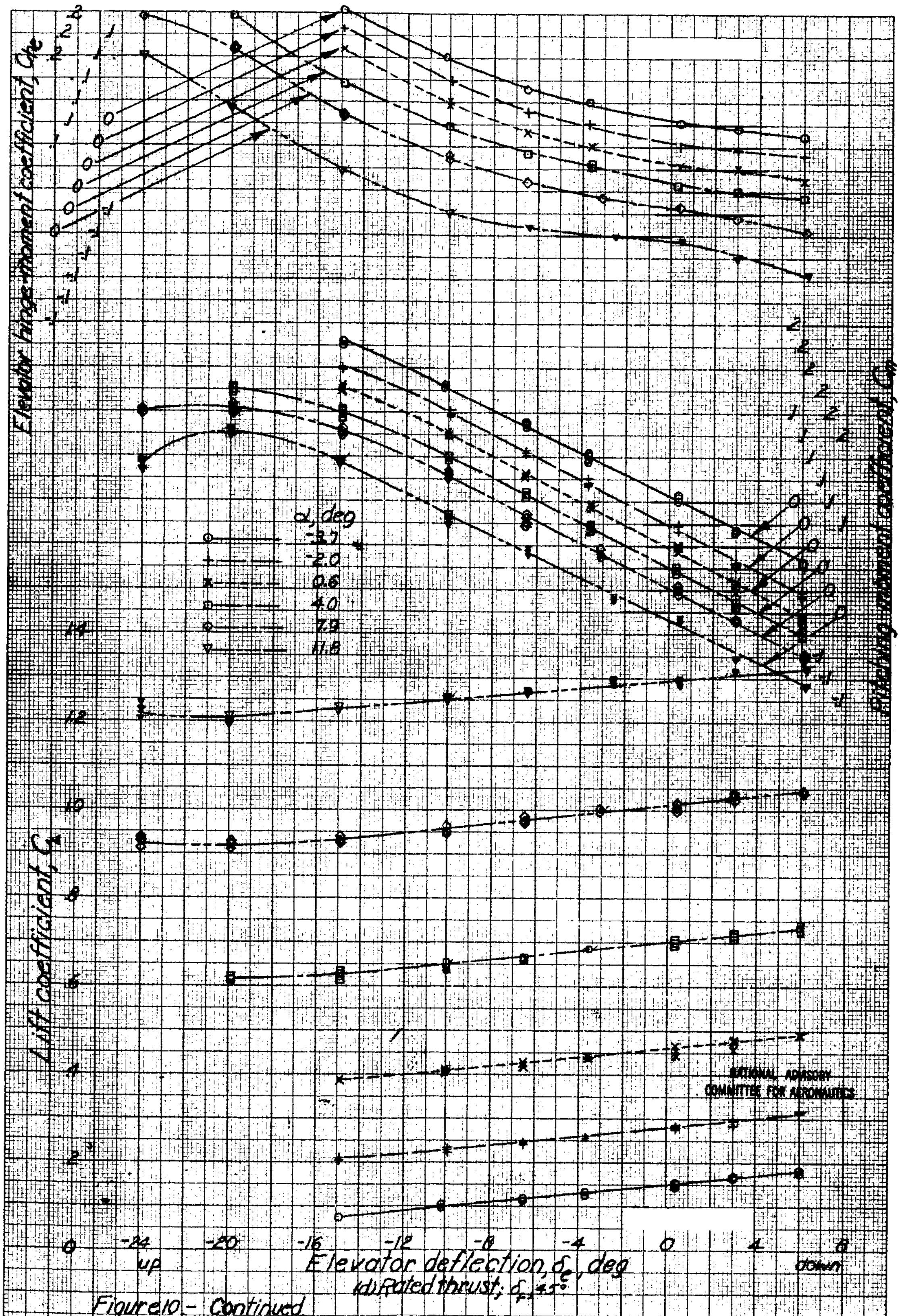

Figure 10 - Continued.

L-526

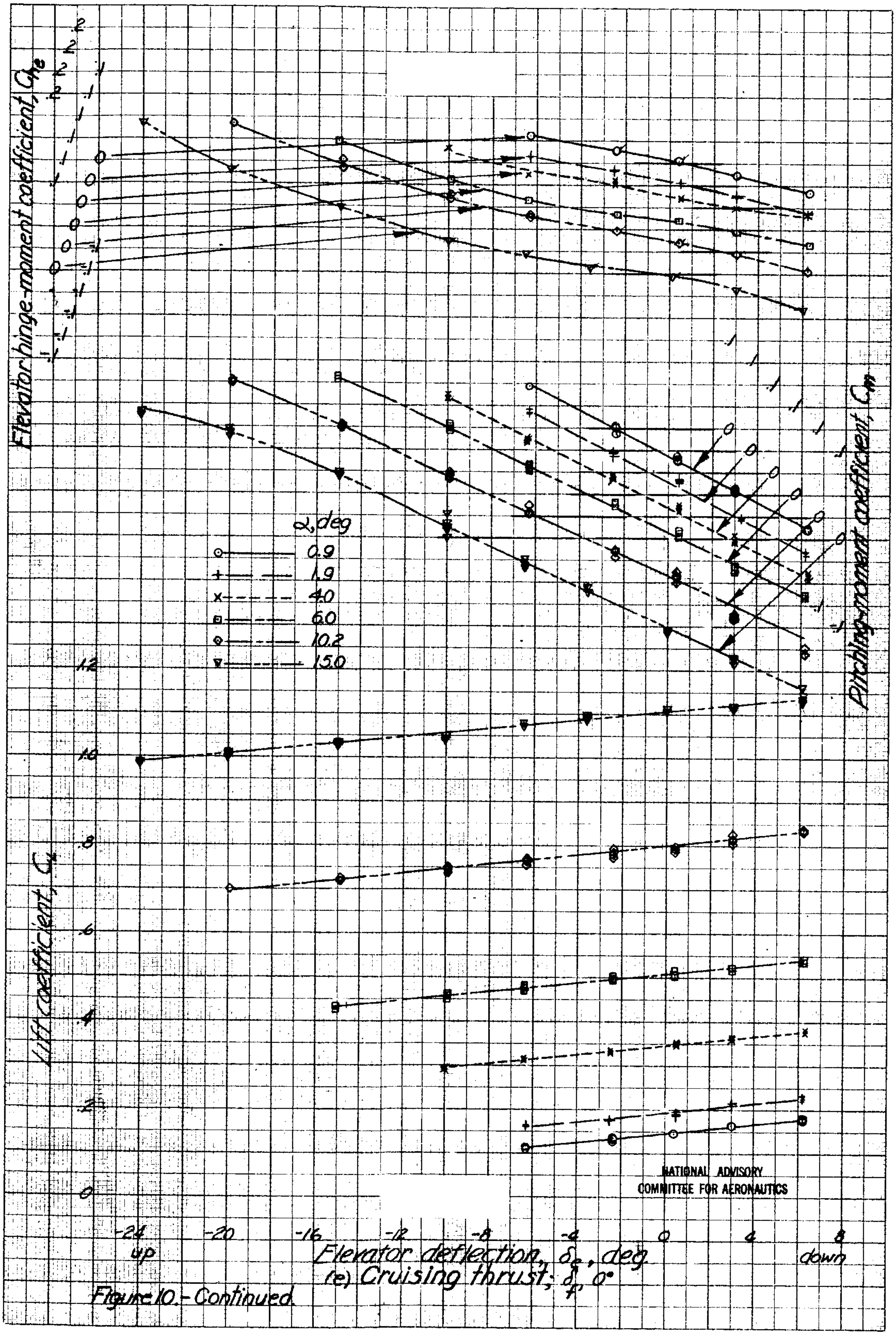

(e) Cruising thrust; δ_f, 0°

Figure 10.- Continued.

L-626

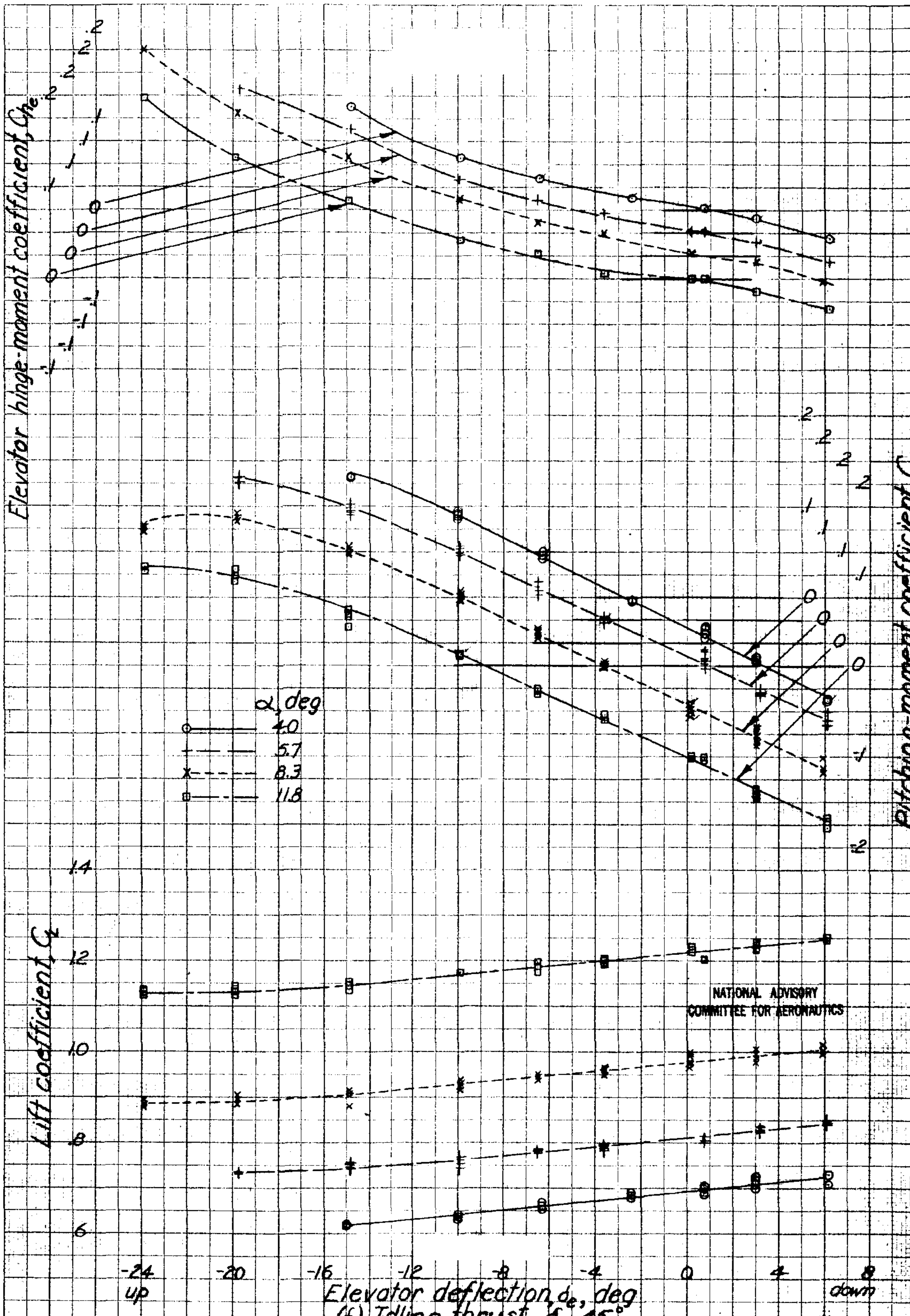

(f) Idling thrust; δ_f, 45°

Figure 10 - Concluded.

L-626

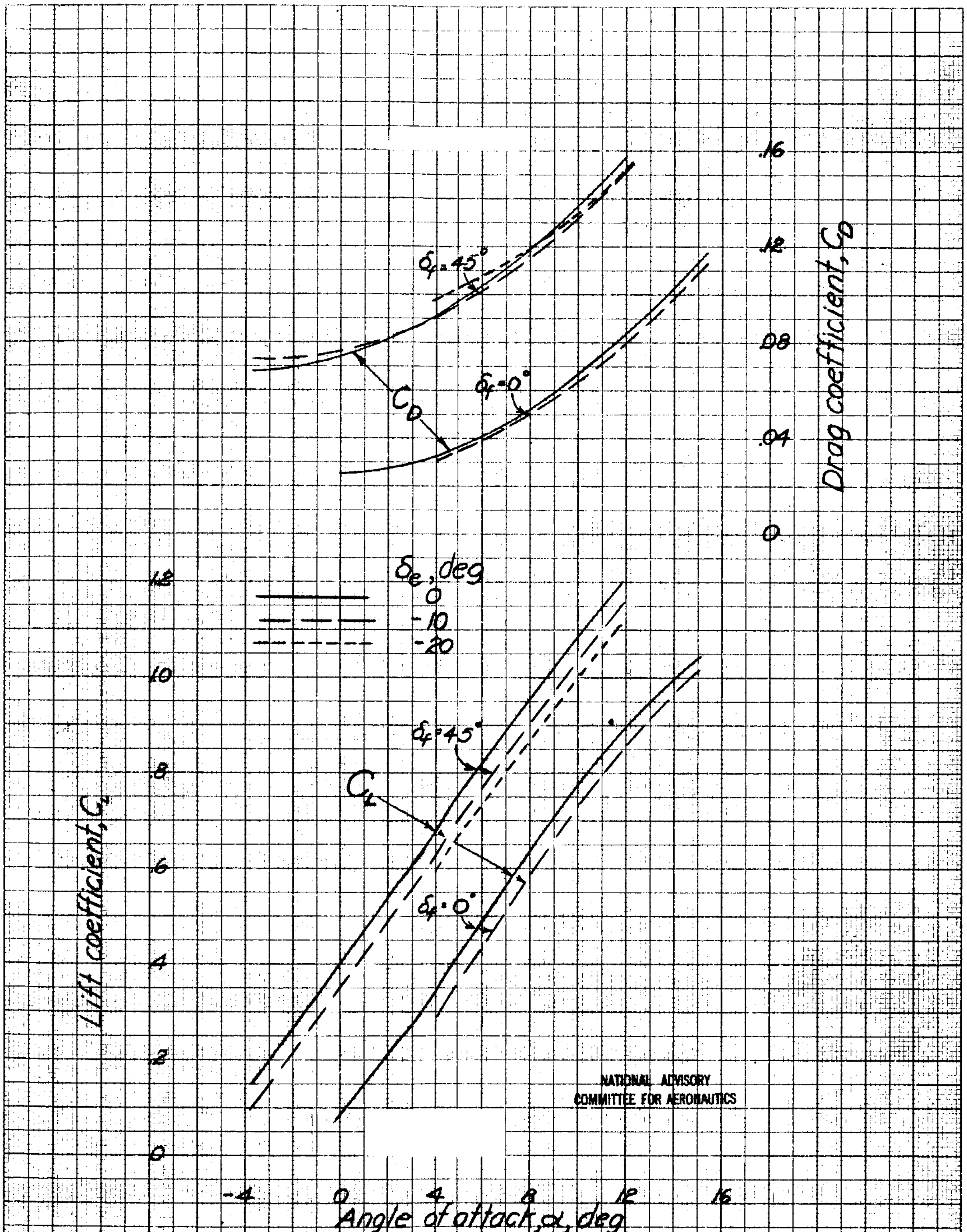

(a) Engines inoperative

Figure 11.- Variation of C_L and C_D with angle of attack for different operating conditions.

L-626

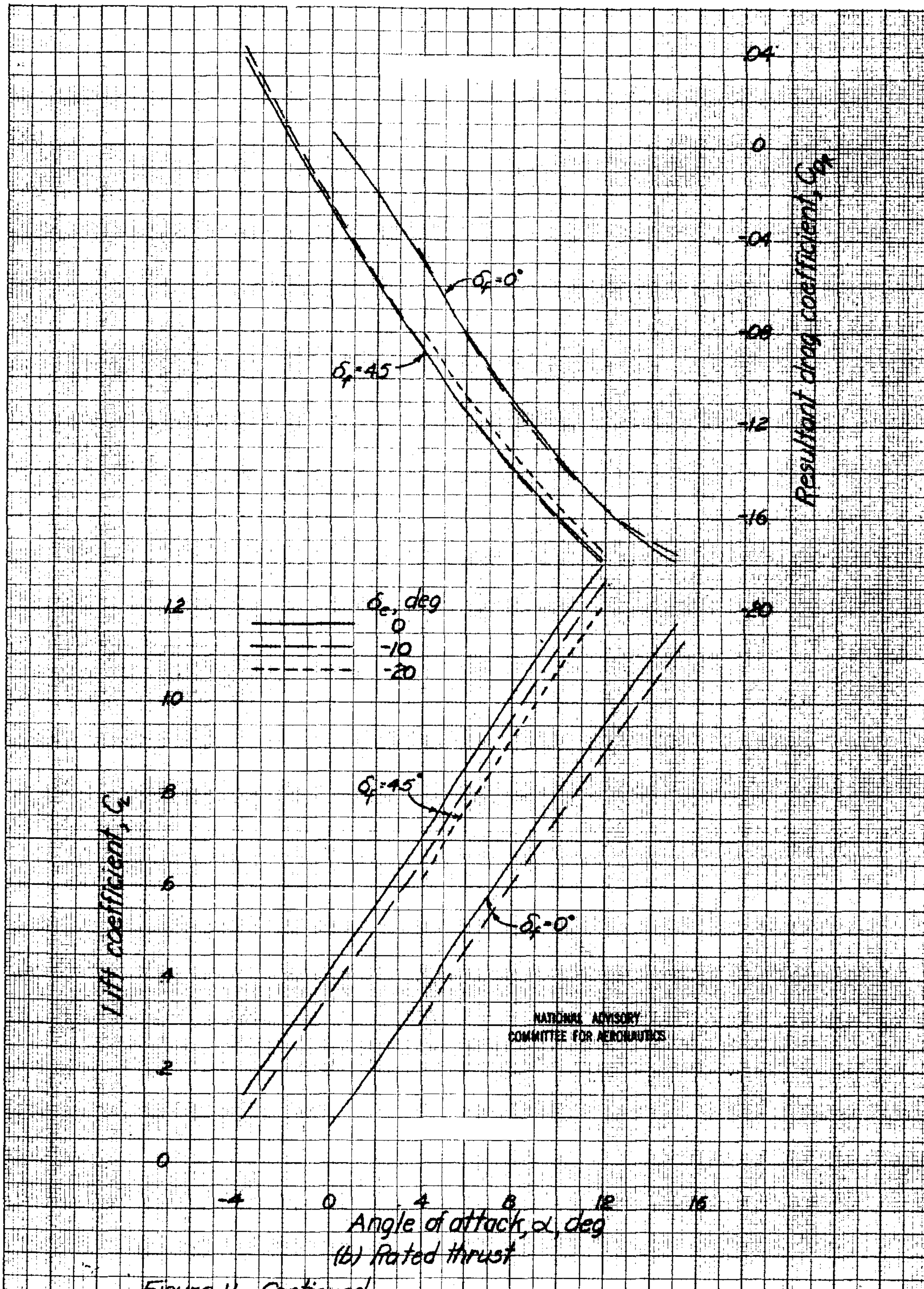

(b) Rated thrust

Figure 11.- Continued.

L-626

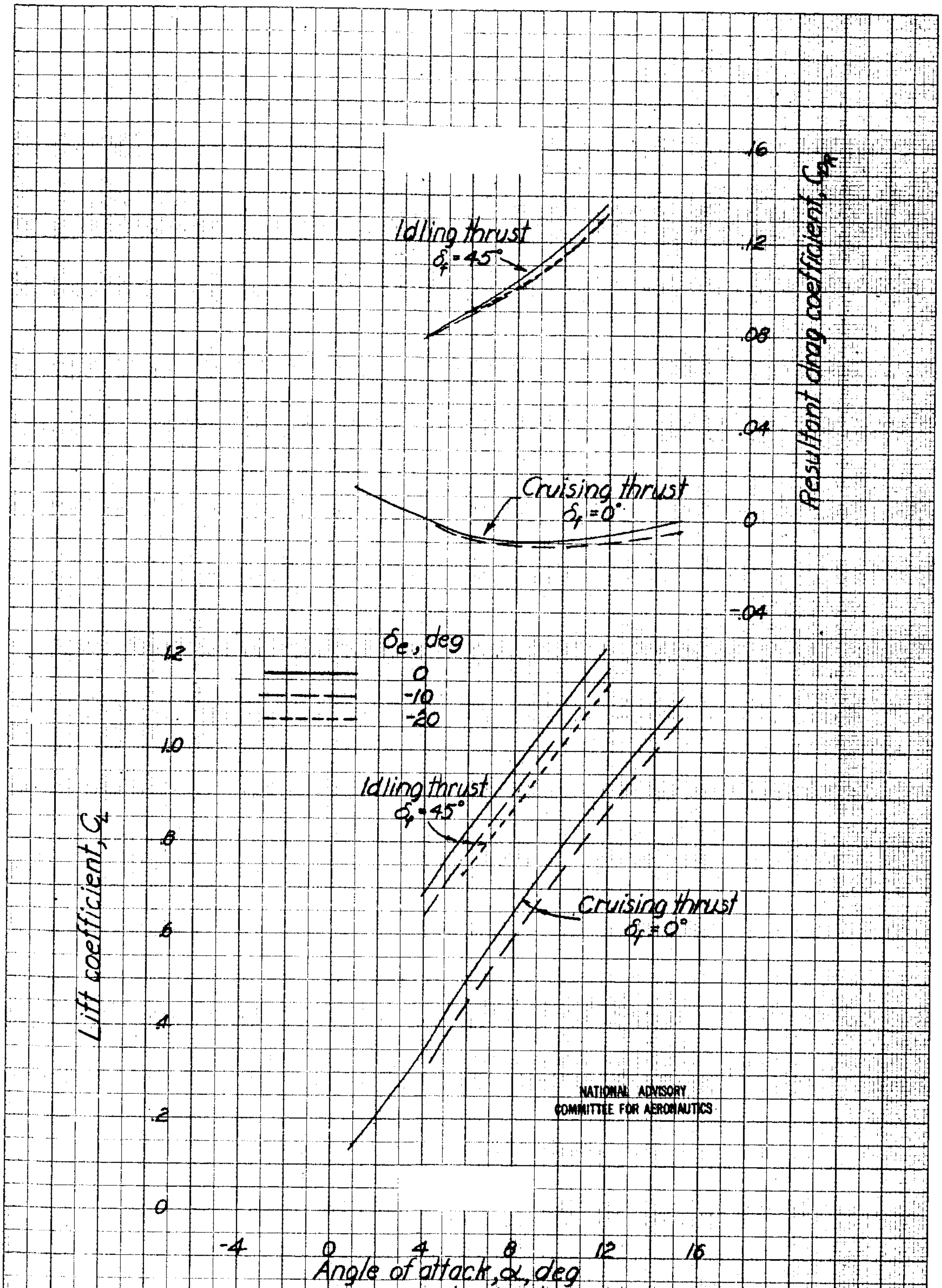

(c) Cruising and Idling thrust

Figure 11.- Concluded.

L-626

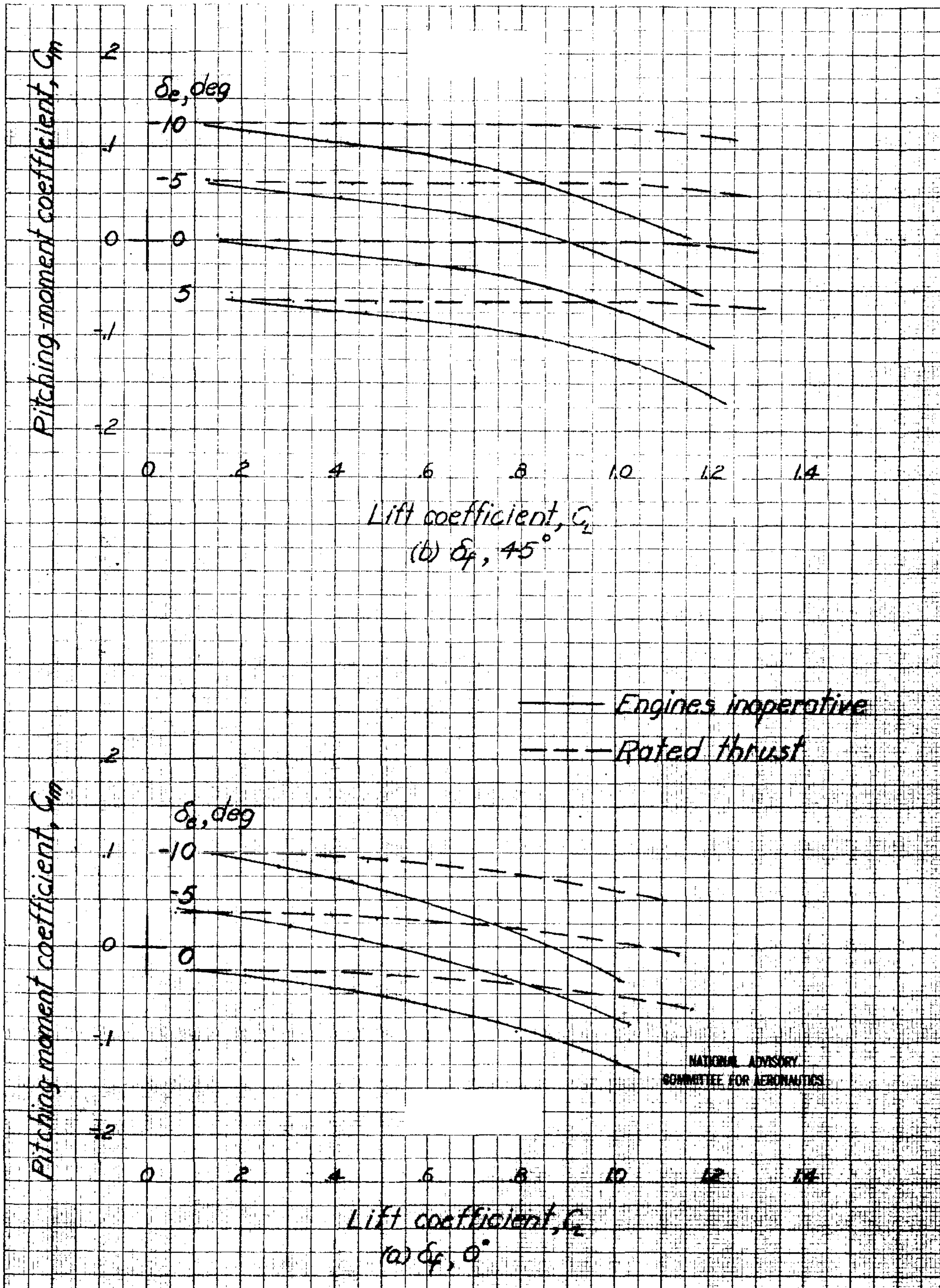

Figure 12.- Effect of rated thrust operation and flap deflection on the variation of C_m with C_L. i_t, 1.25°.

L-626

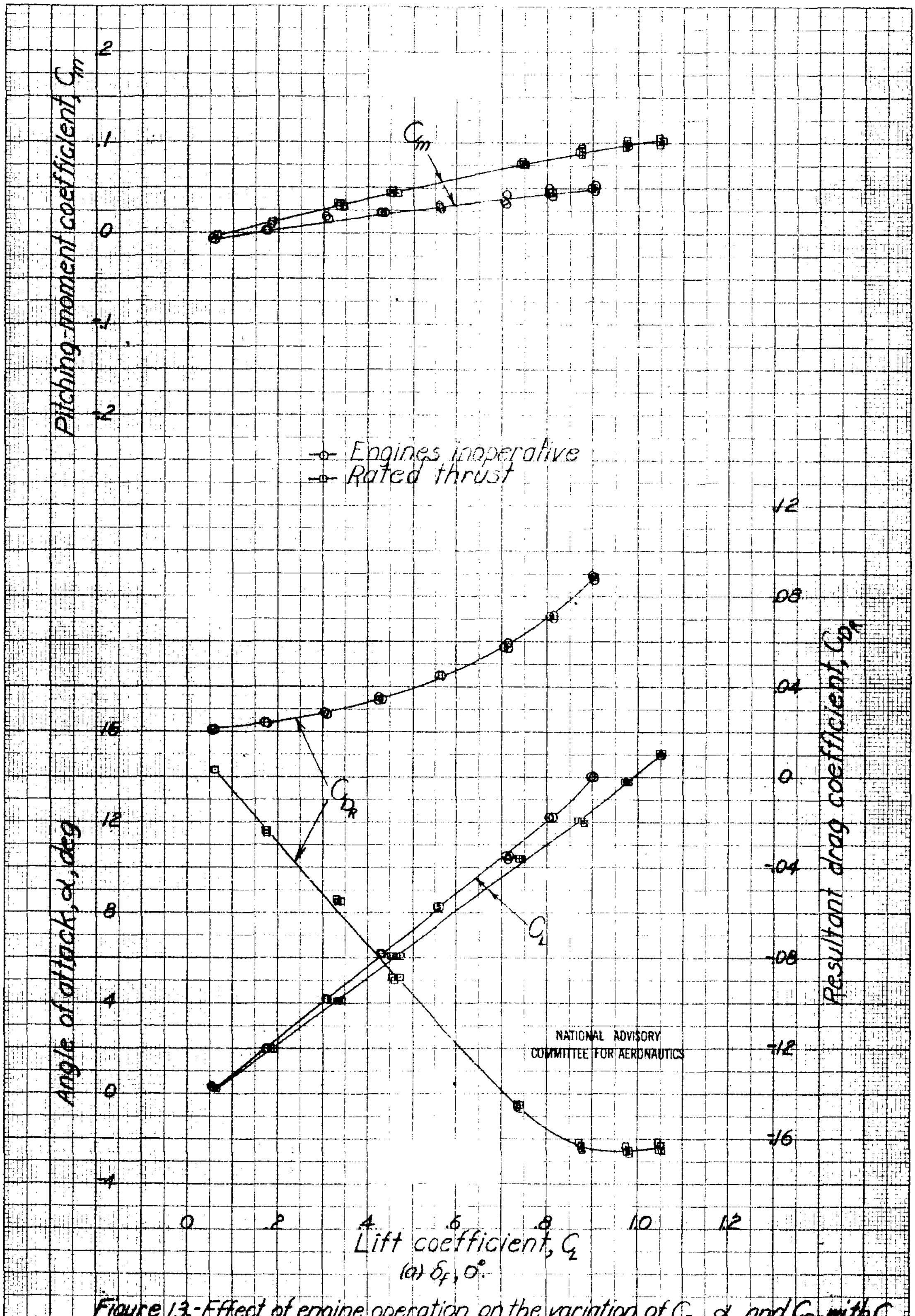

(a) δ_f, 0°.

Figure 13.- Effect of engine operation on the variation of C_m, α, and C_{D_R} with C_L. Horizontal and vertical tail surfaces removed.

L-626

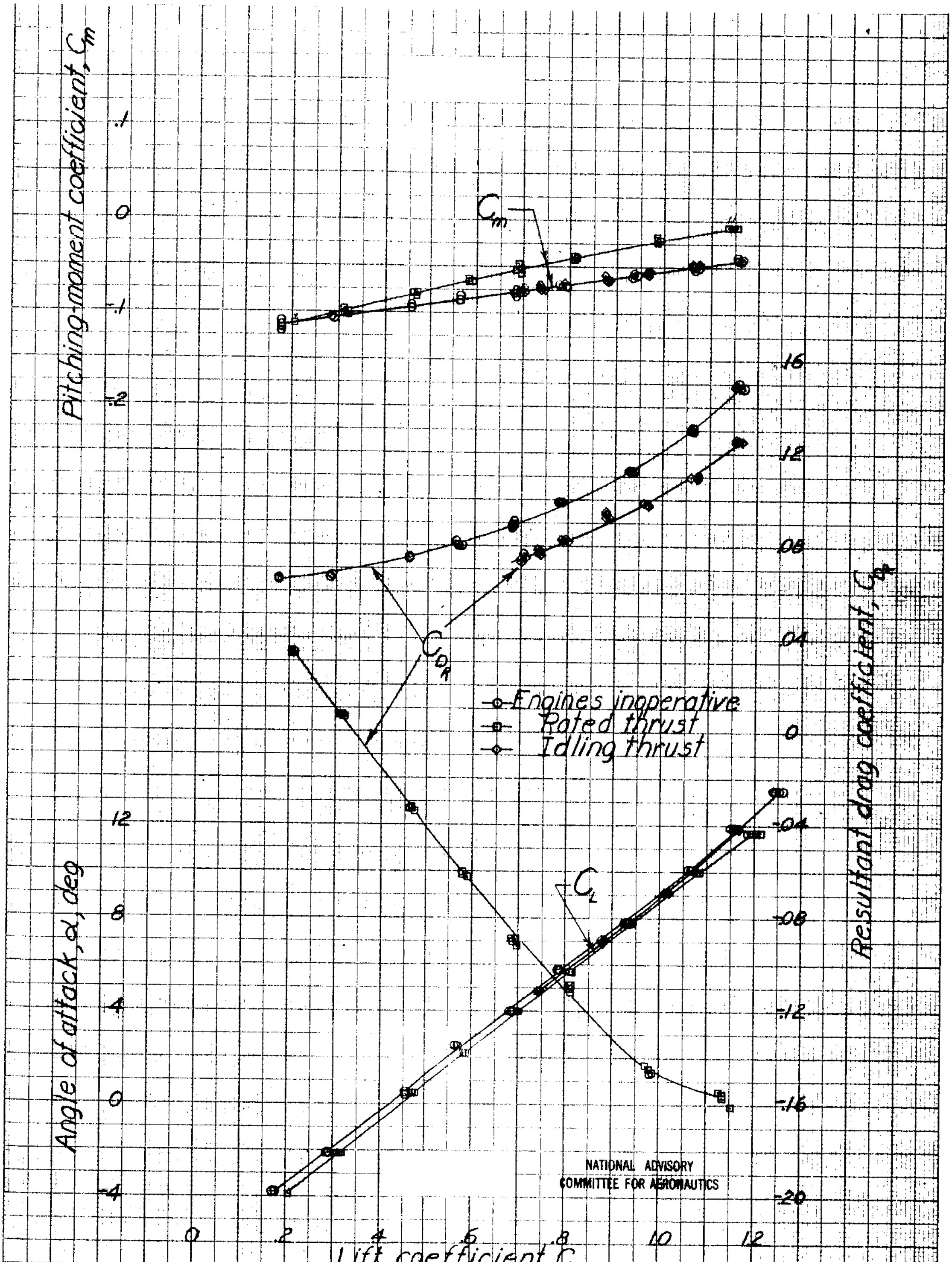

(b) δ_f, 45°

Figure 13.- Concluded.

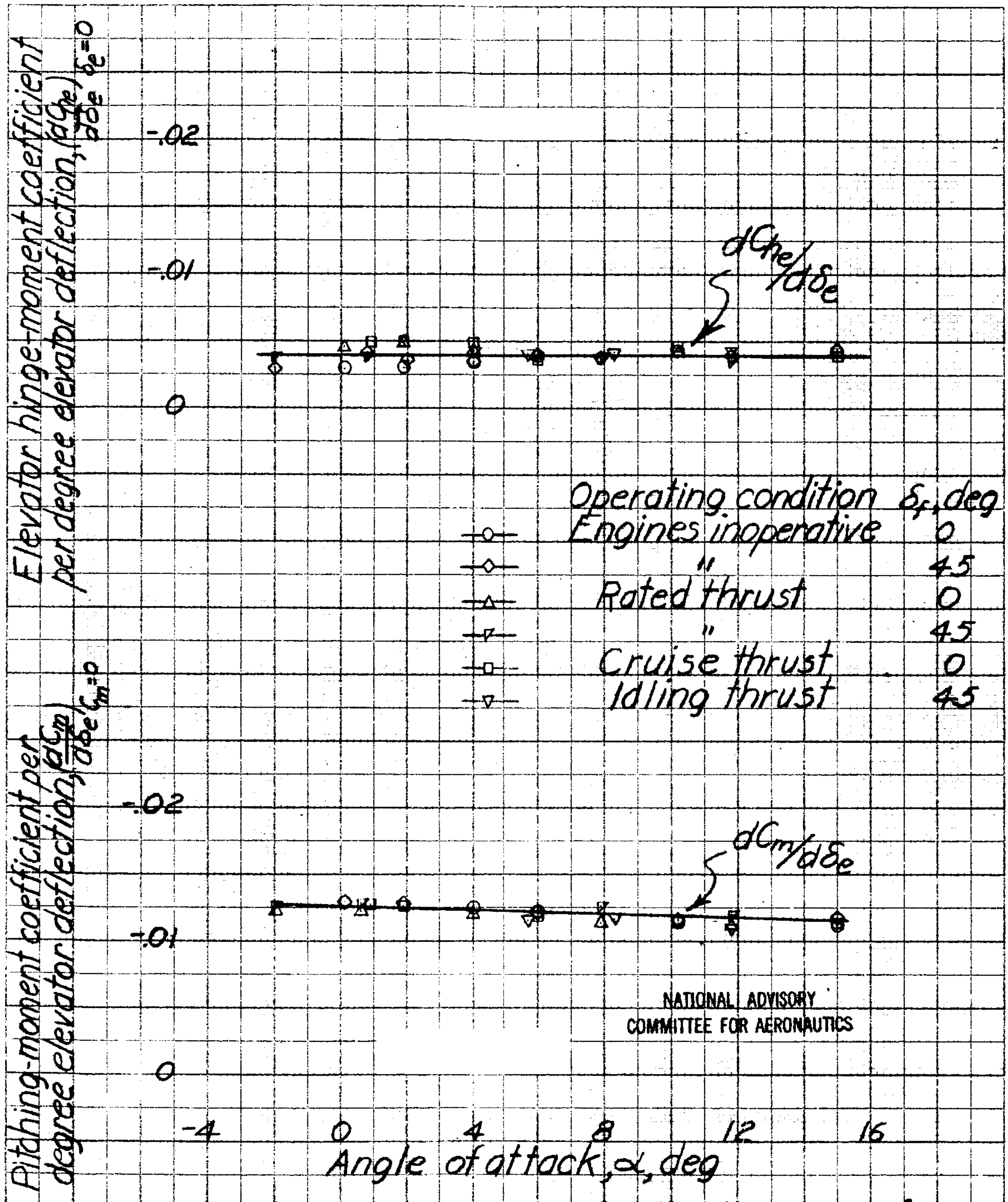

Figure 14.- Effect of engine operation and flap deflection on the elevator control effectiveness and hinge-moment coefficients. δ_e, 0°; i_t, 1.25°.

L-626

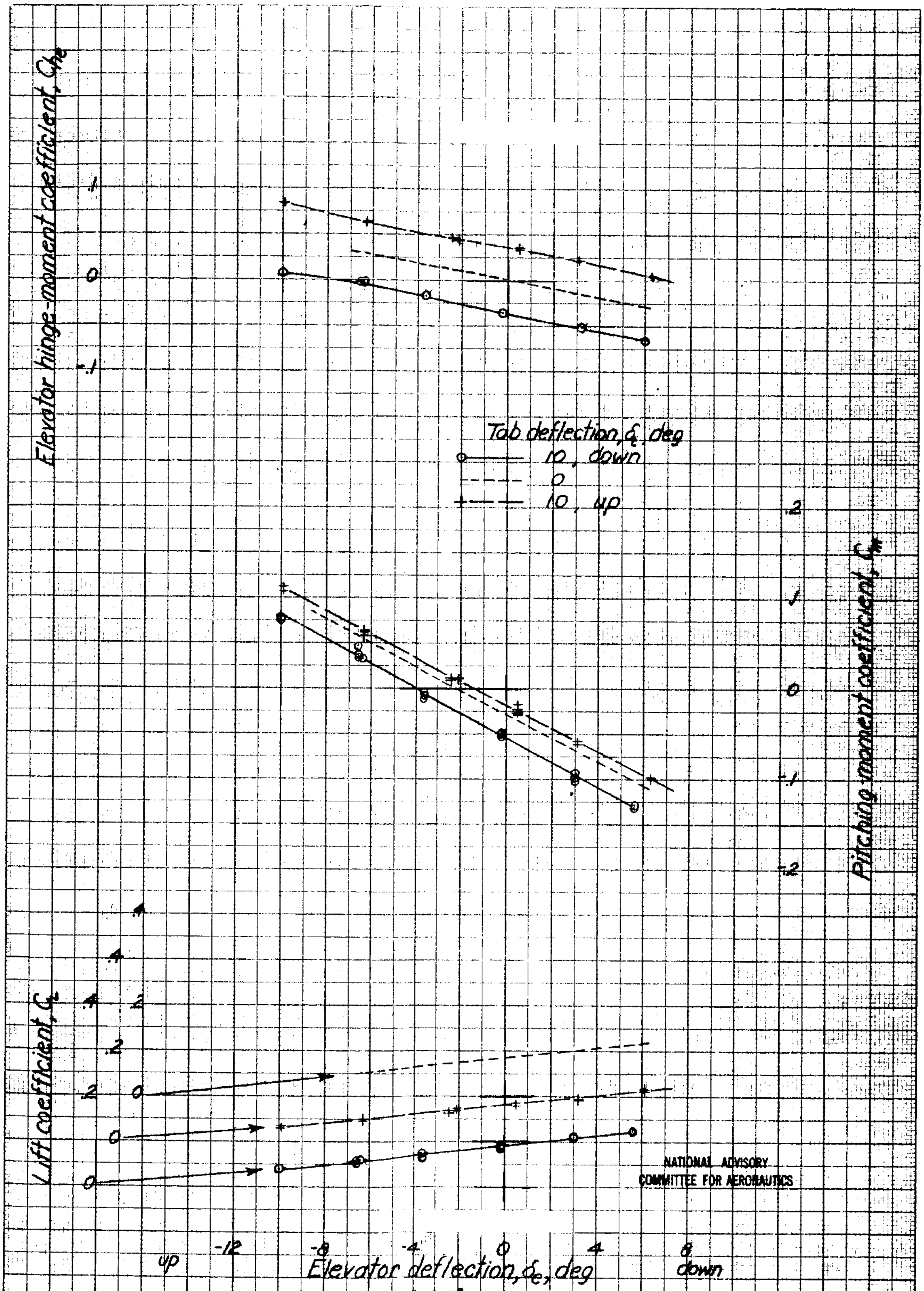

(a) α, 0.1°

Figure 15.- Effect of elevator and tab deflection on the aerodynamic characteristics of the XP-59 airplane. Rated thrust; δ_f, 0°; i_t, 1.25°.

L-626

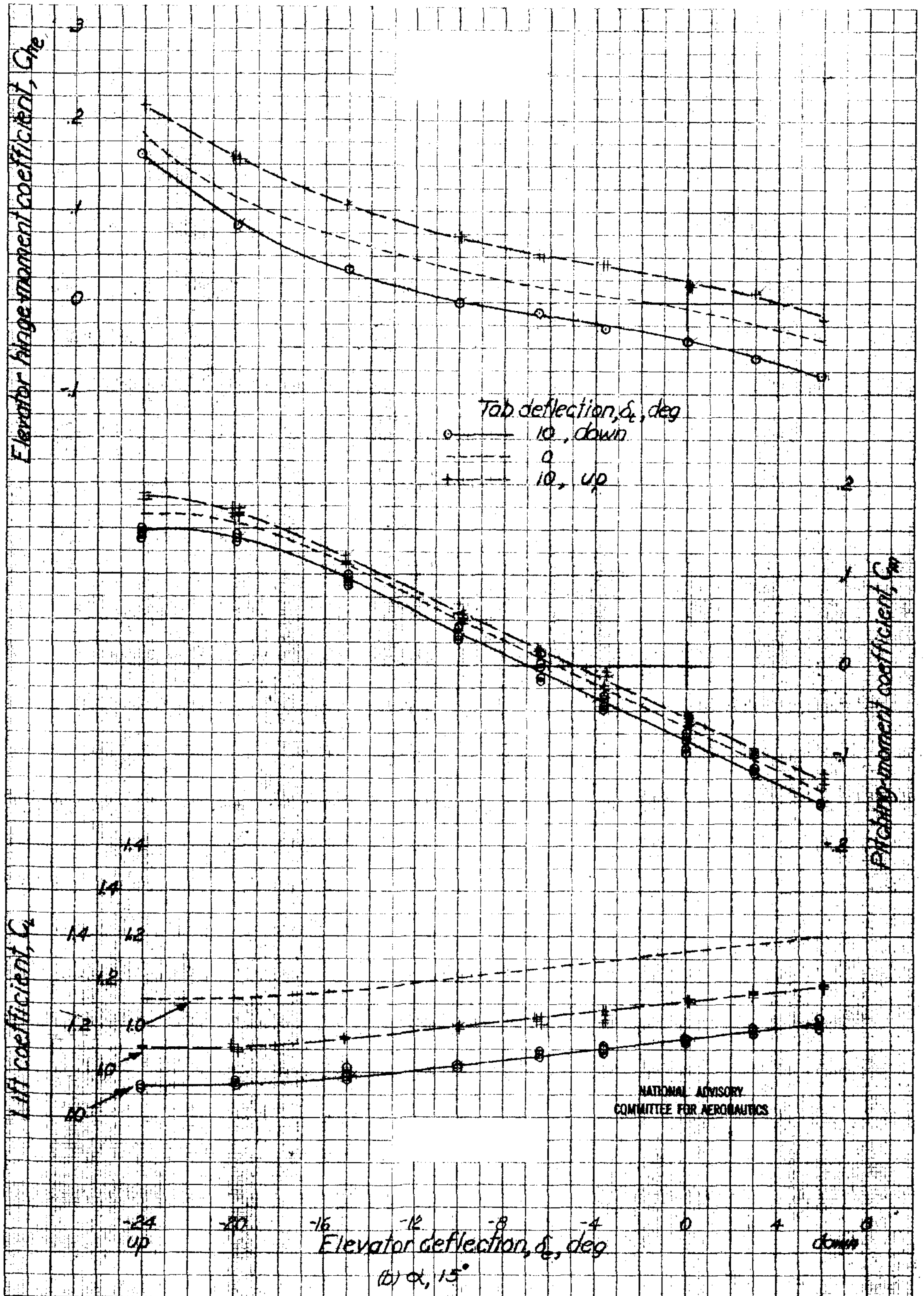

(b) α, 15°

Figure 15.- Concluded.

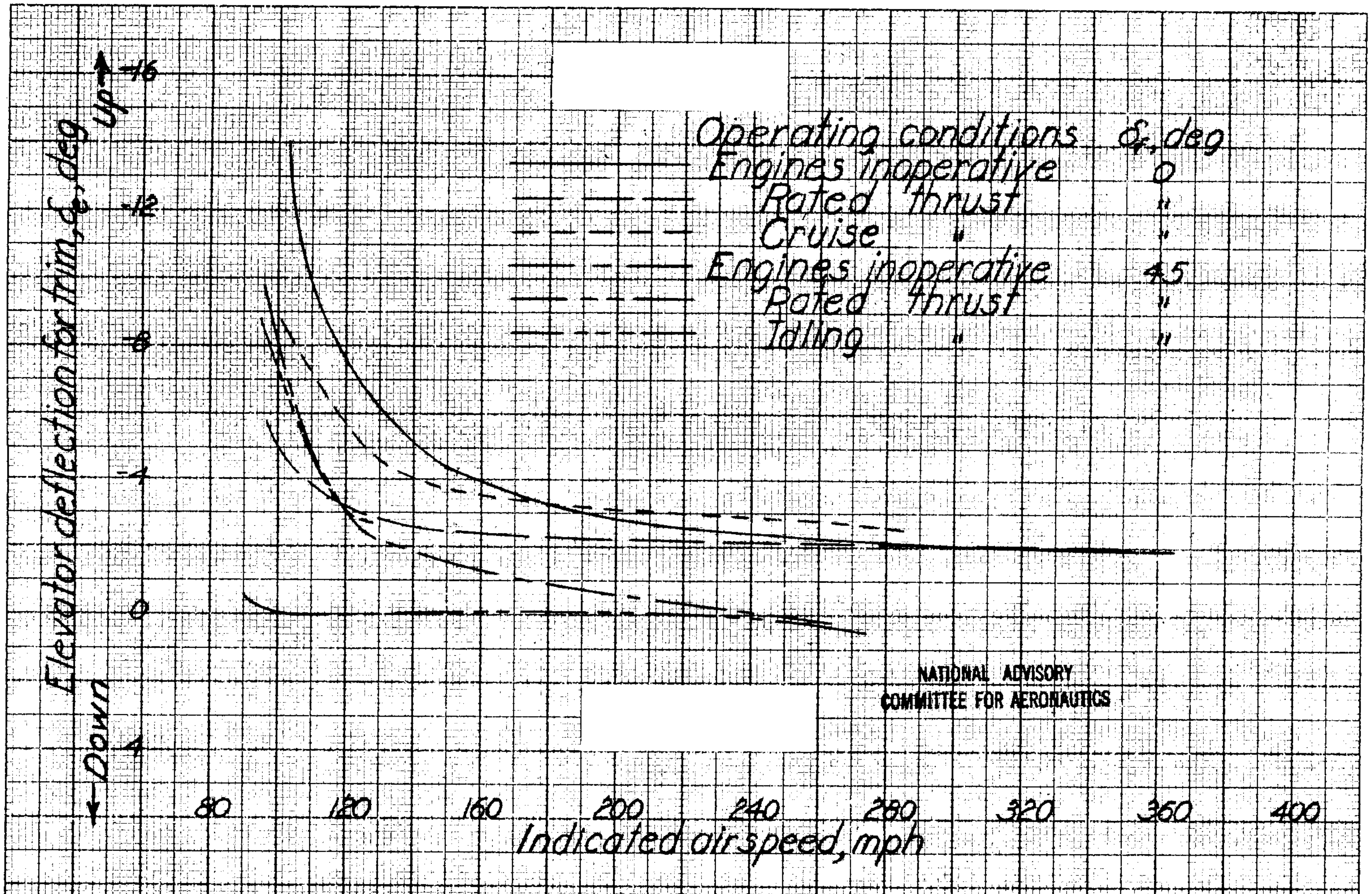

Figure 16.- Effect of engine operation and flap deflection on the variation of elevator deflection for trim with indicated airspeed. i_t, 1.25°; tab neutral.

L-626

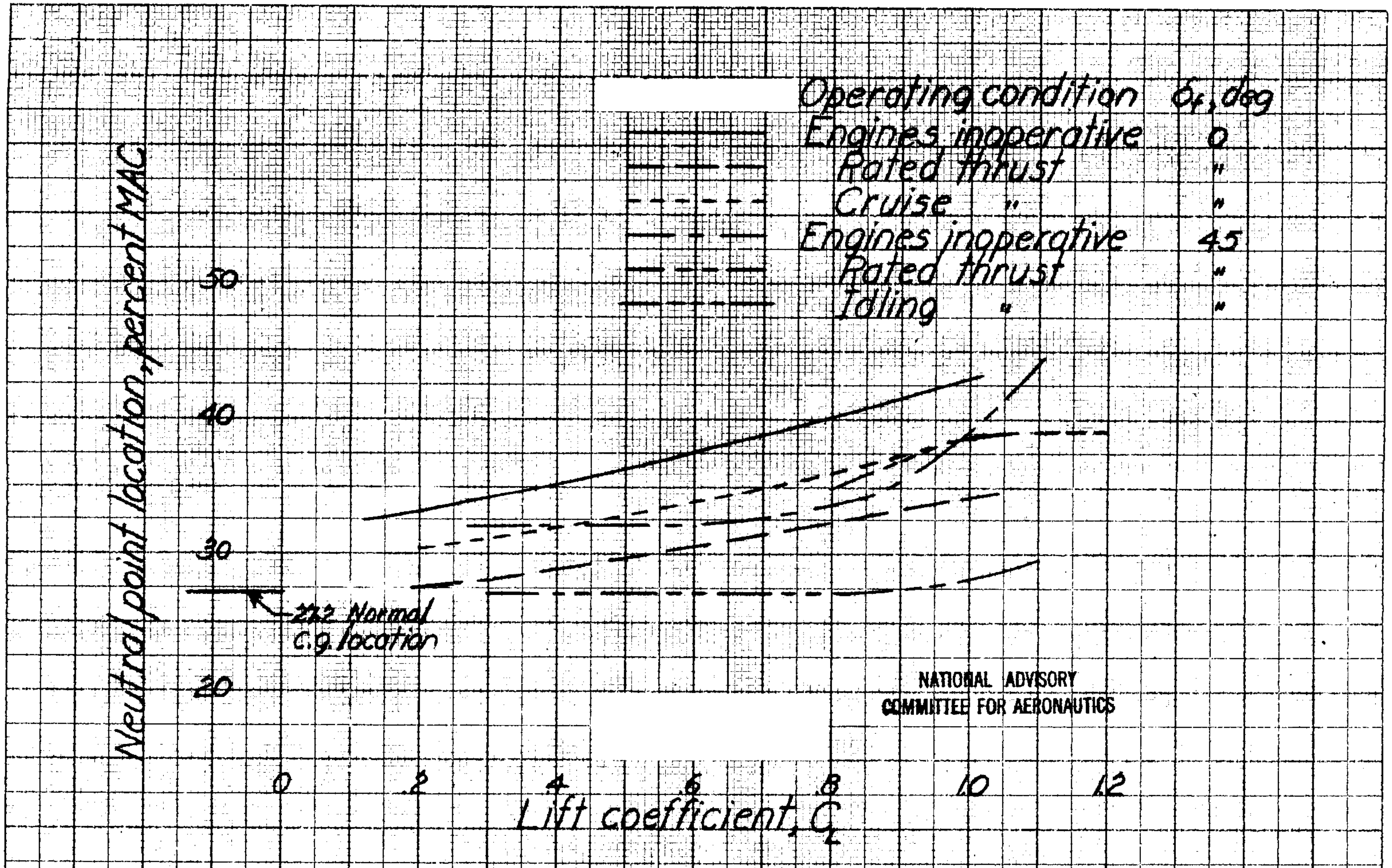

Figure 17.- Effect of engine operation and flap deflection on the variation of neutral points with lift coefficient. Stick fixed; i_t, 1.25°; W/S, 27.2.

L-626

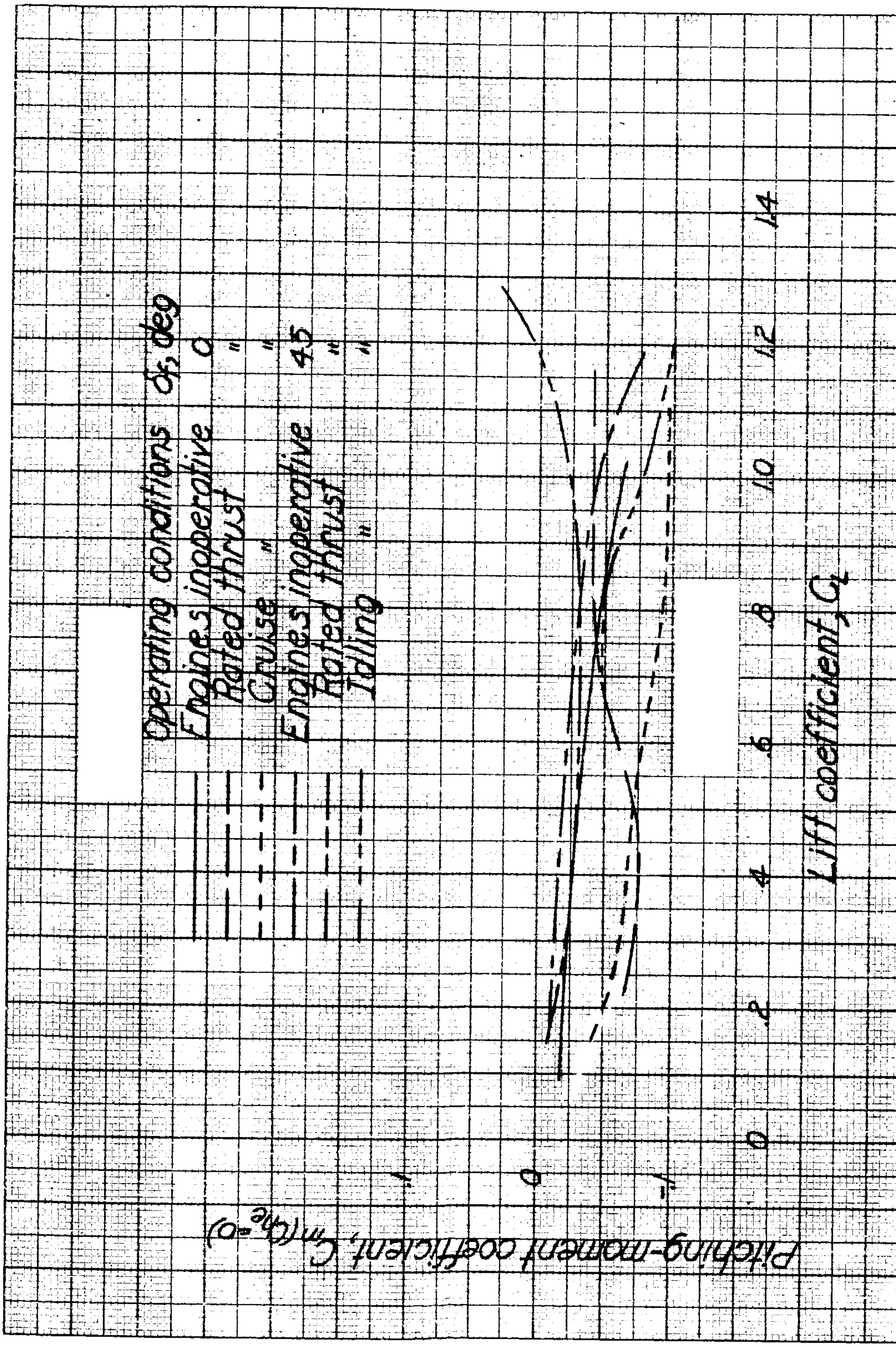

Figure 18.- Variation of pitching-moment coefficient, stick free, with lift coefficient. i_t, 1.25°; tab neutral.

L-626

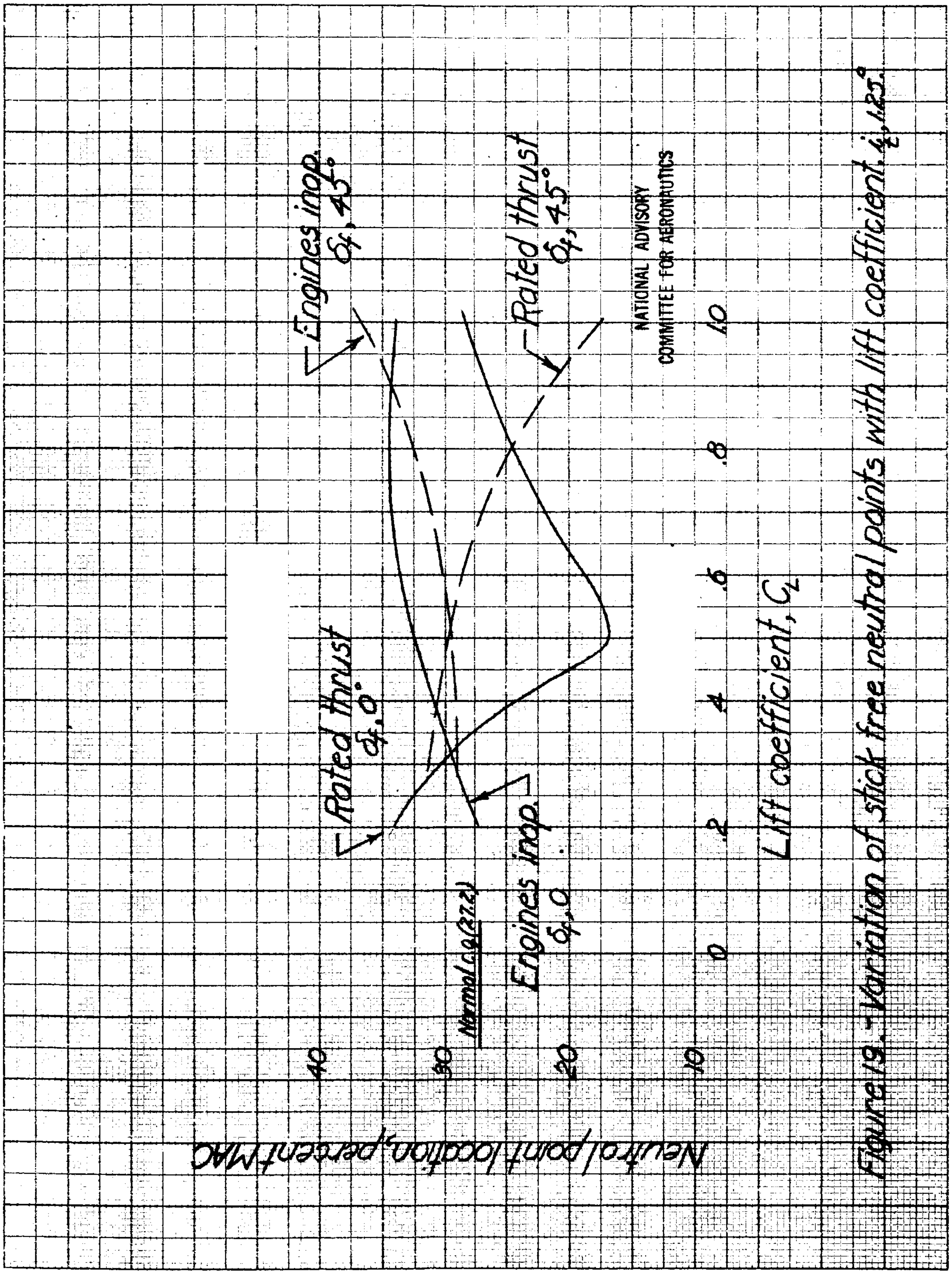

Figure 19.- Variation of stick free neutral points with lift coefficient. i_t, 1.25°.

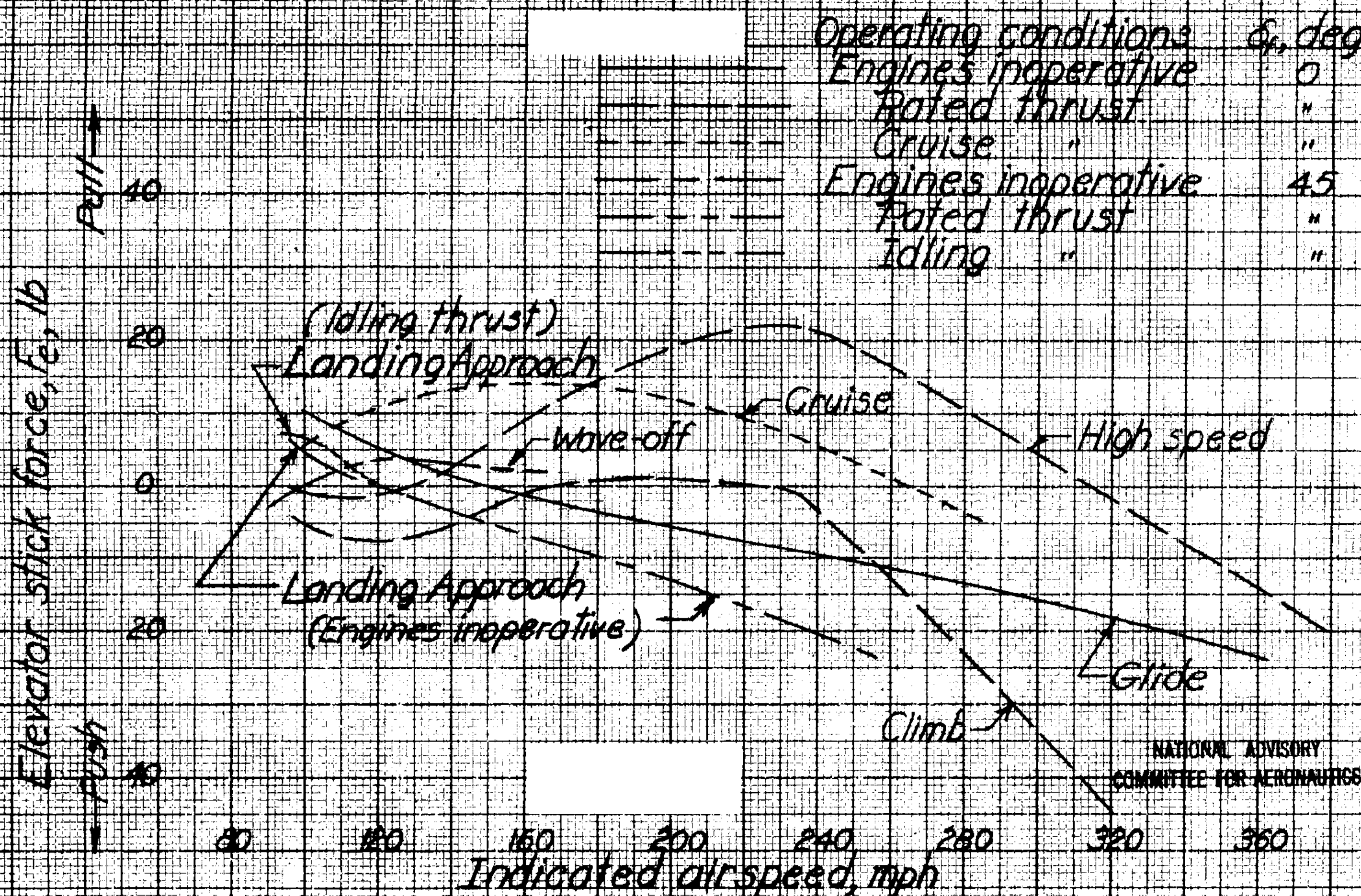

Figure 20.- Variation of elevator stick force with indicated airspeed with the tab set for trim in steady flight for each of the flight conditions. i_t, 1.25°; center of gravity at 27.2 percent MAC; W/S, 27.2.

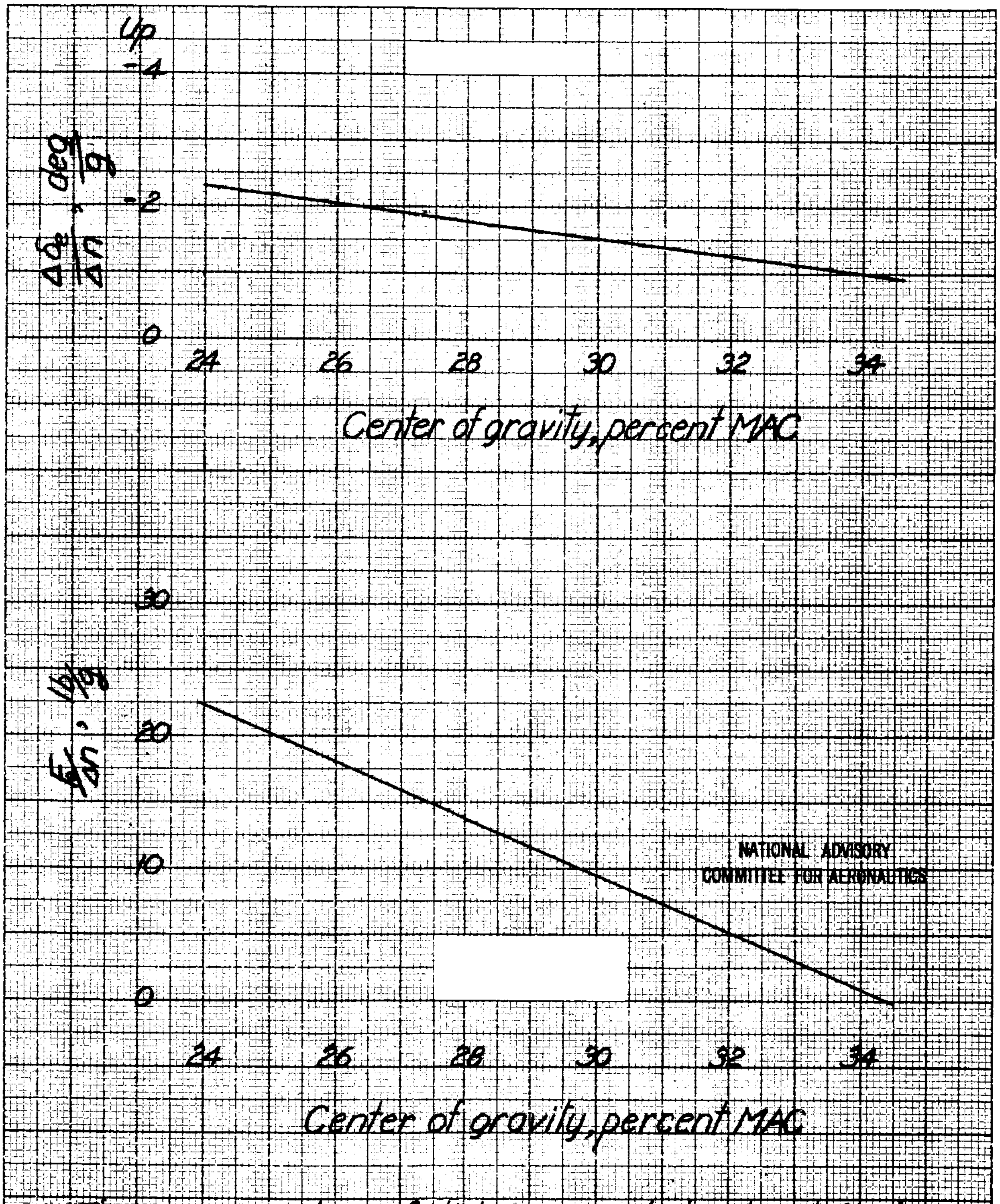

Figure 21.-Variation of stick force and elevator deflection with center of gravity location for a steady turn maneuver. $\Delta n = 8$ at $C_L = 1.0$.

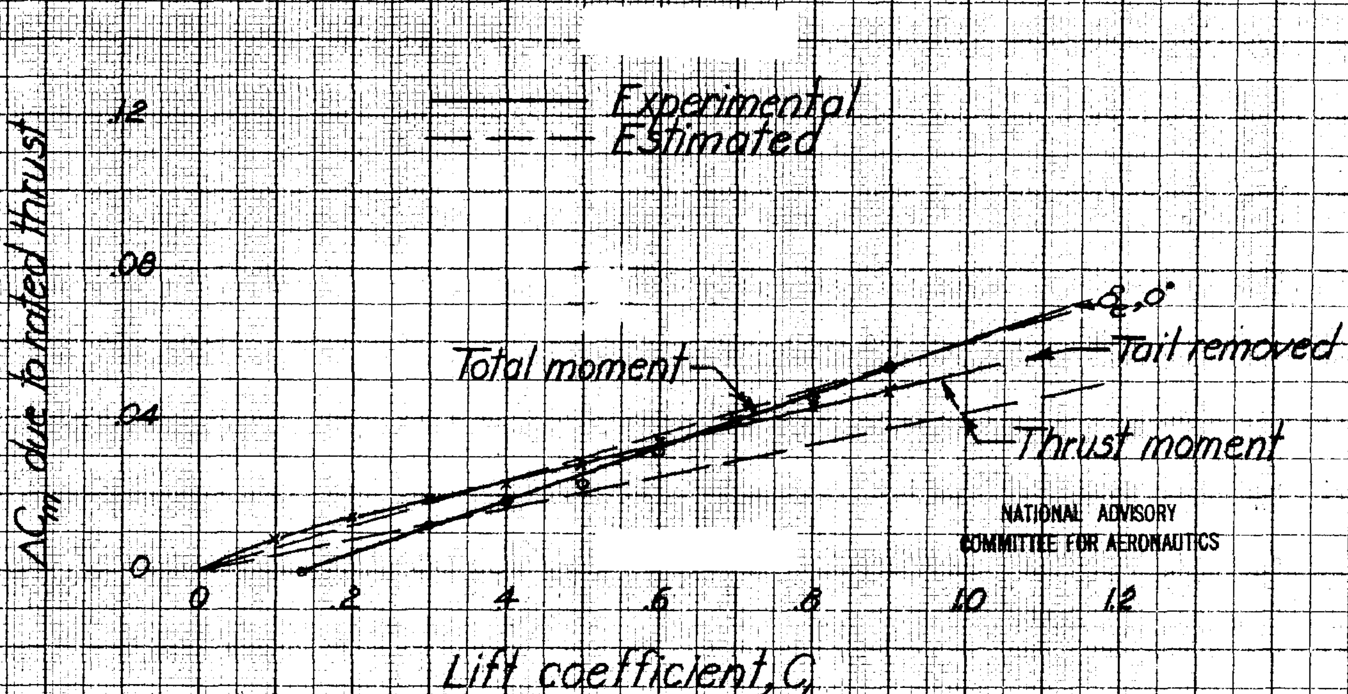

(a) δ_f, 0°

Figure 22.- Comparison of experimental and estimated increments of pitching-moment coefficient due to rated thrust operation.

L-626

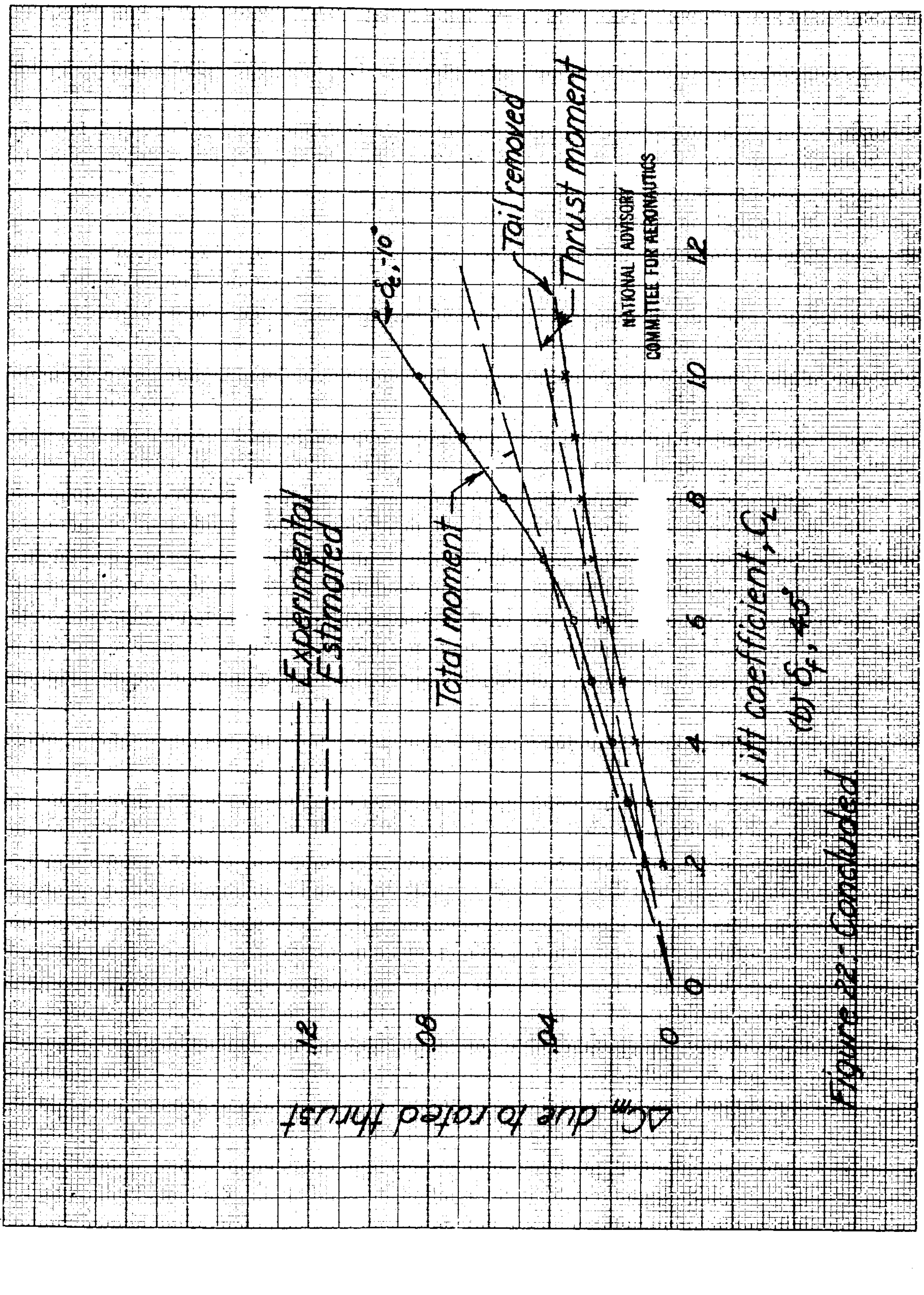

Figure 22.- Concluded.

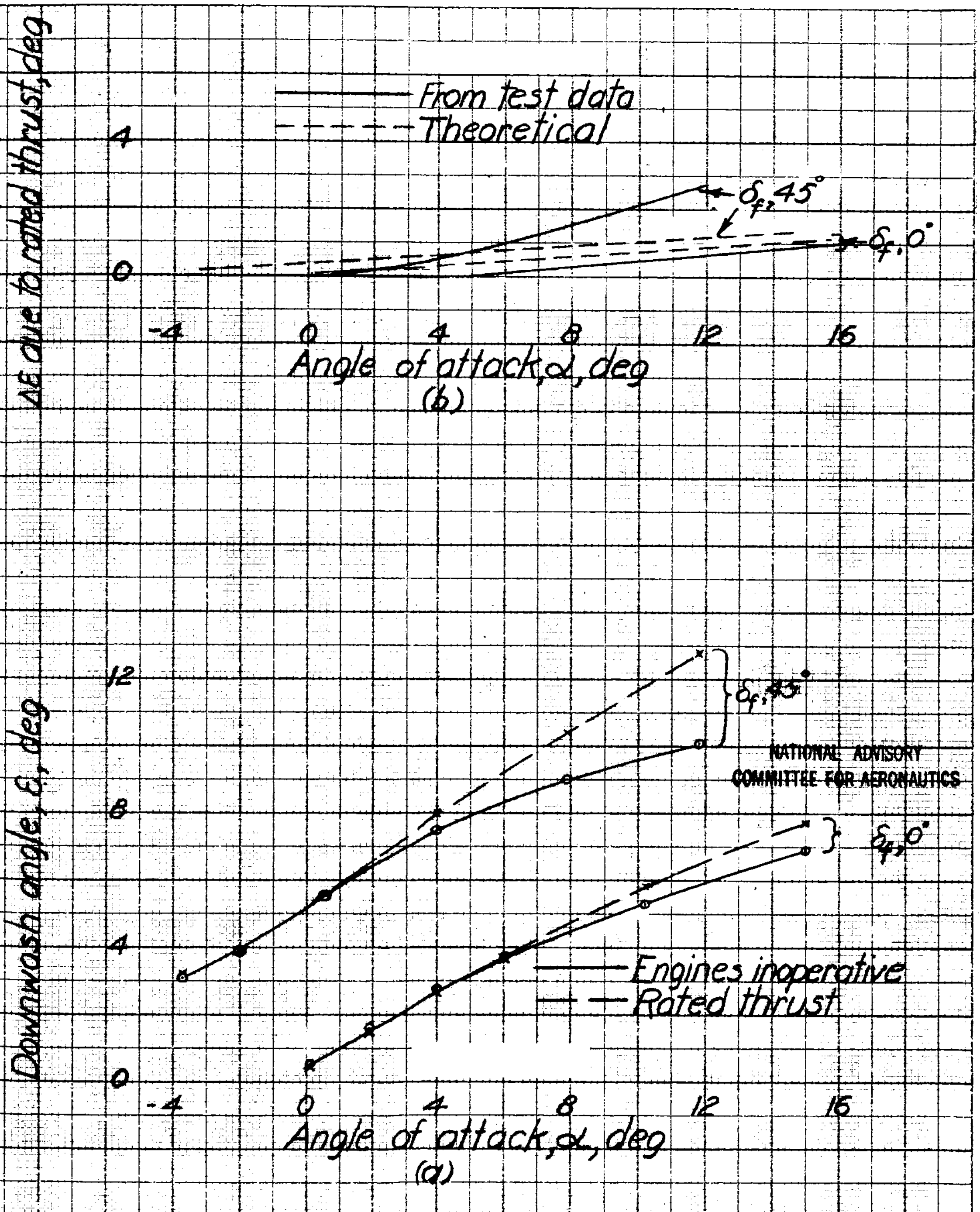

Figure 23.- Effect of rated thrust engine operation on the downwash angle at the tail of the YP-59A airplane for flap deflections of 0° and 45°.

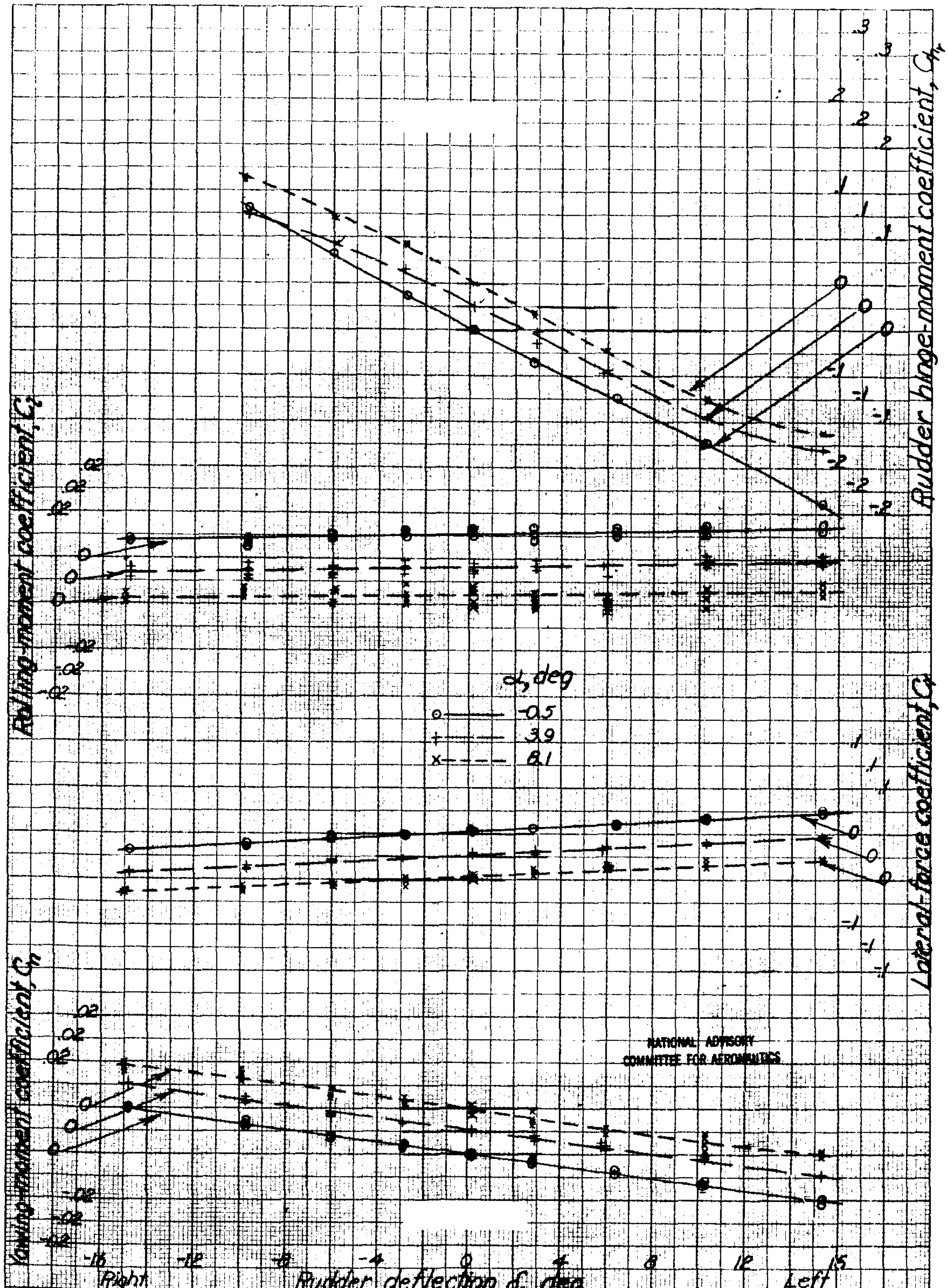

Figure 24.- Effect of rudder deflection on the aerodynamic characteristics of the YP-59A airplane in yaw. Prism deflectors installed on the fin trailing edge and beads on the rudder trailing edge. δ_t, 0°; δ_e, 0°; δ_r, 0°; engines inoperative.

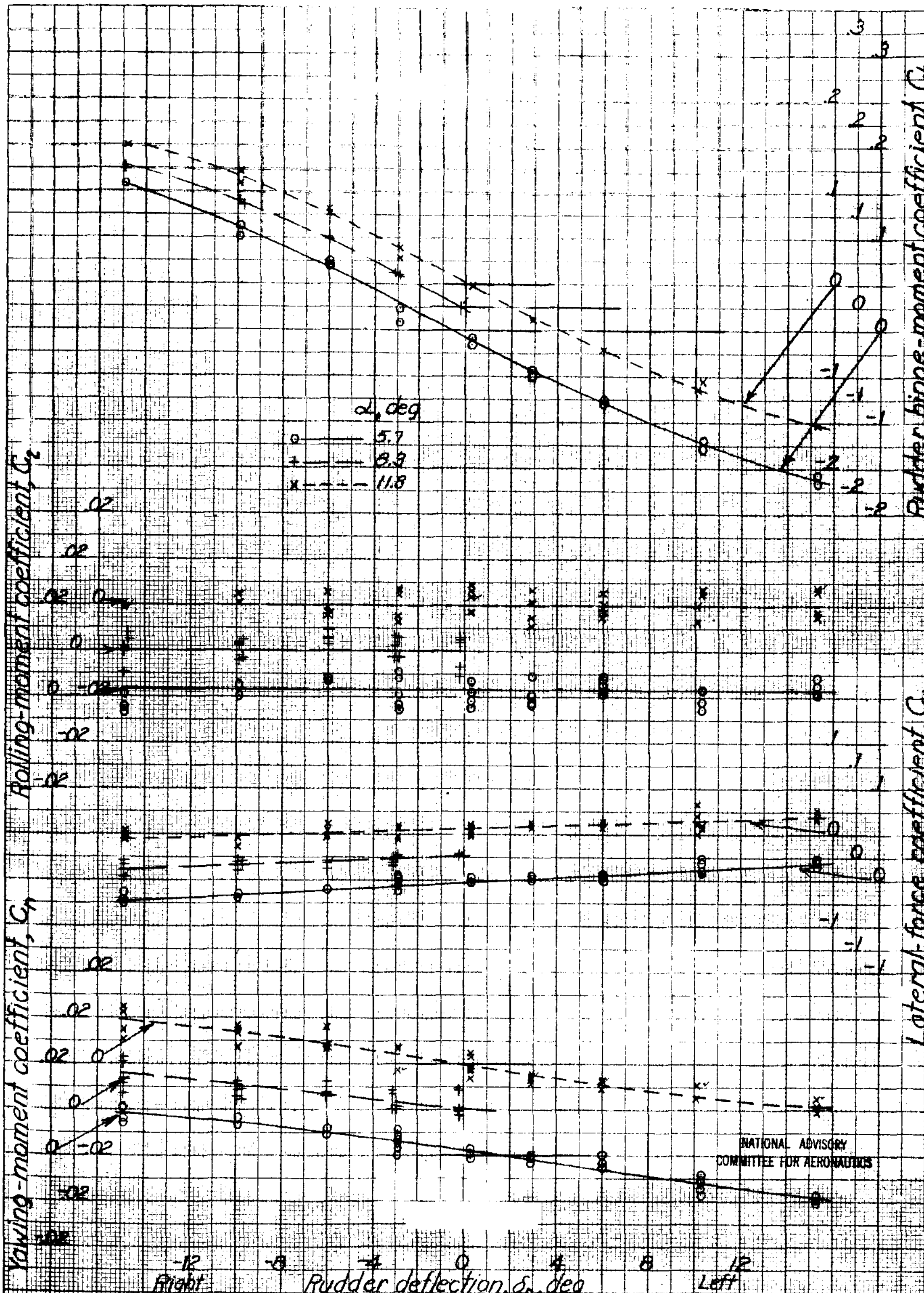

(b) ψ, 0°; δ_t, 45°

Figure 24- Continued.

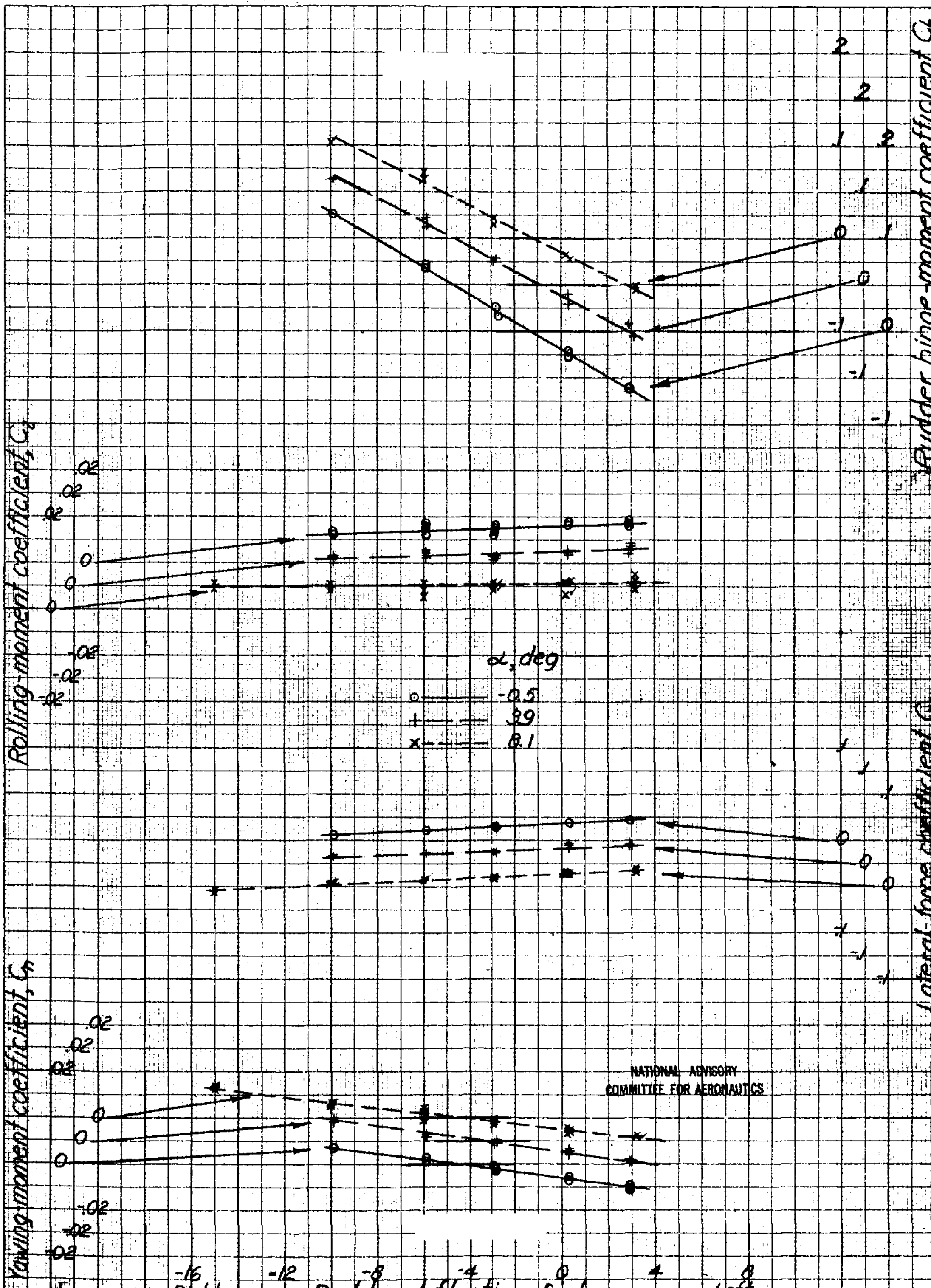

(c) ψ, 3°; δ_t, 0°

Figure 24.- Continued.

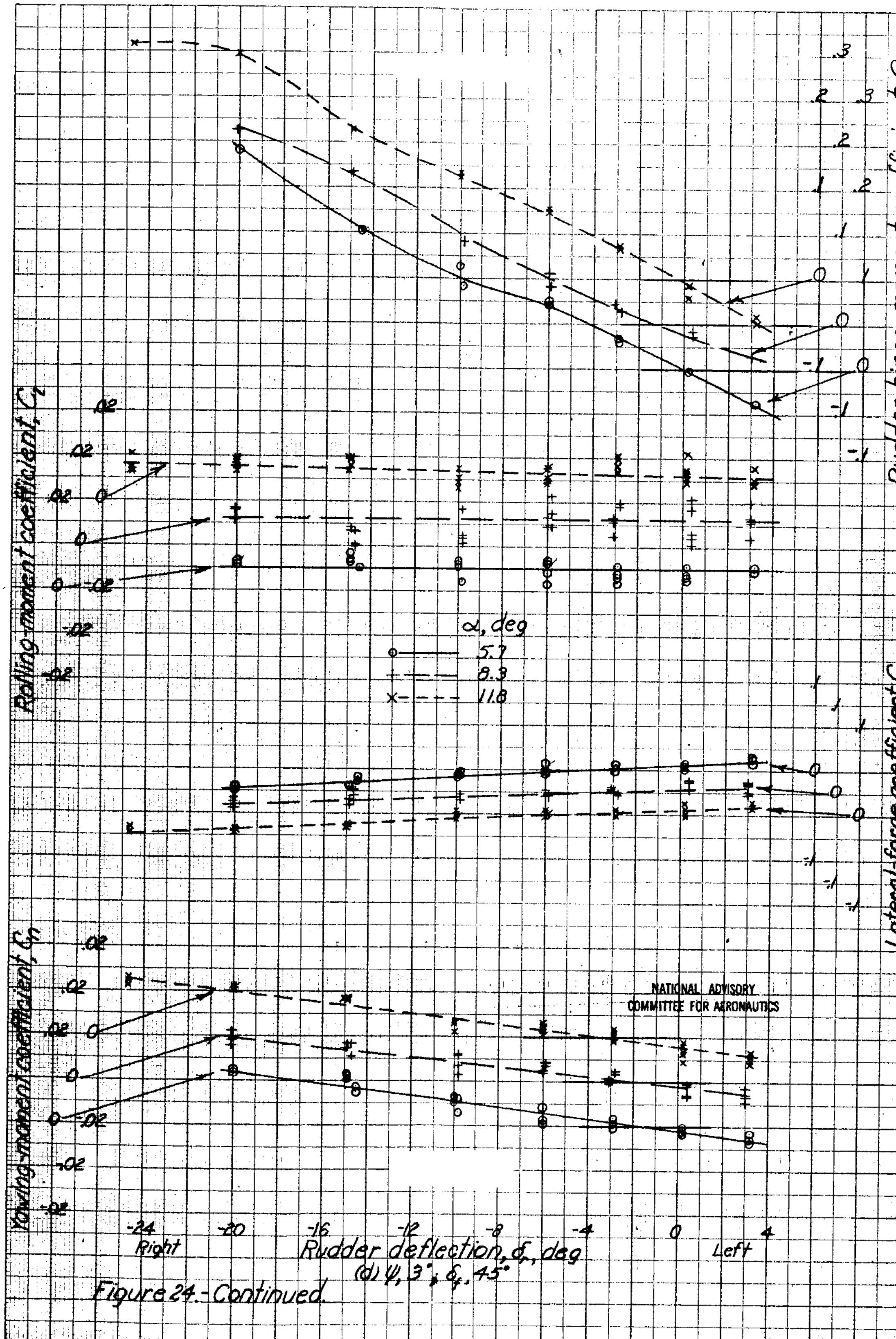

Figure 24.- Continued.

L-626

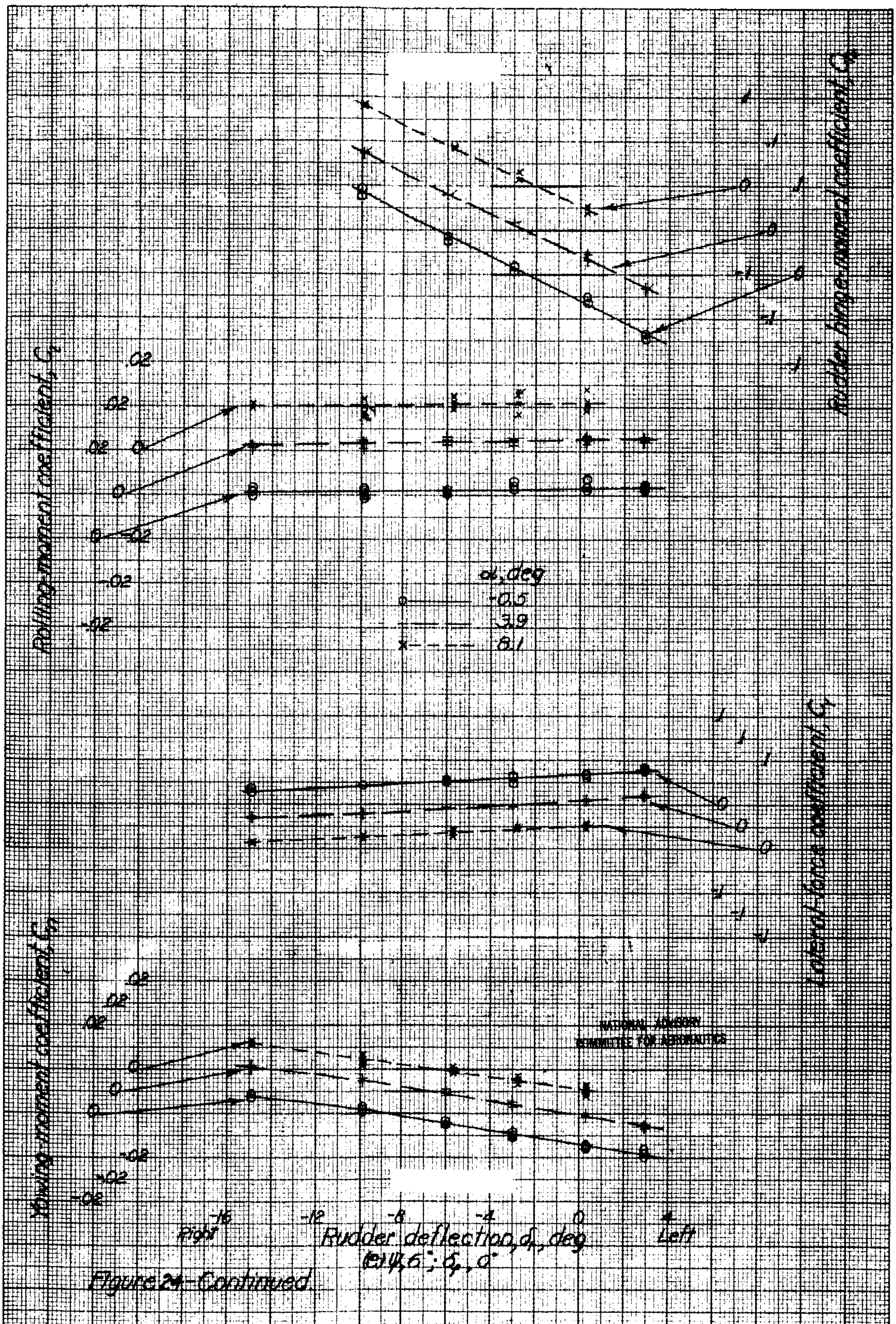

(e) ψ, 6°; δ_t, 0°

Figure 24- Continued.

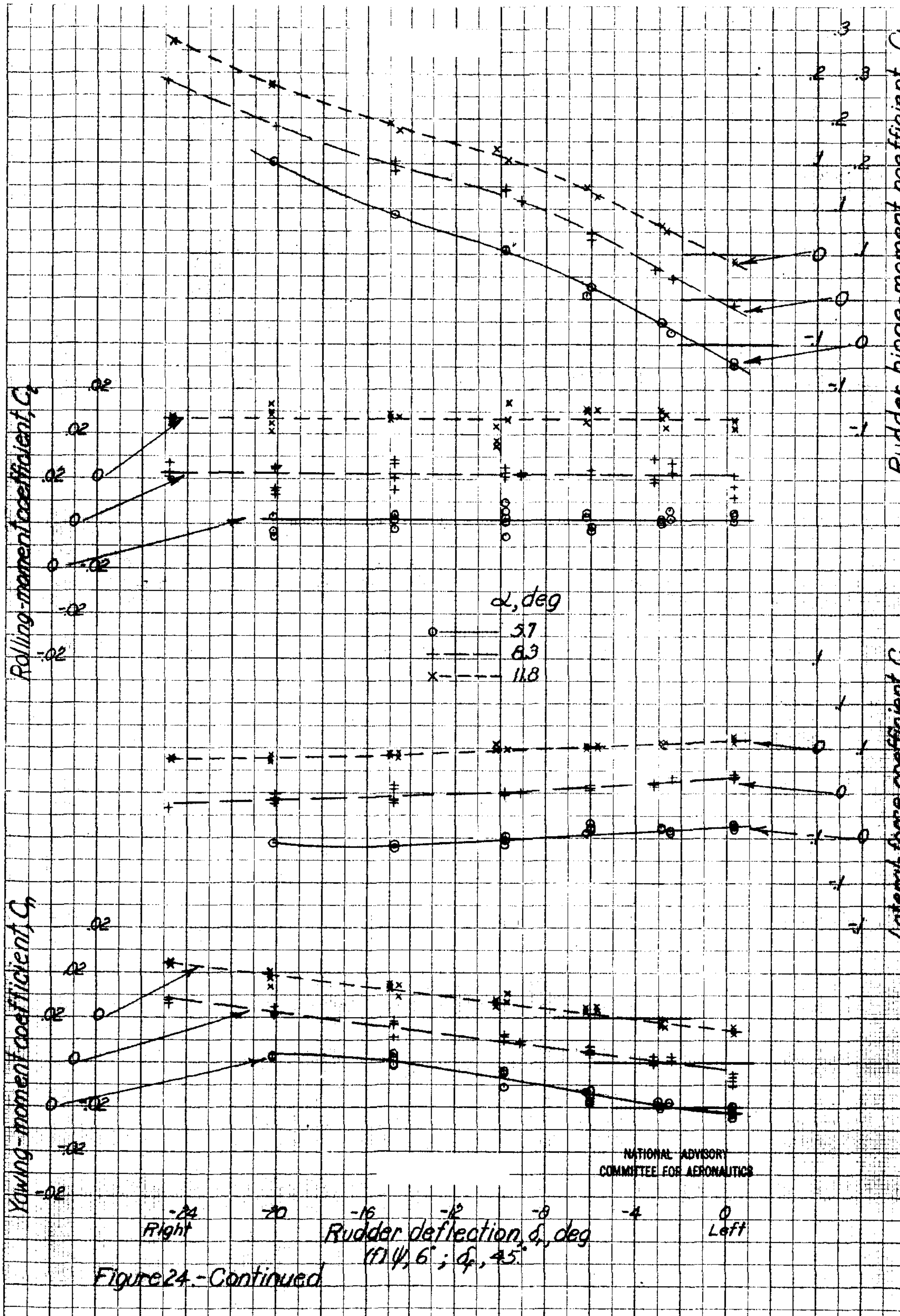

(f) ψ, 6°; δ_f, 45°

Figure 24.- Continued

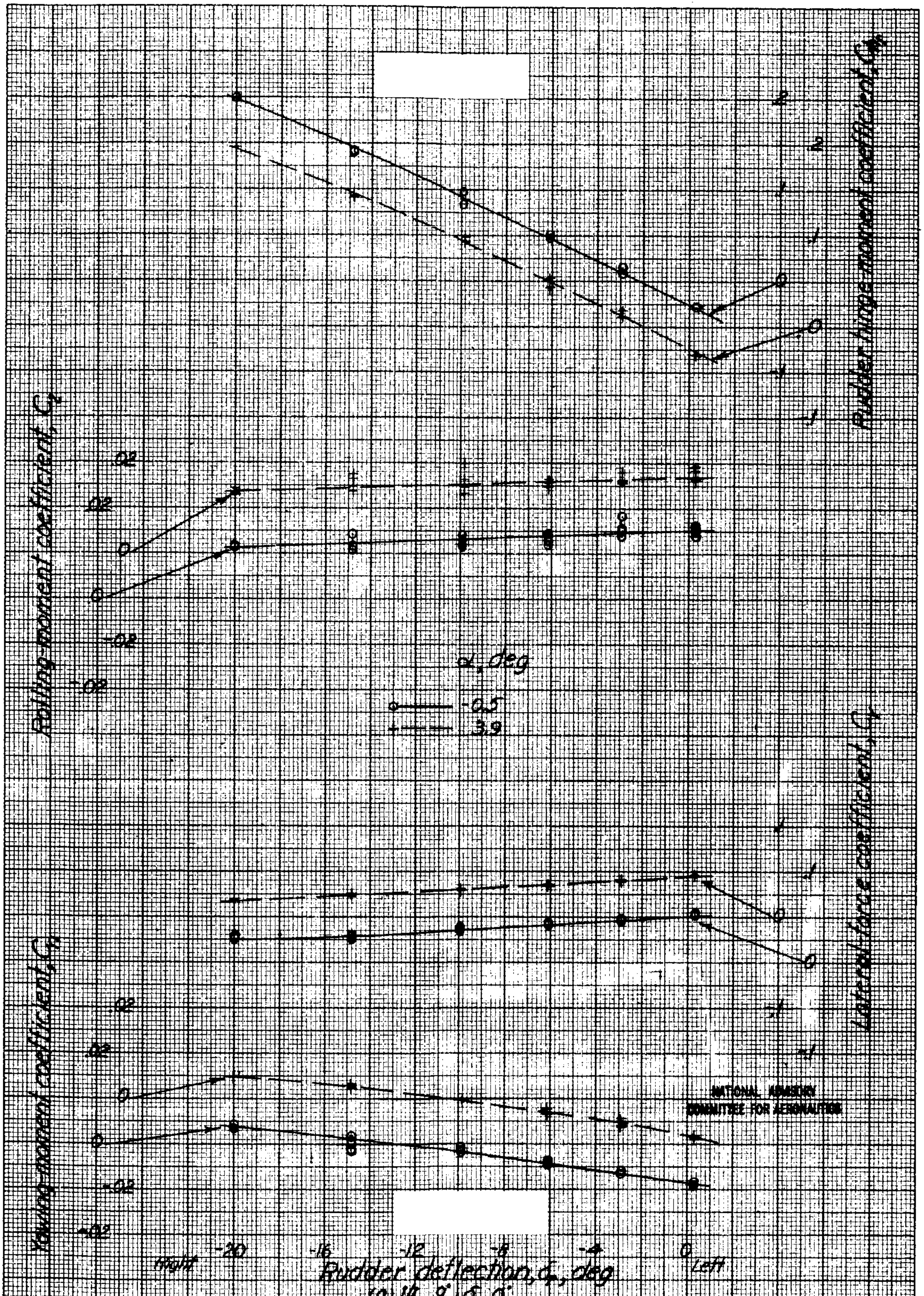

(g) ψ, 9°; δ, 0°.

Figure 24.- Continued.

L-626

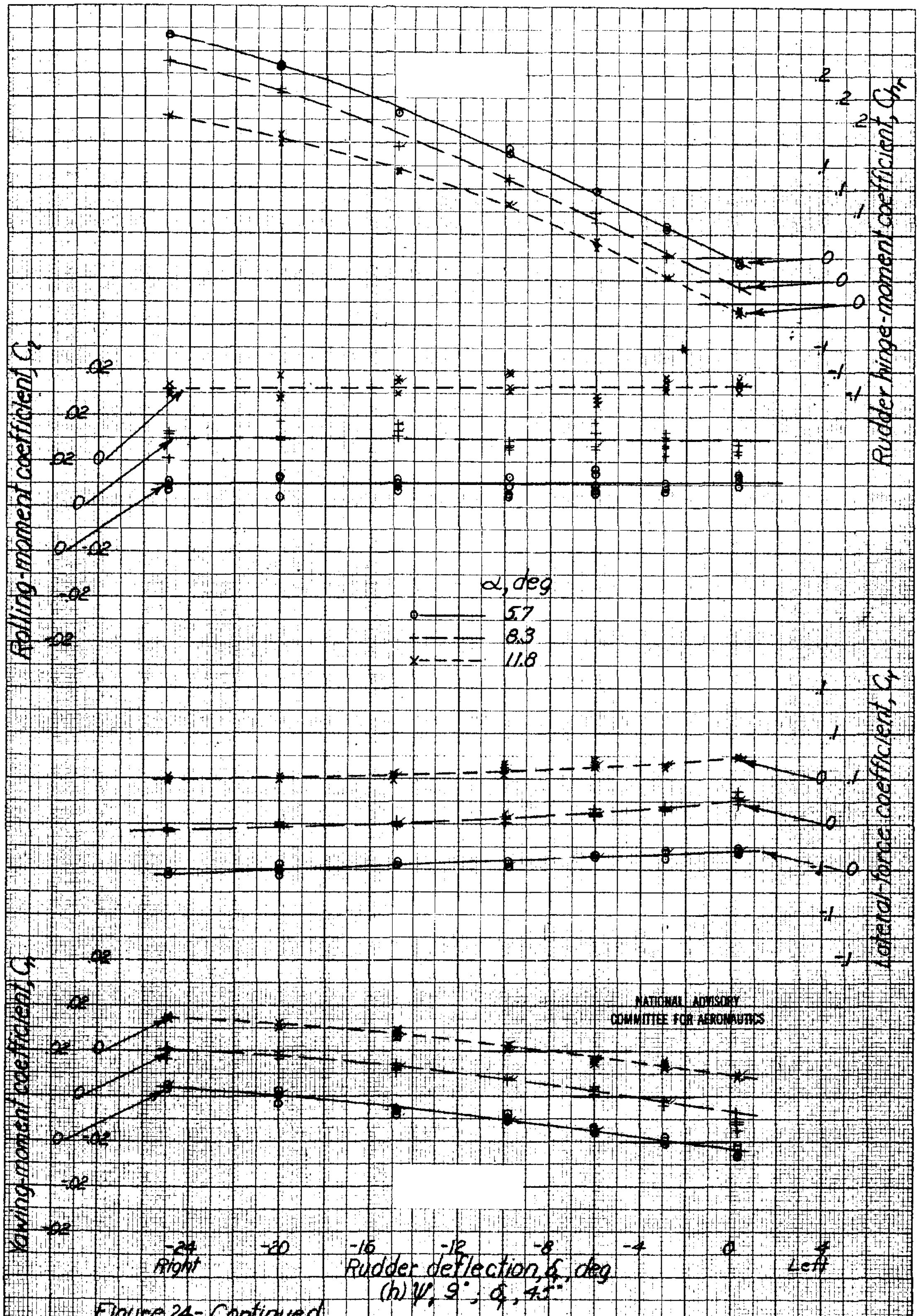

(h) ψ, 9°; δ_f, 45°

Figure 24- Continued.

L-626

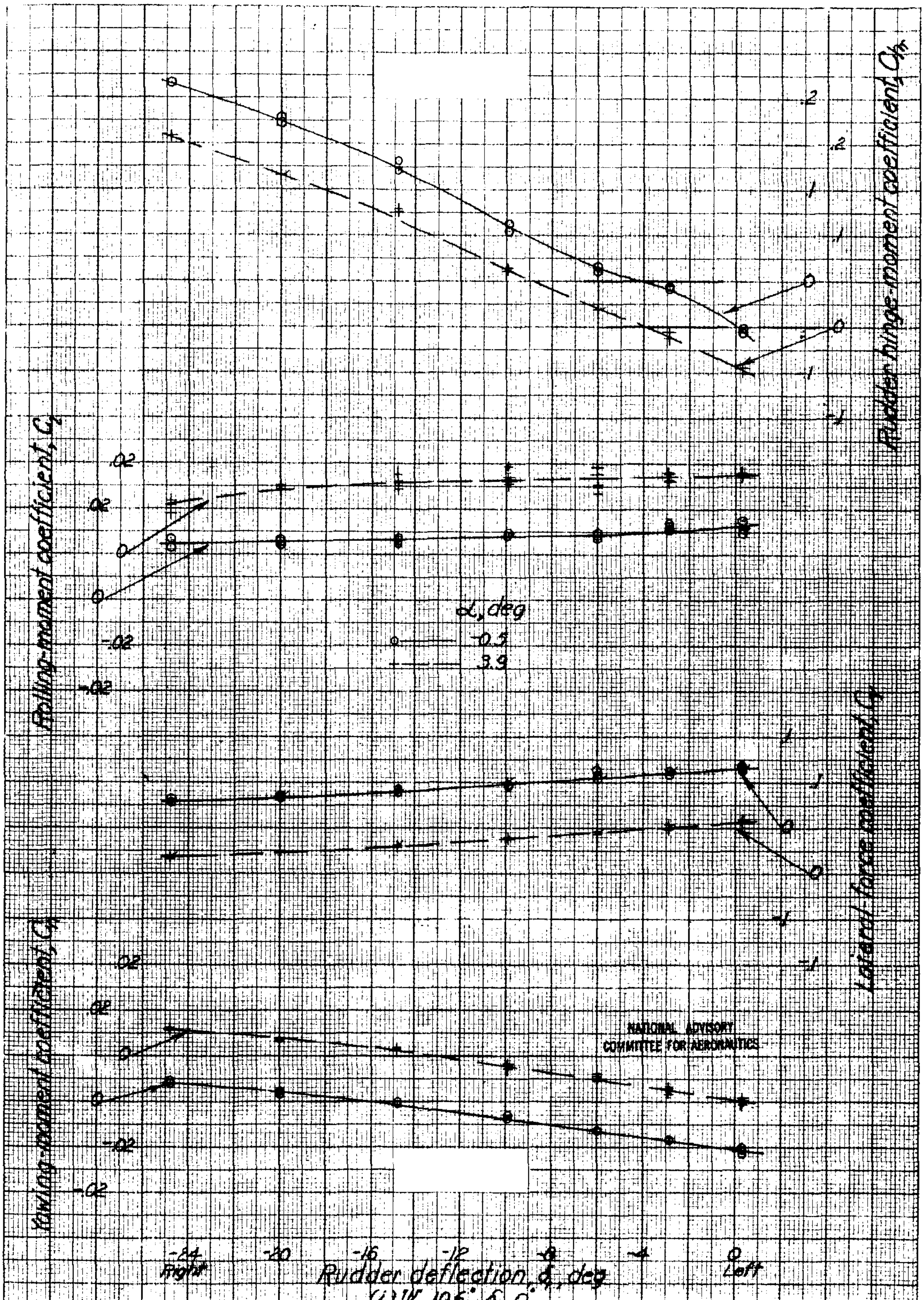

(i) ψ, 10.6°; δ_f, 0°

Figure 24.- Continued

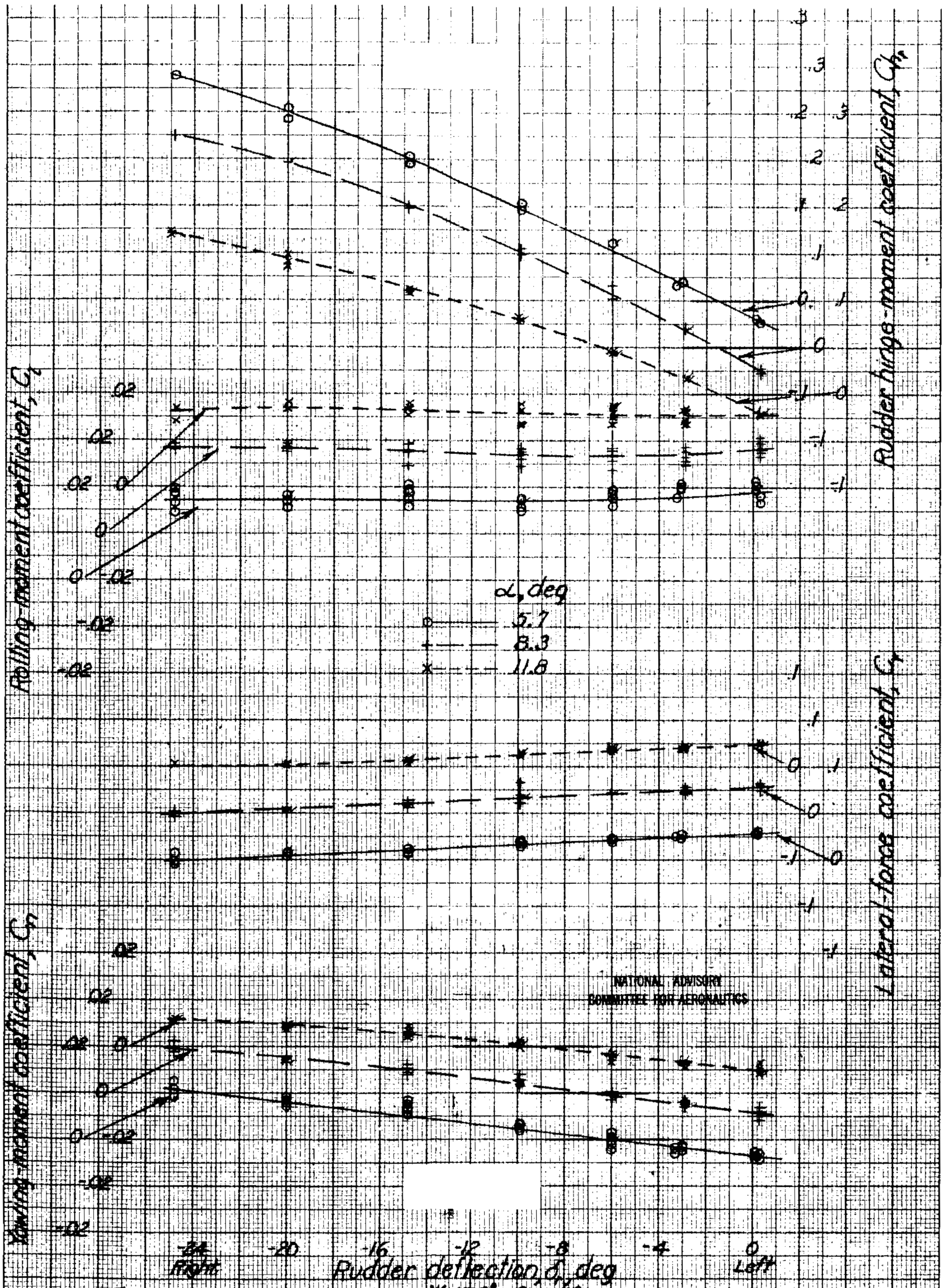

(j) ψ, 10.6°; δ_a, 4.5°.

Figure 24.- Concluded.

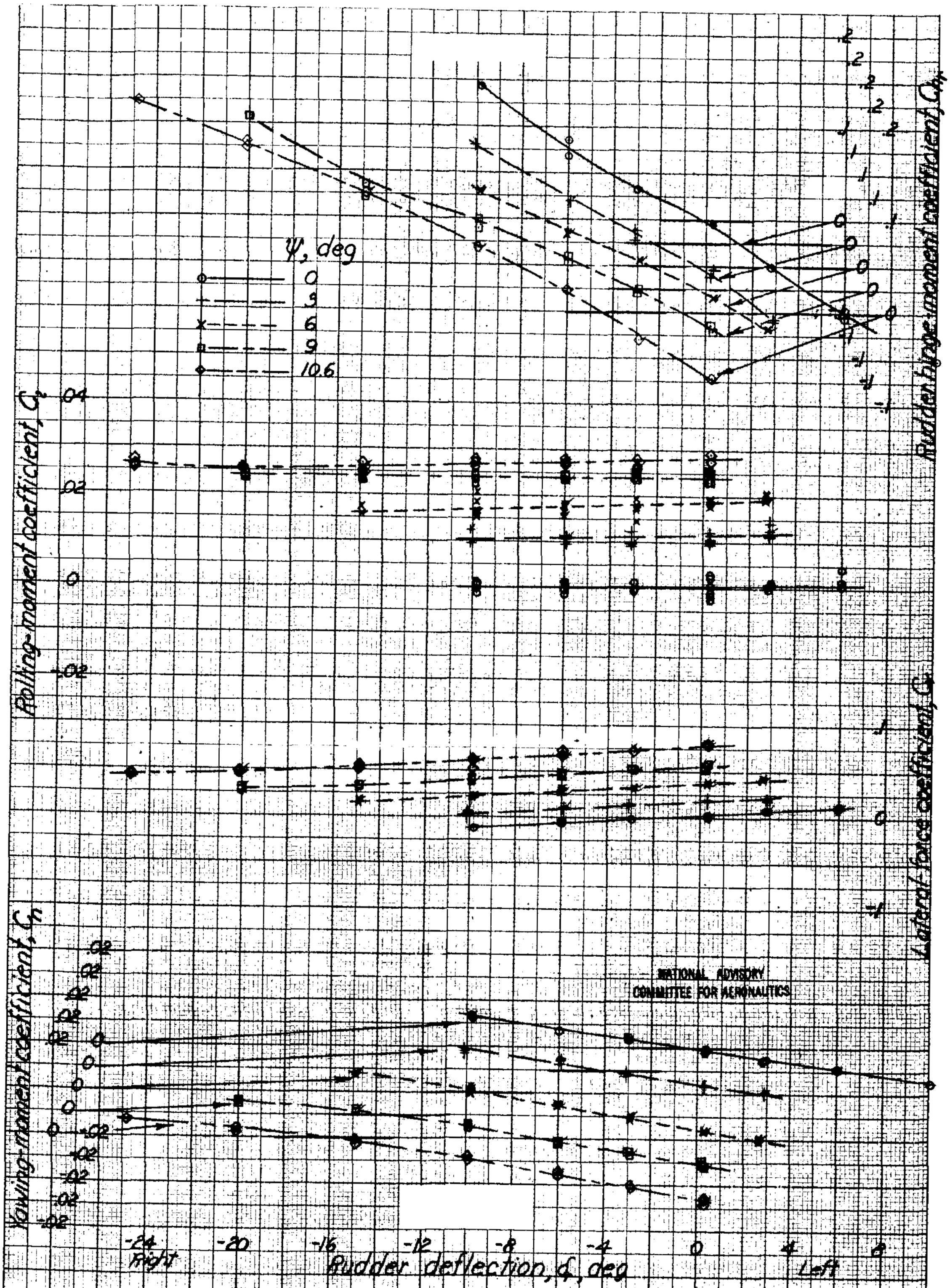

Figure 25.- Effect of rudder deflection on the aerodynamic characteristics of the YP-59A airplane in yaw with engines operating at rated thrust. Prism deflectors installed on the fin trailing edge and beads on the rudder trailing edge. α, 3.9°; δ_f, 0°; δ_e, 0°; δ_a, 0°; δ_t, 0°; T_c', 0.09

L-626

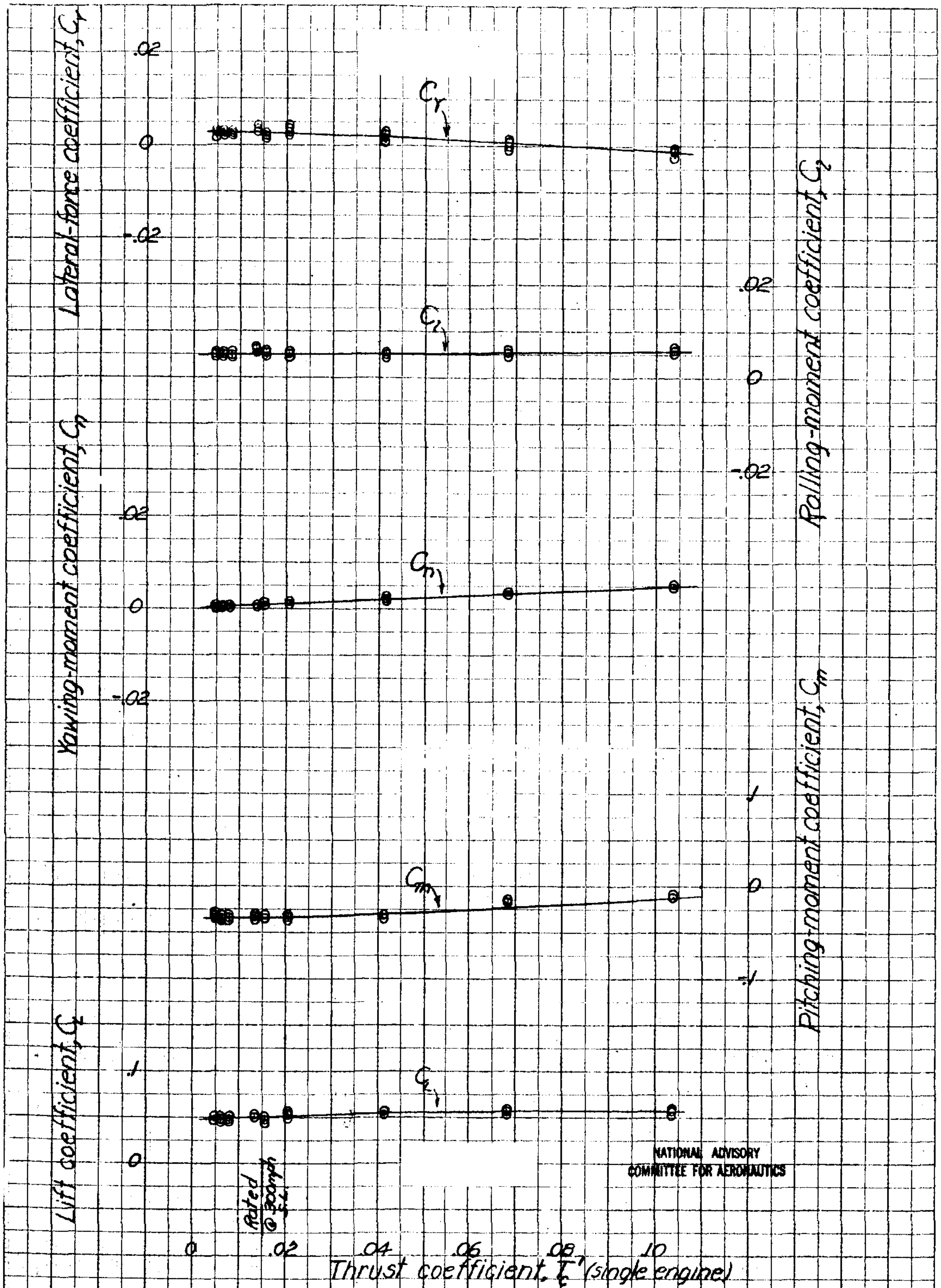

Figure 26.- Effect of single engine operation on the aerodynamic characteristics of the YP-59A airplane. Prism deflectors installed on fin trailing edge and beads on the rudder trailing edge. $\psi, 0°$; $\alpha, -0.5°$; controls neutral; left engine operating.

L-626

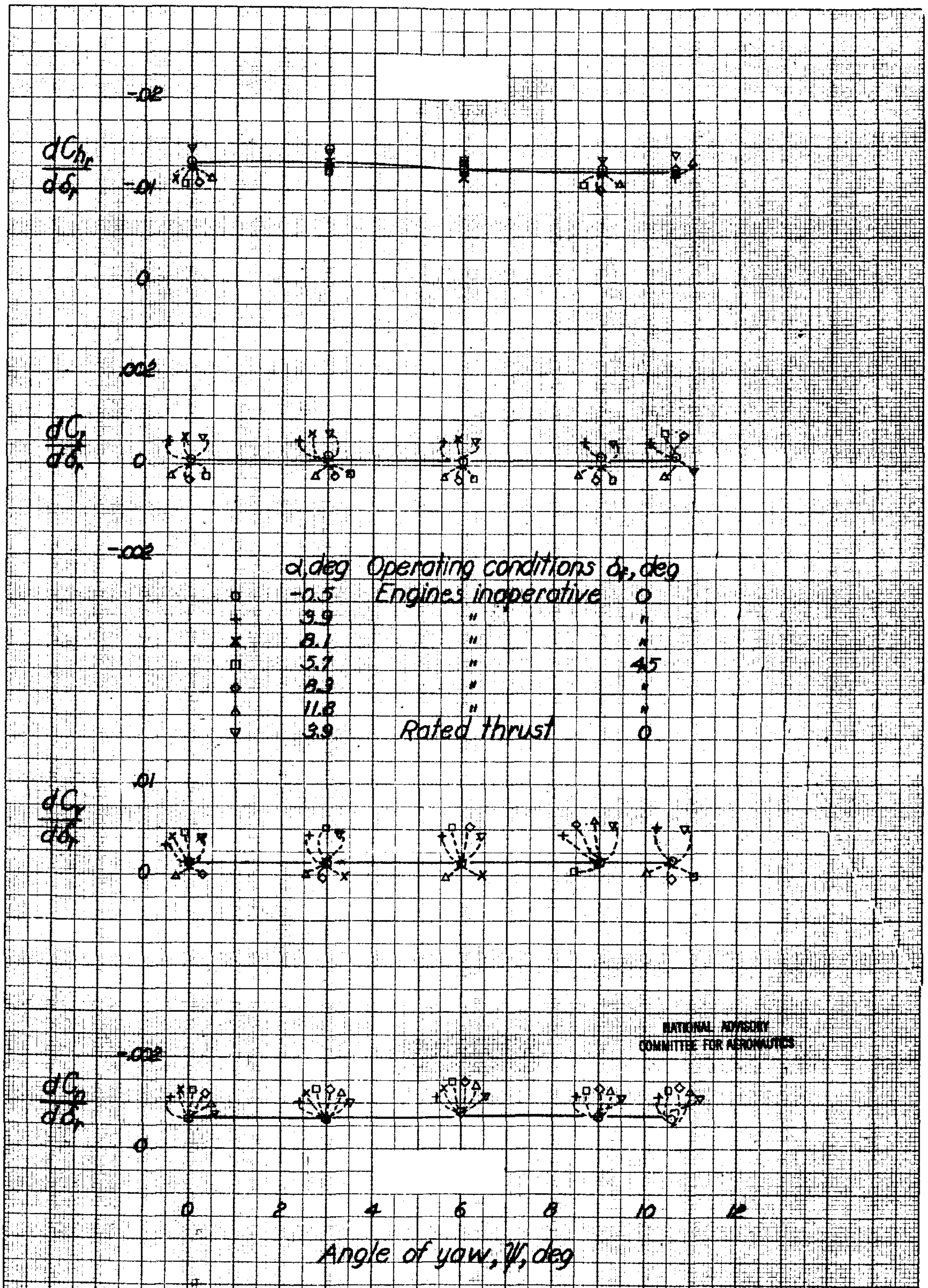

NATIONAL ADVISORY COMMITTEE FOR AERONAUTICS

Figure 27.- Variation of $\frac{dC_n}{d\delta_r}$, $\frac{dC_Y}{d\delta_r}$, $\frac{dC_l}{d\delta_r}$, and $\frac{dC_{h_r}}{d\delta_r}$ with angle of yaw.

L-626

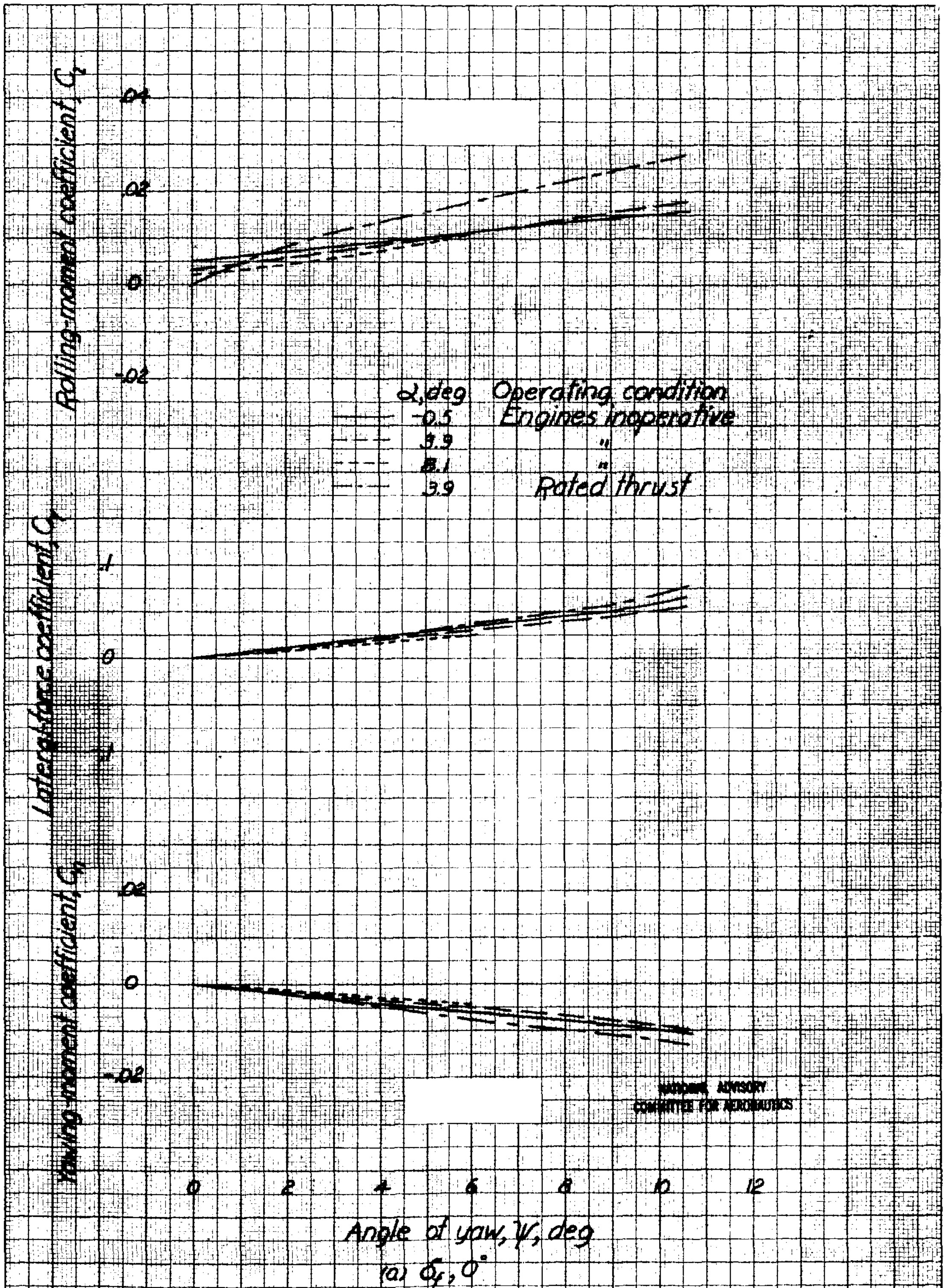

(a) δ_f, 0°

Figure 28.- Variation of C_n, C_Y, and C_l with angle of yaw. δ_r, 0°; δ_a, 0°; δ_e, 0°.

L-626

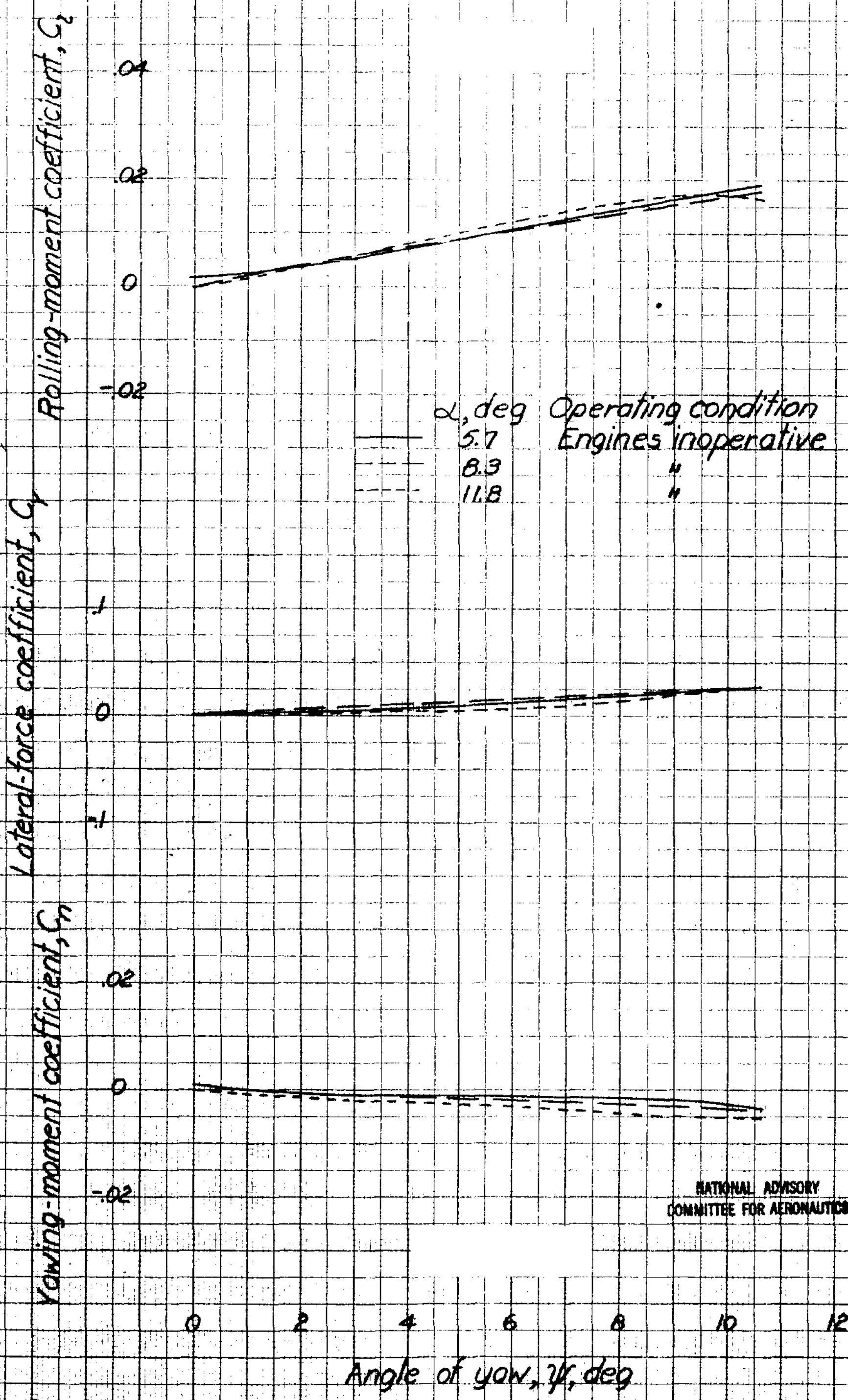

(b) δ_f, 45°

NATIONAL ADVISORY
COMMITTEE FOR AERONAUTICS

Figure 28.- Concluded.

L-626

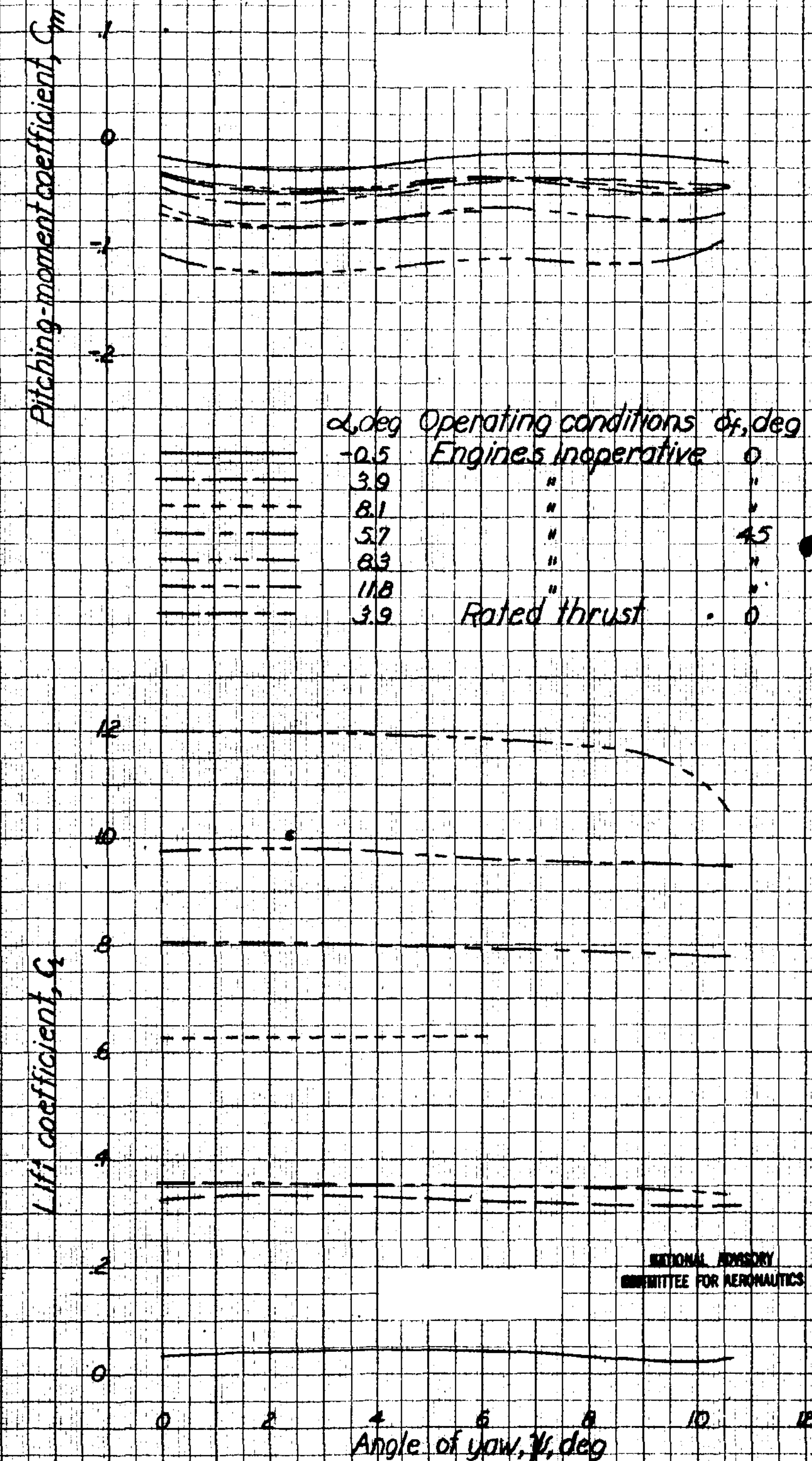

Figure 29.- Variation of C_m and C_L with angle of yaw. $\delta_a, 0°$; $\delta_w, 0°$; $\delta_e, 0°$.

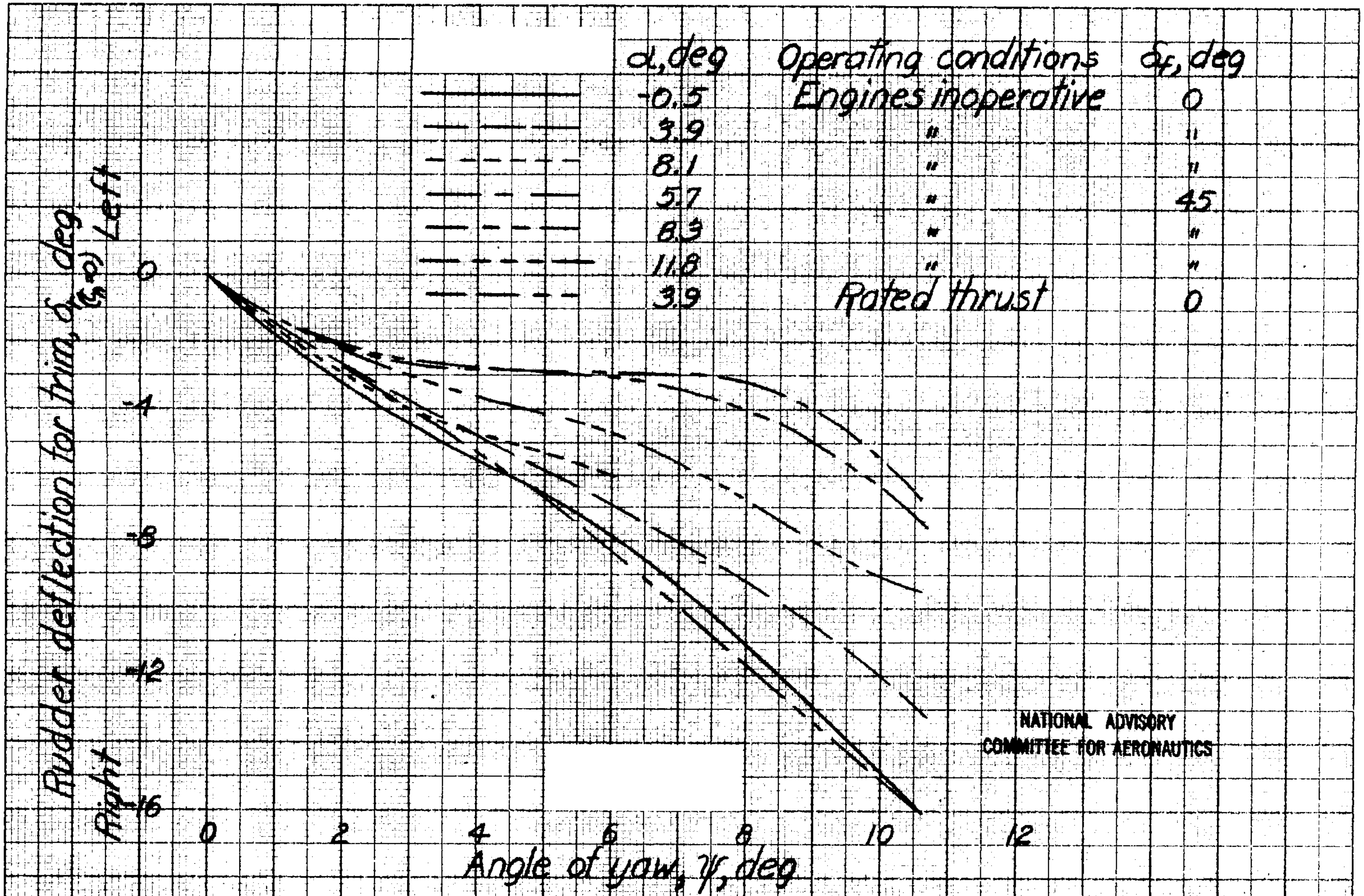

Figure 30.- Variations of rudder deflections for trim with angle of yaw. δ_e, 0°; δ_a, 0°; δ_f, 0°. Prism deflector installed on the fin trailing edge and beads on the rudder trailing edge.

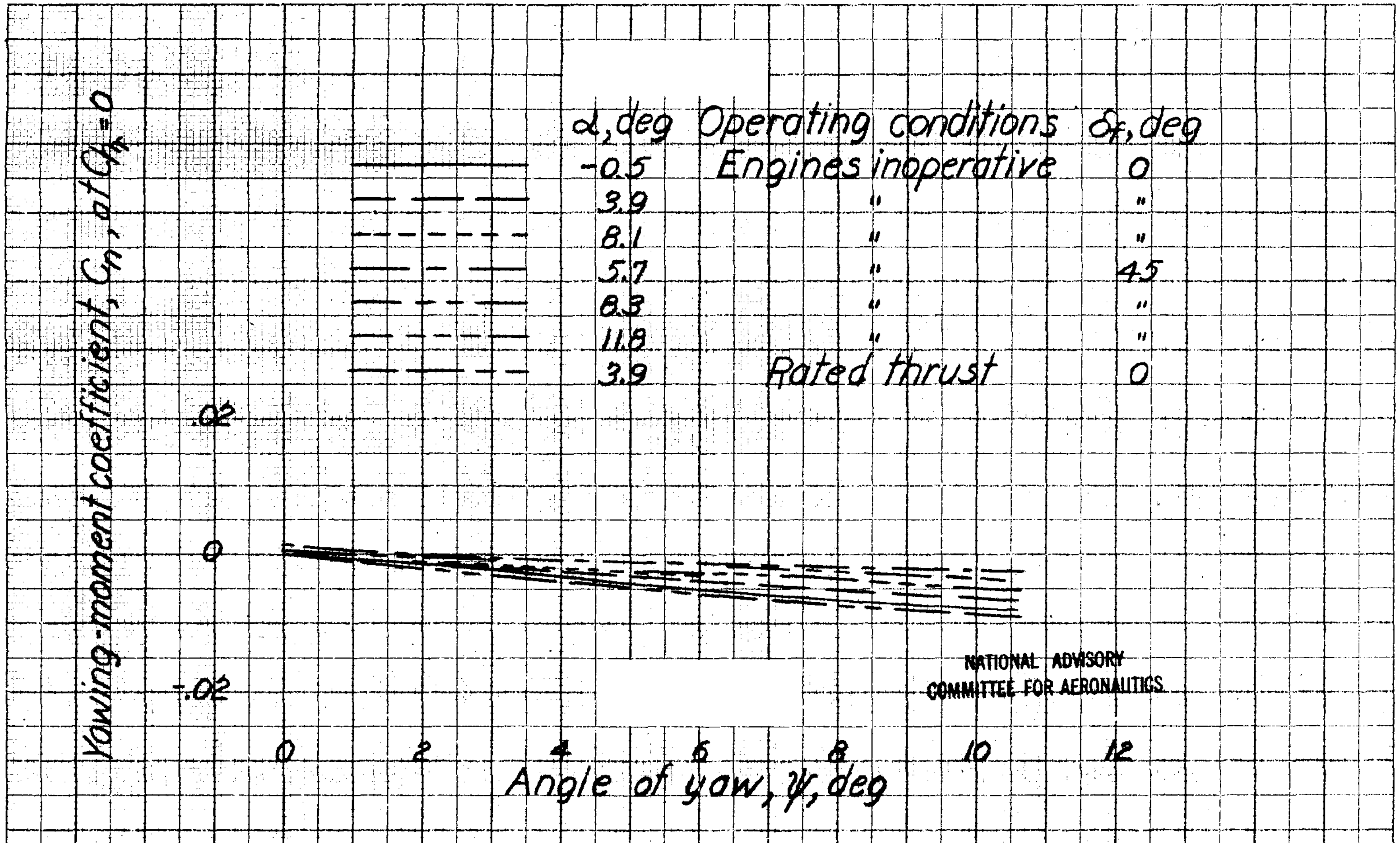

Figure 31.- Variation of yawing-moment coefficient, rudder free, with angle of yaw. δ_e, 0°; δ_a, 0°; δ_r, 0°; prism deflector installed on the fin trailing edge and beads on the rudder trailing edge.

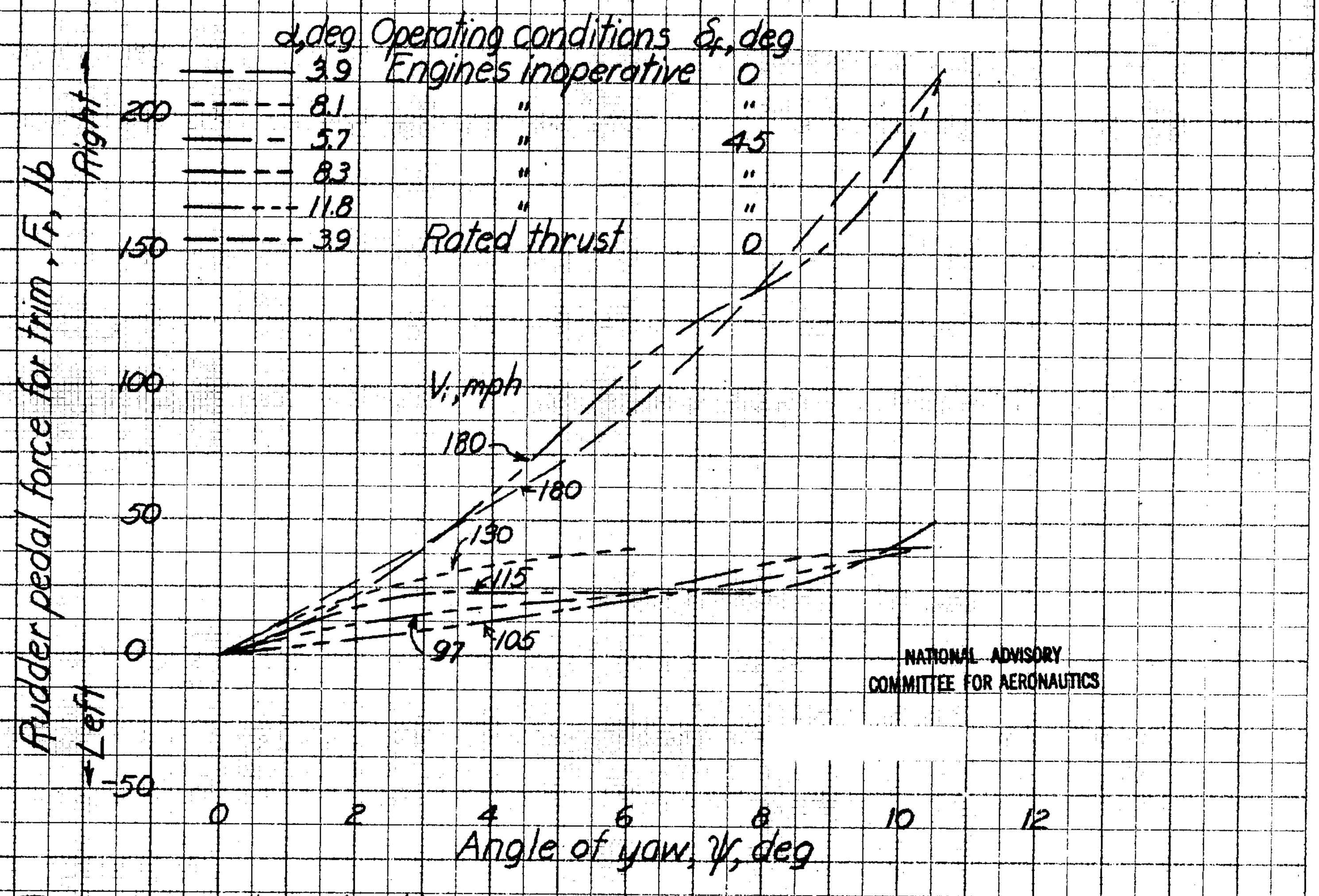

Figure 32.- Variation of rudder forces for trim with angle of yaw. δ_e, 0°; δ_a, 0°; δ_{t}, 0°; prism deflector installed on the fin trailing edge and beads on the rudder trailing edge.

L-626

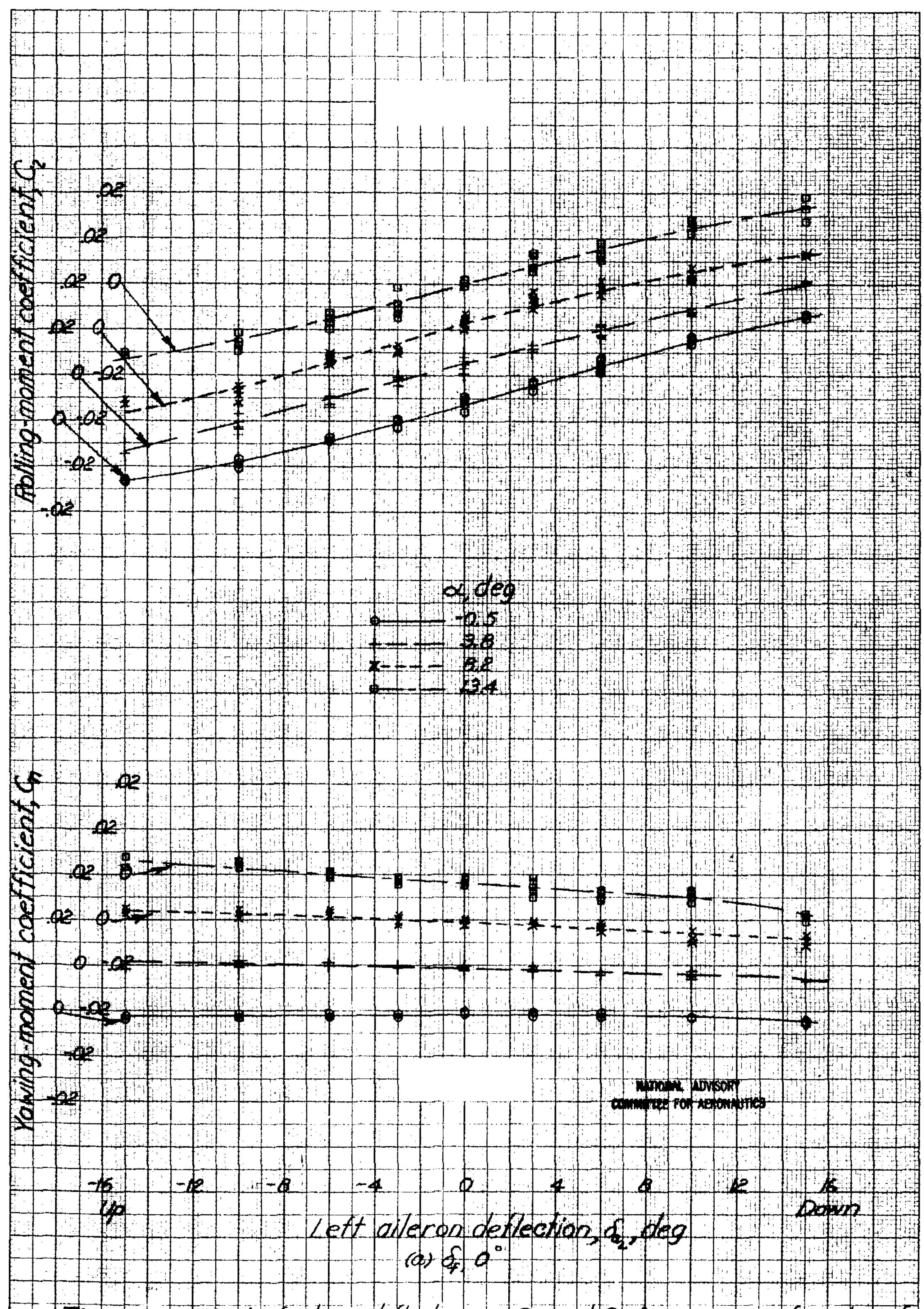

(a) δ_f, 0°

Figure 33.- Effect of aileron deflection on C_n and C_l for a range of angles of attack. ψ, 0°; δ_e, 0°; δ_f, 0°; δ_a, 0°; right aileron locked; engines inoperative.

L-626

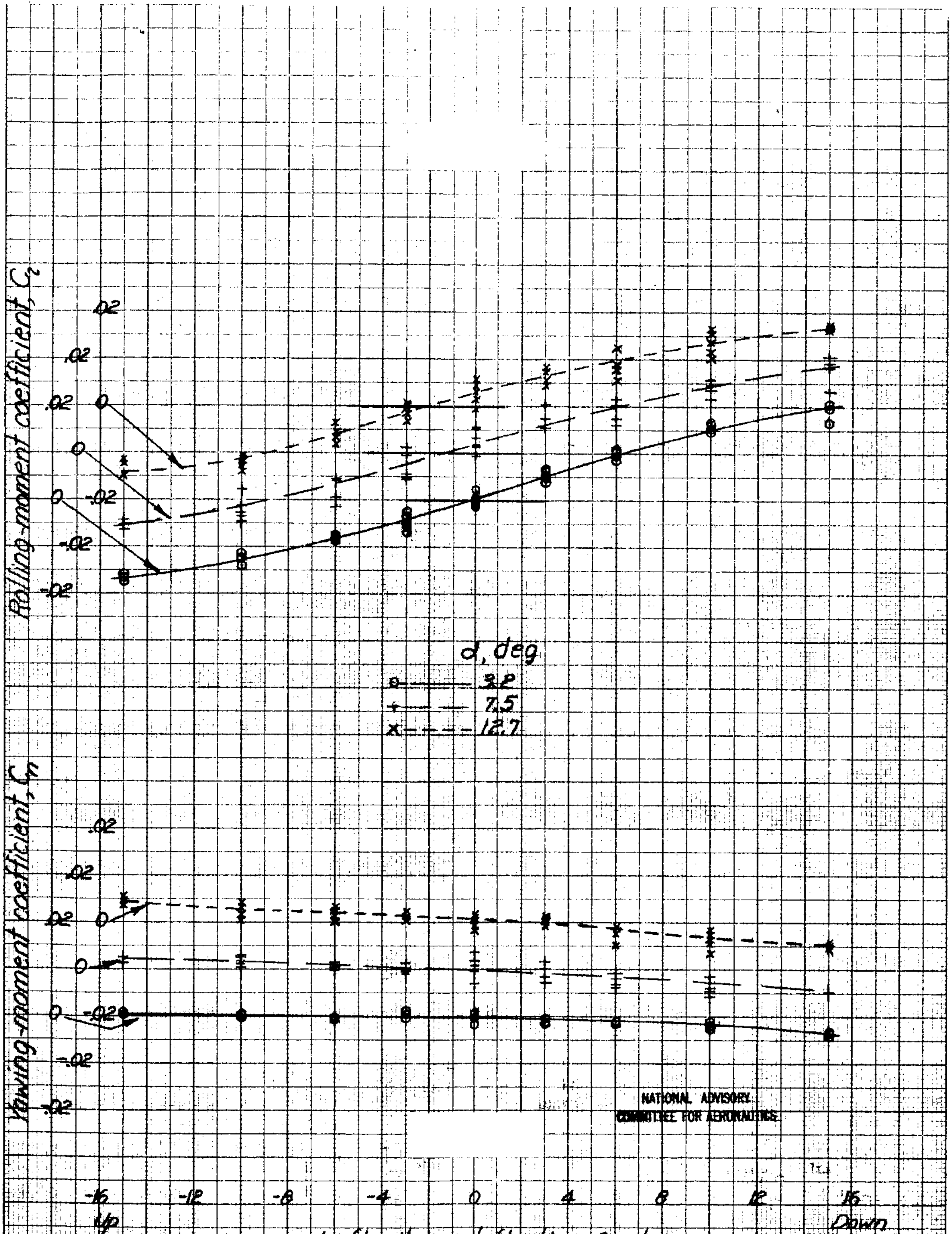

(b) δ_f, 45°

Figure 33-Concluded.